BLIND CHANNEL ESTIMATION AND MULTIUSER DETECTION FOR MULTI-RATE CDMA COMMUNICATIONS

Lei Huang

B.Sc., M.Sc.

SUBMITTED IN FULFILLMENT OF THE REQUIREMENTS FOR THE DEGREE OF DOCTOR OF PHILOSOPHY

School of Electrical Engineering

Faculty of Science, Engineering and Technology

Victoria University of Technology

Melbourne, Australia

August 2003

To my dear wife, Lingfeng Liu

Table of Contents

Abstract

The future wireless communications systems should be able to offer wide variety of applications, which have vastly different quality of service (QoS) requirements. The time-variable QoS may require the support of variable bit rates on the wireless links to the individual users. Multi-rate DS/CDMA is a promising basis on which to support the variable bit rates on the individual wireless links. Currently, the study on channel estimation and multiuser detection for multi-rate DS/CDMA, which makes full use of the nature of multi-rate signals, is still at its early stage.

The thesis deals with the application of subspace-based techniques to blind channel estimation and multiuser detection for multi-rate DS/CDMA, including single-carrier and multicarrier scenarios. For the single-carrier case, space-time blind linear multiuser detection is investigated for synchronous dual-rate systems over the AWGN channel. The performance is evaluated analytically. The multi-rate generalization and the asynchronous extension are discussed. Two-stage space-time dual-rate blind detectors are also presented. Furthermore, blind adaptive channel estimation and detection schemes for asynchronous dual-rate systems over frequency-selective multipath channels are developed. In the context of multicarrier DS/CDMA, based on a finite-length truncation approximation on the band-limited chip waveform, blind timing acquisition and channel estimation scheme is proposed for multi-rate systems. The channel estimation error due to the finite-length chip waveform truncation is analyzed by exploiting a first-order perturbation approximation.

Acknowledgements

First of all I would like to thank my principal supervisor, Associate Professor Fu-Chun Zheng, for his continual financial support and research guidance. He brought me to the field of signal processing for wireless communications, and constantly entertained me with intriguing discussions and questions. His knowledge, experience and commitment have benefited me tremendously during this research. It is my great pleasure to have such an opportunity to work with him.

My deep gratitude goes to Professor Mike Faulkner, my co-supervisor, for his support and help in my research. His enthusiasm for research and devotion to work have been constant sources of inspiration and encouragement for my advancement.

I am truly indebted to Associate Professor Jack Singh, Dr. Ying Tan, Ms. Shukonya Benka and Ms. Shirley Herrewyn for their genuine help.

My thanks should also go to my colleagues at Center for Telecommunications and Microelectronics and my friends. The memories I shared with Leon, Alex, Mladen, Ronny, Hai, Melvyn, Nghia, Don, Wei, Kai, Trung, Gavin, Edward, Shane, and Holly will always remain with me.

Special thanks should go to Australian Telecommunications Cooperative Research Center (ATcrc) for its financial support.

Finally, I wish to express my foremost gratitude for the support and encouragement I have received from my parents as well as my two sisters.

Abbreviations

3G	Third-generation
AWGN	Additive white Gaussian noise
BER	Bit-error-rate
BPSK	Binary phase-shift keying
CDMA	Code division multiple access
DDFD	Decorrelating decision feedback detector
DS	Direct-sequence
DOA	Direction of arrival
EVD	Eigenvalue decomposition
FDD	Frequency division duplexing
FDMA	Frequency division multiple access
FFT	Fast Fourier transform
FIR	Finite impulse response
GSIC	Groupwise successive interference cancellation
HRD	High-rate decorrelator
ISI	Inter-symbol interference
LMS	Least-mean-square
LRD	Low-rate decorrelator
MAI	Multiple access interference
MC	Multicode
ML	Maximum-likelihood
MMSE	Minimum mean-squared error

MOE	Minimum output energy
MRC	Maximal ratio combining
MSC	Mobile switching center
MVDR	Minimum-variance distortionless response
NFR	Near-far resistance
OFDM	Orthogonal frequency division multiplexing
OVSF	Orthogonal variable spreading factor
PAST	Projection approximation subspace tracking
PIC	Parallel interference cancellation
PSTN	Public switching telephone network
QoS	Quality of service
RLS	Recursive least-squares
RMSE	Root mean-squared error
SNR	Signal-to-noise ratio
SIC	Successive interference cancellation
SINR	Signal-to-interference-plus-noise ratio
ST	Space-time
STBC	Space-time block coding
SVD	Singular value decomposition
TDD	Time division duplexing
TDMA	Time division multiple access
VCR	Variable chip rate
VSF	Variable spreading factor
WLAN	Wireless local area network

Chapter 1

Introduction

1.1 Cellular Wireless Communications

Cellular wireless communications has undergone enormous growth over the past two decades, and nearly all market projections have indicated that this trend will last well into the future. In fact, it is expected that the number of wireless customers will surpass that of conventional wireline customers in most developed countries in the near future. The main challenges that the wireless communications industry now faces come from the limited resources in terms of frequency spectrum and the hostile radio propagation environment. As a consequence, how to increase spectrum efficiency and improve link quality is of great commercial interest.

The success of cellular radio systems is mainly due to the **cellular** concept [1]. By dividing a large geographic area into small areas known as cells and then using the same radio channels in the cells located some distance away from each other, cellular radio systems can support a large number of users over a large geographic area using a limited frequency spectrum. In addition, sophisticated handoff techniques enable a call to proceed

without being interrupted when the user moves from one cell to another.

A basic cellular radio system consists of mobile units, base stations, and a mobile switching center (MSC). Each cell contains a base station, which is responsible for communicating to mobile units in the cell by radio links. The base station then connects the simultaneous mobile calls via cables or microwave links to the MSC. The MSC coordinates the activities of all the base stations and connects the entire cellular system to the public switching telephone network (PSTN). Cellular radio systems allow simultaneous bidirectional transmission between the mobile units and their base station, which can be achieved either via frequency division duplexing (FDD) or via time division duplexing (TDD). The transmission from a base station to a mobile unit is called downlink or forward link, and that from a mobile unit to a base station is named uplink or reverse link.

Frequency division multiple access (FDMA), time division multiple access (TDMA), and code division multiple access (CDMA) are the three major access schemes which allow multiple users to access the cellular network simultaneously. Unlike FDMA and TDMA, which allocate different frequency bands or time slots to different subscribers, respectively, CDMA users share all time and frequency resources concurrently. In CDMA, the narrowband message signal for each user is multiplied by a preassigned user-specific spreading waveform whose bandwidth is far greater than that of the message. This is the so-called direct-sequence (DS) spread spectrum. Fig. 1.1 (a) shows the DS/CDMA transmitter of the kth user for binary phase-shift keying (BPSK) modulation, where $s_k(t)$ is the spreading waveform for the kth user. The spreading waveforms also allow the receiver to demodulate the message signals transmitted synchronously or asynchronously

by multiple users of the channel.

Since a CDMA system has valuable properties such as soft capacity, soft handoff, and anti-multipath capabilities, it is particularly suitable for applications such as mobile cellular telephony and personal communications. As a result, all the proposals for third-generation (3G) wireless networks, e.g., Wideband CDMA and cdma2000, employ CDMA-based air interfaces [1], [2], [67], [102].

1.2 Multiuser Detection for DS/CDMA

In a multipath propagation environment, several time-shifted and scaled versions of the transmitted signal arrive at the receiver. In existing DS/CDMA systems, such as IS-95, a RAKE structure is used to combine the time-delayed versions of the original signal in order to improve the signal-to-noise ratio (SNR) at the receiver and to enhance the system performance. A single-user DS/CDMA RAKE receiver is shown in Fig. 1.1 (b), where D is the number of resolvable paths and d_i $(i = 1, \ldots, D)$ is the delay of the ith path. However, the conventional RAKE receiver treats multiple access interference (MAI) as noise, and therefore is **interference-limited** [3], [4]. Moreover, it encounters the **near-far problem**, which occurs when users far away from the receiver are received at lower powers than those situated nearby. A stringent power control mechanism is employed in the IS-95 system to combat this problem [3], [4].

For the sake of overcoming the above restrictions of the conventional RAKE receiver, multiuser detection techniques, which exploit the structure of the MAI rather than treat it as noise, have been proposed (see [5] and references therein). It has been shown that

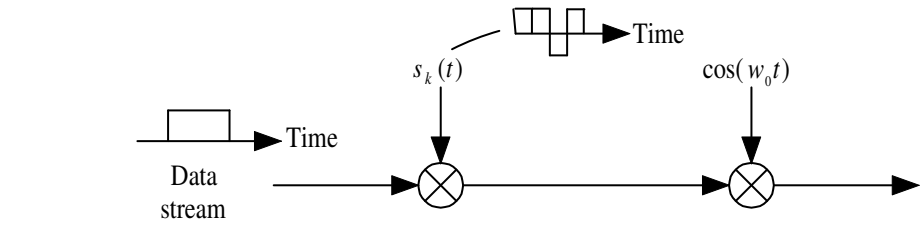

(a) Transmitter

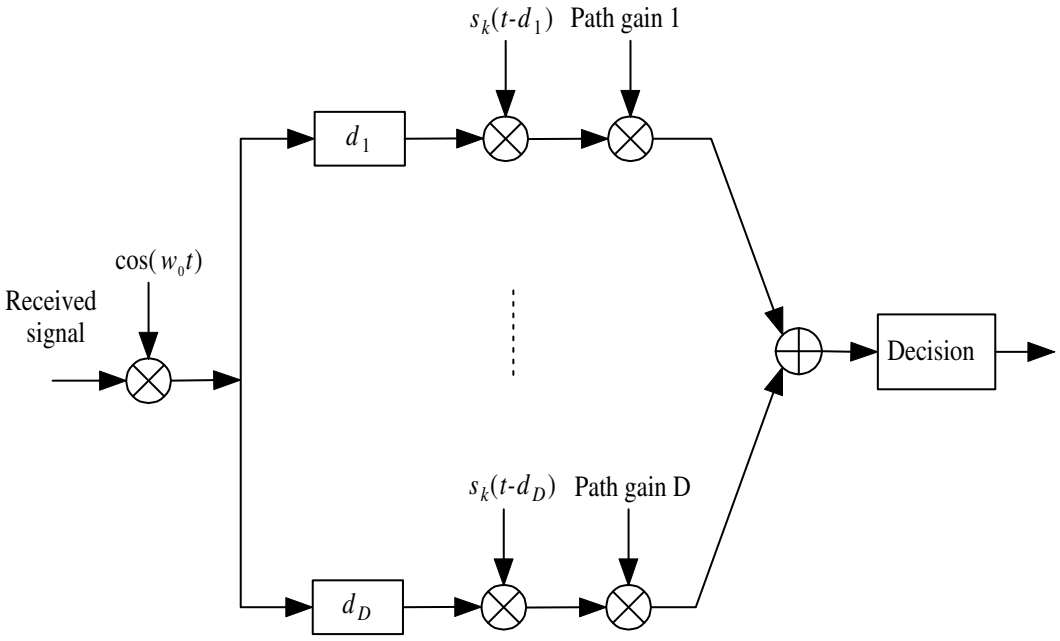

(b) RAKE receiver

Figure 1.1: A DS/CDMA transmitter/receiver.

multiuser detection can not only increase capacity by suppressing interference, but also relax the power control requirement by alleviating the near-far problem.

The effectiveness of multiuser detection was first rigorously demonstrated by Verdú in [6], where it is shown, under a mild condition, that the near-far problem does not occur if optimal maximum-likelihood (ML) detection is used. However, the complexity of implementing ML detection is exponential in the number of active users. Much effort has therefore focused on the design of **suboptimal** receivers with lower complexity. Most of these bit-level receivers fall into the following three categories:

- linear multiuser detectors, such as the decorrelating detector [7] and the minimum mean-squared error (MMSE) detector [8];
- subtractive interference cancellation receivers, e.g., parallel interference cancellation (PIC) [9], successive interference cancellation (SIC) [10], and a hybrid of PIC and SIC [11]; and
- combined schemes, such as decorrelating decision feedback detector (DDFD) [12] and the decorrelator/PIC detector [13].

All these approaches assume a front end consisting of a bank of filters matched to the spreading waveforms and the channels of active users, where each filter is synchronized to the corresponding user, even if only a particular user is of interest. As is well known, however, accurate channel estimation can be difficult in a wireless environment. Furthermore, only spreading waveform of the desired user is available to mobile units and only spreading waveforms of all intracell users are attainable to base stations.

Note that in DS/CDMA systems based on short spreading codes, where a specific spreading code is selected for a particular user and then repeated for each data symbol of that user, the MAI is clearly cyclostationary provided that the channels for the users vary relatively slowly. This observation inspired the invention of several adaptive chip-level receiver structures based on the MMSE criterion [14], [15], [17] which process the samples obtained by chip-matched filtering followed by sampling at (a multiple of) chip rate. The only knowledge required by the receiver is a training sequence transmitted by the desired user, which allows the receiver to be implemented adaptively using standard least-mean-square (LMS) algorithm or recursive least-squares (RLS) algorithm [16]. It has been shown that adaptive MMSE reception not only suppresses interference, but also provides automatic multipath combining for the desired user [4]. In addition to the adaptive MMSE receiver, adaptive techniques based on decorrelator and interference cancellation have also been invented [14].

1.3 Blind Channel Estimation and Multiuser Detection

It is noteworthy that in order to track the severe time variations of a wireless channel, adaptive multiuser receivers need to be regularly trained using periodically transmitted pilot symbols. Unfortunately, frequent use of training sequences decreases the spectral efficiency. As a consequence, blind techniques for multiuser detection, which only require prior knowledge of the spreading sequence of the user of interest [4], [17]-[26], have been explored for DS/CDMA to eliminate the need for training sequences. Obviously, a blind

scheme is very attractive when considering implementation of multiuser detection strategies in portable handset terminals. Among the existing techniques for blind multiuser detect suitable for the CDMA downlink, **constrained optimization** and **subspace-based** methods are the two main categories.

The first solution based on constrained optimization was developed in [20], where it is shown that an MMSE receiver can be obtained by minimizing the receiver's output energy with the response of the desired user constrained to remaining constant. This so-called minimum output energy (MOE) detector is very sensitive to signal mismatch created by multipath effects or timing errors. An extension of the MOE detector to the multipath case was provided in [21], by forcing the receiver response to delayed copies of the signal of interest to zero. The additional constraints alleviate the signal cancellation due to mismatch, but this method still suffers from inferior performance since it treats part of the useful signal as interference. An improvement was proposed in [22], where the constraint values are optimized by a max/min approach rather than being set to one or zero. The performance of this method tends to be close to that of the optimal MMSE receiver at high SNR in the presence of multipath. However, the complexity is higher too due to the use of an eigen-decomposition. In [23], Tian et al. developed a robust constrained receiver by employing multiple linear constraints, which match a nominal multipath profile, and a quadratic inequality constraint. The latter constraint provides robustness to residual mismatch. This scheme has relatively low complexity compared to methods using optimized constrained parameters. Notably, adaptive implementations of these constrained linear detectors have been proposed using LMS and RLS techniques,

and no explicit channel estimation is required for these detectors.

So far as the subspace-based methods are concerned, the subspace-based blind adaptive detector was constructed in closed form based on signal subspace estimation [24]. This detector has been shown to outperform the blind MOE detector [20] in steady state. Since the method in [24] only deals with low rate CDMA systems where inter-symbol interference (ISI) is negligible, an extension was presented in [26] to combat both MAI and ISI in high rate dispersive CDMA systems. In this scheme, the ISI channel is estimated first, and then the receiver is constructed based on channel estimates. Apart from such a two-step procedure, a low-complexity subspace-based blind adaptive detector was constructed in [25] without channel estimation as an intermediate step.

Additionally, the application of subspace-based techniques for channel parameter estimation in CDMA systems, such as delay and channel estimation [26]-[31], is also currently an active area of research. It is worth noting that differential encoding at the transmitter and differential detection at the receiver can be used to solve the problem of phase ambiguity in channel estimates, encountered by subspace-based blind methods.

The subspace-based blind approaches typically require not only a long duration of observation, but also some form of eigen-decomposition. The computational burden can therefore be prohibitively high. Furthermore, the channel is often required to be time-invariant during this long observation period, which typically makes these algorithms impractical for wireless communications. One feasible solution to this issue is to develop low complexity adaptive algorithms with capability for tracking the time variation of a wireless channel (e.g., [24]). Another interesting strategy is semi-blind methods [32],

which exploit the statistics of the unknown data as well as the known pilot signal and require a short duration of observation to achieve the same performance as the blind methods.

The above blind techniques for multiuser detection in the CDMA downlink aim to demodulating a given user's data with prior knowledge of only the spreading sequence of that user. In the CDMA uplink, however, typically the base station receiver has knowledge of the spreading sequences of all intracell users. In such scenarios, a substantial amount of work is available in the literature about blind multiuser detection [33]-[38]. Especially, group-blind techniques have received much interest [35]-[38]. They make use of the spreading sequences and the estimated multipath channels of all known users to suppress the intracell interference, while blindly suppressing the intercell interference. It has been demonstrated that the group-blind linear multiuser detection techniques offer substantial performance gains over the blind linear multiuser detection methods in a CDMA uplink environment.

1.4 Multicarrier DS/CDMA

As described above, the interest in applying DS/CDMA techniques to wireless communications is mainly due to its multiple access capability, robustness against fading, and anti-interference characteristics. On the other hand, **multicarrier modulation** schemes, often denoted as orthogonal frequency division multiplexing (OFDM), are highlighted as emerging signaling methods for broadband wireless access. Recently, OFDM has been accepted as the next generation standard for wireless local area network (WLAN) systems,

including IEEE 802.11 as well as HIPERLAN/2 [39], [40]. The main advantage of OFDM systems is that they can resolve the difficult ISI problems occurring with high data rate transmission in multipath channels.

Naturally, it is interesting to combine multicarrier modulation with CDMA, which forms a new multiple access scheme, denoted as multicarrier CDMA [41], [42]. Multicarrier CDMA signals can be easily transmitted and received using a fast Fourier transform (FFT) device without increasing the transmitter and receiver complexities. Furthermore, they have the attractive feature of high spectral efficiency.

Multicarrier CDMA systems may be classified into two categories, depending upon whether time domain or frequency domain spreading is employed. In the first class (the so-called multicarrier DS/CDMA), the transmitted symbols are multiplied by low rate spreading sequences in time, yielding conventional, narrowband DS waveforms. The complete DS/CDMA waveform is then transmitted at different carrier frequencies, such that the net bandwidth allocation is equal to that of a single-carrier DS/CDMA system using a higher rate spreading waveform [43]-[48]. In the second class, however, the spreading sequence is serial-to-parallel converted such that each chip modulates a different carrier frequency, and thus, the data symbol is transmitted in parallel [49]-[54]. This means that the number of carriers should be equal to the spreading factor. Both classes of multicarrier CDMA systems show a similar capability in mitigating the effects of fading. **However, the time spreading class, in general, employs a smaller number of carriers relative to the frequency spreading class, and thus, is less complex** [43]. As a consequence, only the class of time spreading multicarrier CDMA systems, i.e.,

multicarrier DS/CDMA, is considered in this thesis.

In multicarrier DS/CDMA systems, to achieve frequency diversity, the same data bit spread by a narrowband DS waveform is usually transmitted over each carrier, and then the signals received from all carriers are combined to give a more robust data estimate [41]. As an example, Fig. 1.2 (a) shows the multicarrier DS/CDMA transmission scheme proposed in [43], where a band-limited DS waveform modulates C carriers. For such a scheme, the maximal ratio combining (MRC) receiver proposed in [43] is shown in Fig. 1.2 (b). Other detection strategies, such as MMSE detection [45] and SIC technique [47], have been successfully applied to multicarrier DS/CDMA. Among the existing blind techniques for channel estimation and multiuser detection, an interesting solution is the subspace-based approach [46]. Since the employed band-limited chip waveform results in a null noise subspace, which disables subspace-based techniques, a finite-length truncation approximation to the chip waveform is performed. Although this approximation causes performance degradation of the subspace-based estimators, it is shown that such a scheme is robust to moderate near-far problems.

1.5 Contribution of The Thesis

Recently, wireless communications services have shifted their focus from voice only to multimedia connections in line with the increasing popularity of Internet services in fixed networks. A combination of wireless communications and Internet services will enable our society to enter a wireless Internet era. Thus, future wireless communications systems should be able to offer a wide variety of applications, such as Web browsing, voice over IP,

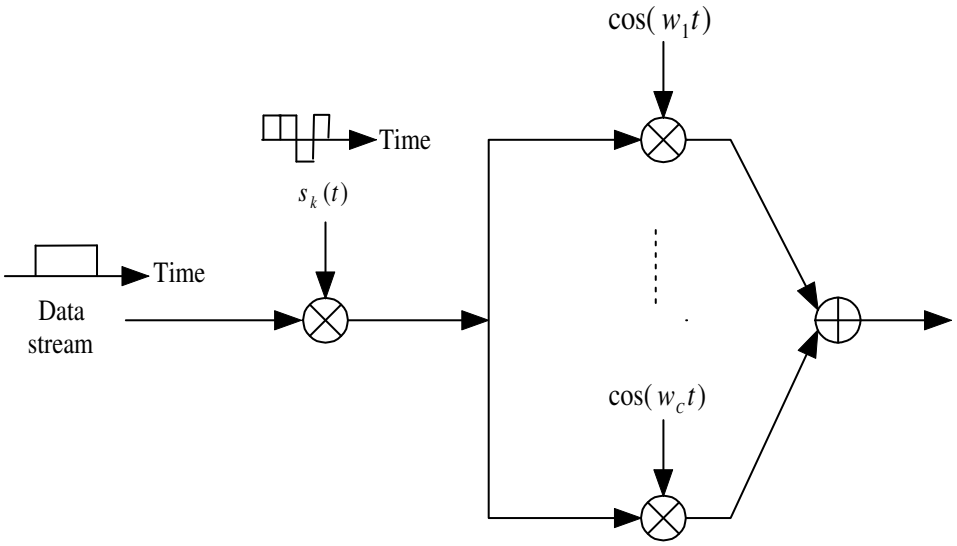

(a) Transmitter

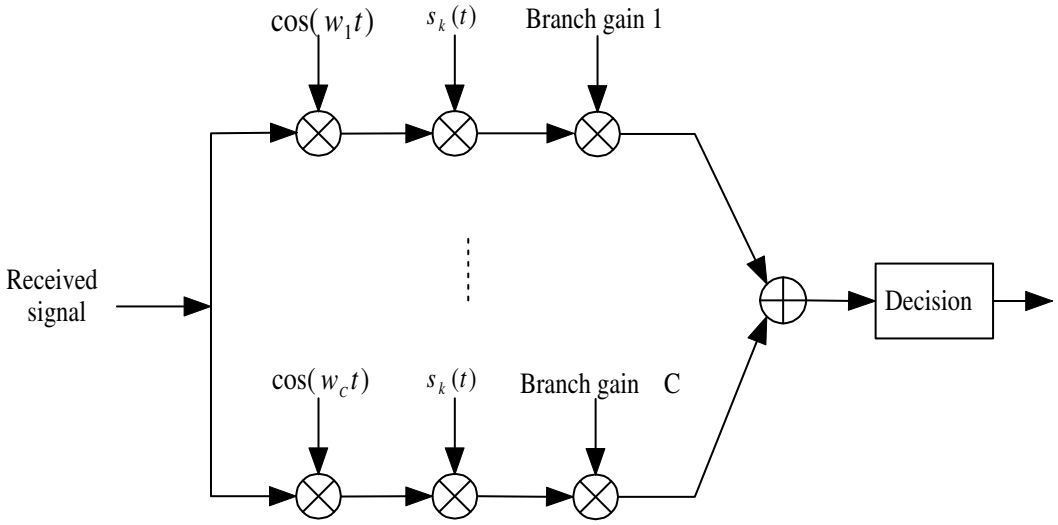

(b) Maximal ratio combining receiver

Figure 1.2: Multicarrier DS/CDMA transmitter/receiver

and video on demand, which have vastly different quality of service (QoS) requirements, e.g., bandwidth, delay, and loss [55]. The time-variable QoS may require support of variable bit rates on the wireless links to the individual users. Considering that CDMA has been proposed as the wireless access technology for 3G wireless systems and beyond, **multi-rate DS/CDMA is a promising basis on which to support variable bit rates on individual wireless links** [55].

Receiver design plays a crucial role in implementing wireless systems. As mentioned above, so far a multitude of research results regarding multiuser detection for single-rate DS/CDMA have been reported, including single-carrier and multicarrier cases. Although multi-rate multiuser detectors have their roots in their single-rate counterparts, multi-rate multiuser detectors should be more elaborately designed due to the inherent properties of multi-rate signals.

As described later in Section 2.4, some results regarding blind channel estimation and multiuser detection for multi-rate DS/CDMA are available in the literature, focusing on constrained optimization methods for single-carrier systems. However, little has been reported on the subspace-based techniques. **The thesis deals with the application of subspace-based techniques to blind channel estimation and multiuser detection for multi-rate DS/CDMA systems**. Most research results in this thesis have been presented, accepted or submitted for publication in IEEE conferences and journals [56]-[62]. For multi-rate single-carrier DS/CDMA, the following contributions are made.

- Space-time (ST) dual-rate blind linear detectors, i.e., blind decorrelating detectors

and blind MMSE detectors, for synchronous systems over additive white Gaussian noise (AWGN) channels are proposed. Purely temporal versions can be obtained as special cases [57], [61], [62].

- Theoretical analyses on the performances of ST dual-rate blind linear detectors are carried out. The conclusions are extended to more general synchronous multi-rate scenarios [57], [61].

- Extension of ST dual-rate blind linear detectors to asynchronous systems is described [57].

- Adaptive implementation for ST dual-rate blind MMSE detection is developed [57], [61].

- Two-stage ST dual-rate blind detectors, which combine purely temporal adaptive dual-rate blind MMSE detectors with non-adaptive beamformer, are presented [57], [61].

- Discrete received signal models for dual-rate systems over frequency-selective multipath channels are established, which take into account both ISI and MAI [56], [60].

- Batch algorithms and their adaptive versions for dual-rate blind channel estimation are developed [56], [60].

- Dual-rate blind MMSE detection for AWGN channels is extended to frequency-selective multipath channels.

For multi-rate multicarrier DS/CDMA, the following contributions are made.

- A discrete-time, chip rate, received signal model is derived for a general multi-rate multicarrier DS/CDMA system, [58], [59].
- Based on the finite-length truncation on the band-limited chip waveform, an approximation to the received signal model is described, which enables the subspace-based techniques [58], [59].
- The algorithms are developed to jointly estimate timing and channel parameters of the desired user [58].
- The channel estimation error due to the finite-length truncation of chip waveform is analyzed by exploiting a first-order perturbation approximation.

1.6 Thesis Overview

The remainder of the thesis is organized as follows. Chapter 2 reviews multiuser detection techniques for multi-rate DS/CDMA. Chapter 3 discusses ST multi-rate blind detectors for single-carrier DS/CDMA systems over AWGN channels. In Chapter 4, dual-rate blind channel estimation algorithms in single-carrier DS/CDMA systems over frequency-selective multipath channels are developed. Blind timing acquisition and channel estimation in multi-rate multicarrier DS/CDMA systems are investigated in Chapter 5. Finally, the conclusions and some discussion on future research are given in Chapter 6.

Throughout the thesis, uppercase letters in boldface denote matrices; lowercase letters in boldface stand for vectors; $(\cdot)^*$, $(\cdot)^T$, $(\cdot)^H$, and $(\cdot)^\dagger$ represent conjugate, transpose,

Hermitian transpose, and Moore-Penrose pseudo-inverse, respectively; $[\mathbf{A}]_{i,j}$ indicates the (i,j)th element of matrix $\mathbf{A}$; $\mathrm{sgn}(\cdot)$ denotes Signum function; $\mathrm{diag}(\cdot)$ represents diagonal matrix; $\mathrm{Re}[\cdot]$ stands for the real part of a complex; $\mathbb{E}$ is expectation operator; $\|\cdot\|$ is two-norm; $\otimes$ is Kronecker product; $\mathbf{I}_d$ is the $d \times d$ identity matrix.

Chapter 2

Multiuser Detection for Multi-rate DS/CDMA

The future multimedia wireless communication networks will have to accommodate a heterogeneous variety of information streams, which inherently possess different data rates, and are to be transmitted with different QoS requirements. As a result, the CDMA-based standards for 3G wireless networks have been designed to support the provision of multi-rate traffic with different QoS requirements. **It is thus of primary interest to investigate possible modulation formats able to accommodate information streams with different data rates over a CDMA network, as well as to devise proper detection structures taking into account the multi-rate nature of the received signal**.

The layout of this chapter is as follows. Section 2.1 summarizes the multi-rate access strategies for CDMA, which form a basis for designing multi-rate multiuser receivers. Multi-rate CDMA signal modelling is discussed in Section 2.2. Section 2.3 reviews the non-blind multiuser detection schemes for multi-rate DS/CDMA. An overview of blind

techniques for multi-rate channel estimation and multiuser detection is given in Section 2.4. In Section 2.5, multi-rate multicarrier DS/CDMA is addressed. Section 2.6 concludes this chapter.

2.1 Multi-rate CDMA Transmission

In DS/CDMA systems, there are three main options to implement multi-rate multiuser communications, i.e., variable spreading factor (VSF), multicode (MC), and variable chip rate (VCR) transmission [63]–[66]. The VSF systems employ the same chip rate for all the users, and data streams at different rates are modulated by spreading codes of the different length. In other words, for a VSF CDMA system with I different data rates, we have

$$T_c = \frac{T_0}{N_0} = \cdots = \frac{T_{I-1}}{N_{I-1}}, \tag{2.1.1}$$

where T_c is the chip duration, and T_i and N_i $(i = 0, \ldots, I-1)$ are the symbol period and the spreading factor of rate i users, respectively. This indicates

$$T_0 q_0 = T_1 q_1 = \cdots = T_{I-1} q_{I-1} = T_{br}, \tag{2.1.2}$$

where $q_0, q_1, \ldots, q_{I-1}$ are co-prime integers which represent the rate ratio, and T_{br} is the least common multiple of $T_0, \ldots, T_{I-1}$. $1/T_{br}$ is called basic rate.

In the MC systems, all data rates are assumed to be multiples of a basic rate. Each data stream is converted into several parallel basic-rate substreams, followed by spreading with different codes. Orthogonal codes are used to prevent interference between the substreams [64]. However, the presence of a dispersive wireless channel results in loss of this

orthogonality. It is easy to see from (2.1.2) that each user at rate i can be viewed as q_i virtual users at the basic rate. Note that all the users share the same bandwidth in both VSF and MC systems.

In the VCR systems, data streams at different rates are spread with different codes of the same length, i.e., different rate users use different chip rates. This means that the available bandwidth for the different rate users is different.

Fig. 2.1 shows an example of how two different rate users would be supported by these three access methods, where the rate ratio is 2:3. In this example, for the VSF scheme, if N_1 is set to be 9, N_2 should be equal to 6. For the MC scheme, each data stream is converted into two (for rate 1 users) or three (for rate 2 users) parallel basic-rate streams, which are spread by the spreading codes with length 18. In the VCR case, the spreading factor is set to be 6 for all the users, while the ratio of the chip duration between rate 1 and rate 2 users is 3:2.

The selection of multi-rate CDMA transmission scheme depends on many other factors rather than the performance only. **Since the VCR scheme introduces extra difficulty for chip synchronization and frequency planning [71], it seems that MC and VSF solutions are preferred over the VCR scheme. Furthermore, 3G wireless networks indeed employ the VSF and MC multi-rate access strategies [67], [102]**. As a result, only VSF and MC multi-rate access schemes are considered in this thesis.

It is a more challenging question which one of the VSF and MC schemes is better. The MC solution can provide orthogonal channels in the forward link which is more difficult for

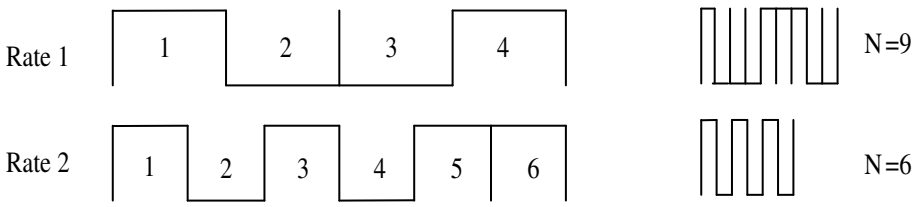

(a) Variable spreading factor scheme

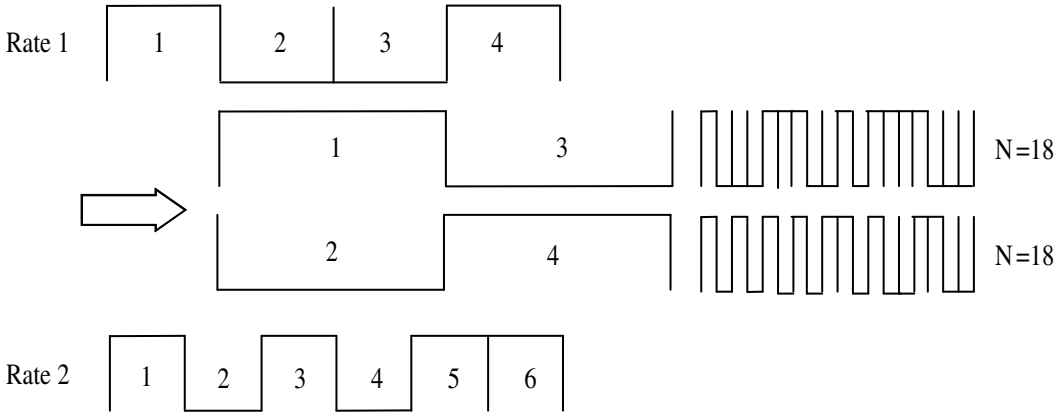

(b) Multicode scheme

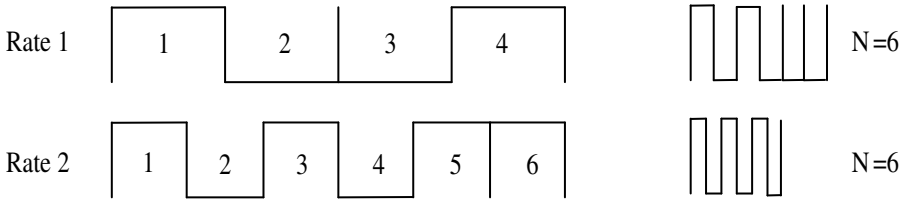

(c) Variable chip rate scheme

Figure 2.1: Three main multi-rate CDMA access strategies

the VSF solution. This is because for the VSF scheme, orthogonal codes can be found only if the spreading factors are constrained to 2^n where n is a positive integer, e.g., orthogonal variable spreading factor (OVSF) codes used in the 3G wireless systems [67], [102]. In addition, because of the larger spreading factor, MC multi-rate signals experience less ISI than VSF multi-rate signals. This leads to the complexity of the receiver in the MC case being lower than that in the VSF solution. On the other hand, the MC system requires a linear amplifier, especially in the reverse link direction, since multiple channels for a particular user give rise to large amplitude variations. The right choice of multi-rate transmission schemes depends, apart from the above points, also on the power control implementation and code allocation. All these factors must be considered before the decision of the technique is made.

2.2 Multi-rate Signal Modelling

Modelling the received multi-rate signal plays a vital role in developing efficient multi-rate multiuser detectors. Let us consider a general VSF multi-rate DS/CDMA system as defined in (2.1.1) and (2.1.2) [74], [79], [92], [95]. All the users are grouped into I classes in accordance with their data rates. In class i, there are K_i users at data rate $\frac{1}{T_i}$ where $T_i = \frac{T_{br}}{q_i}$. Without loss of generality, assume that $\frac{1}{T_0} < \frac{1}{T_1} < \cdots < \frac{1}{T_{I-1}}$, and thus $q_0 < q_1 < \cdots < q_{I-1}$. Users are indexed by two variables: i indicates the class and k indicates the user number within the class.

The received baseband signal can be modelled as

$$y(t) = \sum_{i=0}^{I-1} \sum_{k=1}^{K_i} A_{ki} x_{ki}(t) + z(t), \tag{2.2.1}$$

where $z(t)$ is an AWGN process with power spectral density σ_z^2, and A_{ki} is the received amplitude for user ki. The received signal $x_{ki}(t)$ for user ki is given by

$$x_{ki}(t) = \sum_{l=-\infty}^{\infty} b_{ki}(l) s_{ki}(t - lT_i), \tag{2.2.2}$$

where $b_{ki}(l)$ is the information stream for user ki and $\mathbb{E}\{|b_{ki}(l)|^2\} = 1$. For simplicity of presentation, BPSK modulation is assumed. The information bits are assumed to be independent from user to user and in time. The **effective** spreading waveform $s_{ki}(t)$ is the convolution of the channel impulse response $h_{ki}(t)$ and the preassigned transmitted spreading code $c_{ki}(l)$, i.e.,

$$s_{ki}(t) = \sum_{l=1}^{N_i} c_{ki}(l) h_{ki}(t - lT_c), \tag{2.2.3}$$

where $c_{ki}(l) \in \{-1, +1\}$, and $h_{ki}(t)$ is the composite channel for user ki, which includes the fixed transmit/receive pulse shaping filters and the unknown multipath physical channel, and can be described as [68]

$$h_{ki}(t) = \sum_{j=1}^{D_{ki}} \alpha_j(t) \phi(t - \tau_j), \tag{2.2.4}$$

where D_{ki} is the number of distinct paths, $\alpha_j(t)$ is the complex gain of the path, τ_j is the propagation delay, and $\phi(t)$ is pulse function (e.g., raised cosine pulse). In this thesis, we will assume **static** multipath, i.e., the channel amplitudes and delays are fixed over the observation duration. For practical purposes, $h_{ki}(t)$ can be modelled as a finite impulse response (FIR) filter [68].

Discretization of the above continuous-time signal model is indispensable for the subsequent digital signal processing. Generally, the received signal $y(t)$ is first filtered by a chip-matched filter and then sampled at the chip rate. After the discrete-time received signal is obtained, the processing interval needs to be determined. It has been shown that the received signal $y(t)$ is cyclostationary with period T_{br} for a multi-rate DS/CDMA system employing short spreading codes [92]. Naturally, the processing interval can be set to be (a multiple of) T_{br} [74], [79], [95]. This is called **basic-rate modelling**. As an alternative to basic-rate modelling, which inherently introduces detection delay for all the users, the received signal can also be modelled based on the symbol period of rate i users for the purpose of detecting rate i users [92]. This is referred to as **rate i modelling**. Since rate i symbols experience periodically time-varying interference with period q_i, q_i different signal models need to be established corresponding to q_i symbol periods within a basic-rate symbol period.

In practice, a special type of multi-rate DS/CDMA systems is often taken into account in which the higher rates are multiples of the lower rates [69]-[72], [76], [78], [81], [84], [86]-[88], [90], [91], [94], [96], [99]. Unless otherwise stated, this type of multi-rate systems is assumed in this thesis. For such multi-rate systems, most of the research results deal with dual-rate (i.e., $I = 2$) cases, where one data rate is M multiples of the other and M is an integer greater than 1. This is because all dual-rate results can be easily generalized to multi-rate scenarios where more than two data rates exist [90]. In dual-rate DS/CDMA systems, the lower data rate is actually the basic rate, and thus basic-rate modelling becomes **low-rate modelling** and rate i modelling reduces to **high-rate modelling**.

It is worth noting that the single-rate system is a special case of the VSF multi-rate system when $I = 1$. Considering that the MC multi-rate system is equivalent to the single-rate system with more virtual users at basic rate, the basic-rate (i.e., low-rate in dual-rate cases) signal model for the VSF case is also applicable to the MC case.

2.3 Multi-rate Multiuser Detection for DS/CDMA

Depending on the form of multi-rate signal modelling, multi-rate multiuser detectors can be classified as basic-rate or rate i detectors. Apparently, rate i detectors are not applicable to MC multi-rate systems. It is also noteworthy that basic-rate detectors can be used for detecting any user; while rate i detectors can generally only be used for the detection of rate i users[1].

Taking dual-rate cases as an example, Fig. 2.2 illustrates the principles of basic-rate (i.e., low-rate) and rate i (i.e., high-rate) detectors. For low-rate detectors, a single time-invariant receiver can be used for detection of each low-rate user. Comparatively, M time-invariant receivers must be deployed for each high-rate user, where the mth receiver is in charge of detecting the mth high-rate symbol within a low-rate symbol period. On the other hand, depending on how to handle the fact that high-rate symbols undergo the periodically time-varying interference with period M, the high-rate detectors can further be partitioned into **time-invariant** and **time-varying** classes. In the first class, M time-invariant receivers are employed corresponding to M high-rate signal models; while in the second class, a single periodically time-varying receiver with period M is used.

[1] In certain situations, however, rate i detectors can also be used for the detection of the users different from rate i ones.

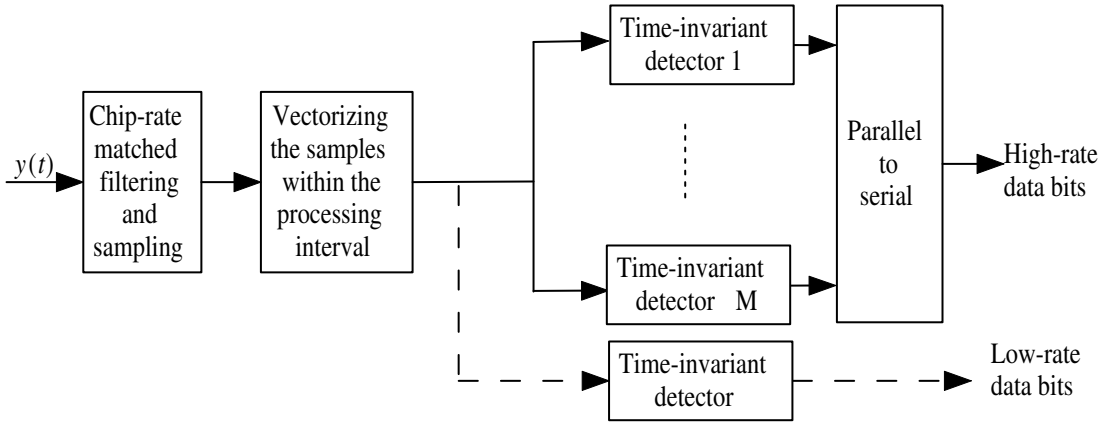

(a) Low-rate detectors

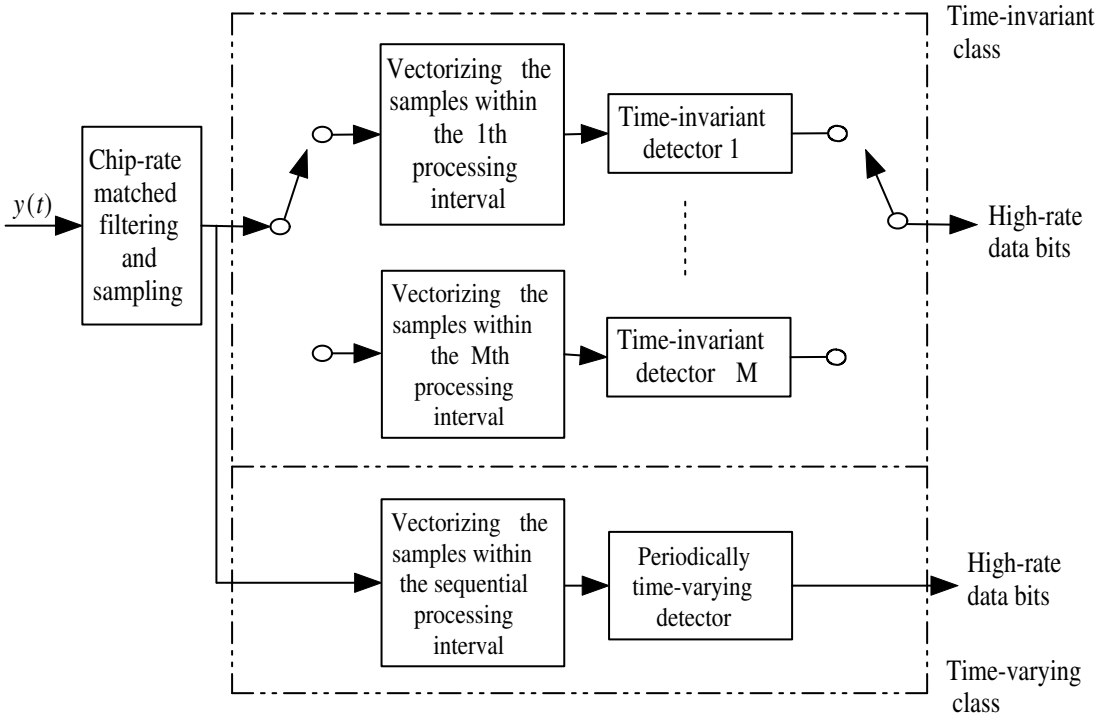

(b) High-rate detectors

Figure 2.2: The principle of low-rate and high-rate detectors

In comparison with the former, time-varying high-rate detectors have a simpler receiver structure but need a much more complicated algorithm.

A number of results regarding multiuser detection have been reported for multi-rate DS/CDMA systems. In [69], the performance of low-rate ML detectors was compared for MC and VSF cases, using particular realizations of spreading sequences. This makes global comparison of multi-rate access schemes problematic [72]. To tackle this problem, in [72], the optimum near-far resistance (NFR) measure was used for performance comparison based on the random signature sequence analysis. It is found that for a high-rate user, the performance in the VSF scheme is better than that in the MC scheme; while for a low-rate user, the performance in the MC scheme is not inferior to the VSF scheme.

Similar to single-rate DS/CDMA, the high complexity of the optimal ML detector has motivated the invention of many suboptimal multi-rate multiuser detectors with lower complexity. In the context of linear multiuser detection, both decorrelator-based receivers [71]–[75], [90] and MMSE receivers [76], [77], [90] have been studied for multi-rate DS/CDMA. A typical example is the dual-rate decorrelator for synchronous VSF systems [71]. This includes a time-invariant high-rate decorrelator (HRD) and a low-rate decorrelator (LRD). Note that the time-invariant HRD is also used for detection of low-rate users by utilizing soft decisions and MRC. Although LRD offers superior performance to HRD for all the users, it does incur additional computational complexity as well as a processing delay for high-rate users. The above dual-rate results were further generalized to synchronous multi-rate cases [70].

In addition, there is much work on the application of interference cancellation for

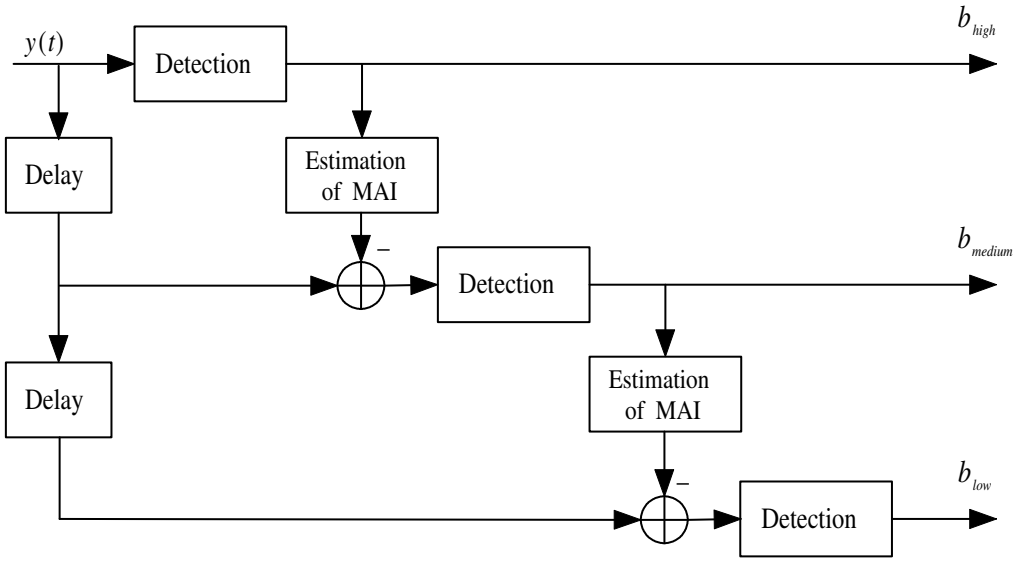

Figure 2.3: General structure for the GSIC receiver

multi-rate DS/CDMA [70], [78]–[84]. One interesting solution is the dual-rate DDFD for synchronous VSF systems [70], which consists of two stages. In the first stage, each high-rate data bit in the first $M-1$ subintervals is detected by an HRD, and then the corresponding signals of high-rate users are reconstructed. In the second stage, the reconstructed signals are subtracted from the received signal and an LRD is used to demodulate the high-rate data bits in the last subinterval and all the low-rate data bits. This scheme incurs no demodulation delay for each high-rate data bit and improves the performance for low-rate users by eliminating the interference from the high-rate data bits in the first $M-1$ subintervals.

Another example is the basic-rate groupwise successive interference cancellation (GSIC) receiver [79]. The application of GSIC to the VSF system is especially appealing due to

the natural grouping of users based on spreading factors. Normally, the same link quality (e.g., the ratio of energy per information data bit to noise power) has to be maintained for different rate users [94]. This implies that a signal with a lower spreading factor has to be transmitted with much larger power than a signal with a high spreading factor, and thus the higher rate users are expected to cause more interference to other users. Based on this observation, for the basic-rate GSIC receiver, the cancellation is started with the users transmitting at the highest data rate. After the highest rate users have been detected and the MAI is cancelled, the users with second highest data rate are detected. A GSIC receiver for a three-rate system is shown in Fig. 2.3. The detection within groups can, in principle, apply any known multiuser detector, such as the decorrelating detector or the PIC detector.

It should be pointed out that a closely related issue to multi-rate multiuser detection is channel estimation for multi-rate DS/CDMA. This is because high performance detectors, such as coherent detectors, need explicit channel information. To this end, multi-rate channel estimation based on training sequence has been investigated in [85] and [86].

2.4 Multi-rate Blind Channel Estimation and Multiuser Detection

Besides the aforementioned non-blind multi-rate multiuser detectors, blind channel estimation and multiuser detection in multi-rate DS/CDMA systems are also active areas of research. Various blind MMSE detection schemes have been derived and analyzed for

multi-rate DS/CDMA systems over AWGN channels [87]-[90] and multipath fading channels [91], [92], [96]. In [87] and [88], based on the inverse of the correlation matrix of the received signal, both low-rate and high-rate blind MMSE detectors were constructed for dual-rate systems over AWGN channels, which have capability of detecting both high-rate and low-rate users. However, the time-invariant high-rate blind MMSE detector is not strictly blind because knowledge of the noise level and interfering users is required to detect a low-rate data bit. On the other hand, blind implementation of periodically time-varying MMSE detection for high-rate users was proposed in [90] by developing a blind cyclic RLS algorithm.

For multipath channels, the design of multi-rate blind multiuser detectors without channel estimation is possible. Such dual-rate blind multiuser detectors were proposed in [91] by applying the MOE criterion. It is observed that a high-rate user experiences the same frequency-selective channel during its M consecutive symbol durations within a low-rate symbol period. A bank of M time-invariant high-rate detectors are derived jointly to detect those M symbols for a high-rate user by minimizing the total output power of these detectors subject to a common constraint for all M high-rate detectors. However, this constrained optimization approach only deals with the case where the delay spread is only a small fraction of the symbol period. Moreover, its performance degrades greatly at low SNR.

Alternatively, the channel can be estimated before the multiuser detection process. Blind channel estimation for multi-rate DS/CDMA has been suggested using subspace-based techniques [95], [96], the correlation matching approach [97] and the frequency

domain method [98]. Semi-blind channel estimation for dual-rate systems has also been investigated in [99]. As an additional dimension to blind channel estimation, the problem of blind time delay estimation in multi-rate asynchronous DS/CDMA systems was also addressed in [101]. Both subspace and non-parametric methods are considered for MC and VSF schemes.

In addition, blind techniques for interference cancellation have been proposed for multi-rate DS/CDMA, such as the blind adaptive DDFD detector [93]. The dual-rate blind adaptive DDFD detector differs from the dual-rate non-blind DDFD [70] in that the time-invariant HRD and LRD in the latter are replaced by time-invariant high-rate blind adaptive bootstrap decorrelator and low-rate adaptive decorrelating detector, respectively. In comparison with its non-blind counterpart, the dual-rate blind adaptive DDFD has a lower computational complexity. Moreover, it is shown that at low SNR, the dual-rate blind adaptive DDFD provides a better performance for low-rate users than the non-blind LRD and a better performance for high-rate users than the dual-rate non-blind DDFD.

2.5 Multi-rate Multicarrier DS/CDMA

The above mentioned multi-rate multiuser detection techniques target primarily single-carrier systems. Multi-rate single-carrier DS/CDMA requires very wide transmission bandwidth to support high data rate multimedia services. It is well known that a signal of wider bandwidth can resolve more multipath [68]. For example, as Wideband CDMA has four times as much bandwidth as IS-95, the channel experienced by the Wideband CDMA signal exhibits higher dispersion. Moreover, multi-rate single-carrier DS/CDMA

can utilize the VSF scheme to provide various transmission data rates. In this case, the multipath delay spread can be comparable to or much longer than the bit duration. For instance, when the IMT-2000 vehicular channel A model is taken into consideration [102], the maximum delay spread is about 2.5μs. If the data rate is 2Mbps, then the channel spans almost 5 bit periods. Consequently, multi-rate single-carrier DS/CDMA suffers much more severe ISI than its single-rate counterpart. On the other hand, as mentioned in Section 1.4, multicarrier DS/CDMA experiences less ISI than single-carrier DS/CDMA having the same transmission bandwidth. **Thus, compared to its single-carrier rival, multi-rate multicarrier DS/CDMA seems to be a more promising solution as the wireless access technology for future wireless communications systems**.

Considering that both single-carrier and multicarrier DS/CDMA employ time-domain spreading, VSF and MC multi-rate access strategies can also be applied to multicarrier DS/CDMA. In addition, multi-rate multicarrier DS/CDMA receivers generally consist of multiple branches, each of which being in charge of one carrier. The received baseband signal at each branch can be modelled in a similar manner to a multi-rate single-carrier signal.

In comparison with single-carrier systems, much less results regarding multi-rate multiuser detection for multicarrier DS/CDMA have been reported in the literature. In [103], MRC receivers were considered for multi-rate multicarrier DS/CDMA systems, where the basic-rate and rate i detectors are used in MC and VSF cases, respectively. The BER of each multi-rate system is obtained by analysis and simulation in a Rayleigh fading channel with perfect channel estimation. It is shown that the MC system has a slightly

better performance than the VSF system. Both systems achieve significant performance improvement by applying SIC techniques.

2.6 Summary

In this chapter, multi-rate access schemes for DS/CDMA are described, followed by multi-rate signal modelling. The existing multiuser detection techniques for multi-rate DS/CDMA are reviewed, including non-blind and blind solutions. Finally, multi-rate multicarrier DS/CDMA is introduced.

Chapter 3

Space-time Blind Multiuser Detection for Multi-rate DS/CDMA Signals

As described in Chapter 2, for VSF dual-rate DS/CDMA systems, the received signal models can be established by low-rate and high-rate modelling, whose processing intervals are (a multiple of) symbol periods of low-rate users and high-rate users, respectively. Various low-rate and high-rate detectors have been developed for the AWGN and multipath fading channels, including non-blind and blind solutions.

In the case of AWGN channels, typical non-blind multi-rate linear detectors are the time-invariant LRD and HRD for synchronous dual-rate systems with a single receive antenna [71], [72], which can be used for the demodulation of both low-rate and high-rate users. It has been proven that the LRD is not inferior to the HRD in terms of probability of error, and the dual-rate results are further generalized to multi-rate scenarios where more than two data rates exist [72]. Typical examples of existing dual-rate blind multiuser detectors are the time-invariant low-rate and high-rate blind MMSE detectors

for synchronous and asynchronous CDMA systems proposed in [87] and [88]. However, the high-rate blind MMSE detector in [87] and [88] is not strictly blind. This is because for the sake of detecting a low-rate user, the signal-to-interference-plus-noise ratio (SINR) of this low-rate user within each subinterval, which involves knowledge of the noise level and interfering users, is required for decision-making. In addition, the performances of low-rate and high-rate blind MMSE detectors in [87] and [88] were compared only by numerical simulations. Note that the above dual-rate blind MMSE detectors, which are based on the inverse of the covariance matrix of the received signals, do not operate in the signal subspace.

Blind adaptive multiuser detection and antenna array processing have recently been viewed as powerful methods for mitigating cochannel interference inherent to non-orthogonal CDMA systems [19], [104], [105], [107]. For instance, Chkeif et al. presented the subspace-based ST blind decorrelator and blind MMSE detector for synchronous single-rate systems [107]. Adaptive implementation for ST blind MMSE detection based on the orthonormal projection approximation subspace tracking (PAST) algorithm [108] has also been developed. **However, so far little has been reported on ST multiuser detection for multi-rate DS/CDMA**. This chapter extends the results in [72] and [107] and proposes the subspace-based ST low-rate and high-rate blind linear detectors, i.e., blind decorrelators and blind MMSE detectors, for a synchronous dual-rate DS/CDMA system over an AWGN channel. An effective blind strategy is proposed to detect low-rate users using ST high-rate blind linear detectors, and theoretical analyses on the performances of these proposed detectors are carried out. The extension to asynchronous systems is also described.

Finally, after adaptive algorithms for ST dual-rate blind MMSE detectors are developed, two-stage ST dual-rate blind detectors are presented, which combine the adaptive purely temporal dual-rate blind MMSE detectors with the non-adaptive beamformer.

This chapter is organized as follows. In Section 3.1, signal models for a synchronous VSF dual-rate system are established. Section 3.2 presents ST low-rate and high-rate blind linear detectors and compares their performances. The asynchronous extension is addressed in Section 3.3. Section 3.4 gives adaptive implementations for ST dual-rate blind MMSE detection. In Section 3.5, two-stage ST dual-rate blind detectors are proposed. Simulation results are described in Section 3.6. Section 3.7 gives some concluding remarks. Most results presented in this chapter can also be found in [57], [61], [62].

3.1 Signal Models

Let us consider a VSF dual-rate DS/CDMA system over an AWGN channel, in which one data rate is M multiples of the other and M is an integer greater than 1. The system is assumed to be synchronous at this stage of problem formulation, and the asynchronous case will be discussed later in Section 3.3. As for the notation used below, unless otherwise stated, please refer to Sections 1.6 and 2.2.

Assume that an array of P antenna elements is employed at the receiver. At the pth antenna element, in accordance with (2.2.1) and (2.2.2), the received complex baseband

signal within the jth low-rate symbol period $[jT_0,\ (j+1)T_0]$ is

$$y_p(t) = \sum_{k=1}^{K_0} A_{k0} b_{k0}(j) s_{k0}(t - jT_0) g_{k0}^p + \sum_{k=1}^{K_1} \sum_{m=0}^{M-1} A_{k1} b_{k1}(jM+m) s_{k1}(t - mT_1 - jT_0) g_{k1}^p + z(t), \tag{3.1.1}$$

where

$$s_{ki}(t) = \sum_{l=1}^{N_i} c_{ki}(l)\phi(t - lT_c),\ i = 0, 1, \tag{3.1.2}$$

is the signature waveform for user ki. The chip waveform $\phi(t)$ is assumed to be rectangular. Generally, the signature waveform is normalized so that

$$\int_0^{T_i} s_{ki}(t)dt = 1,\ i = 0, 1. \tag{3.1.3}$$

The complex vector $\mathbf{g}_{ki} = [g_{ki}^1, \ldots, g_{ki}^P]^T$ expresses the spatial signature for user ki. For a linear array, the pth component of this spatial signature is given by

$$g_{ki}^p = \frac{1}{\sqrt{P}} \exp\left(j \frac{2\pi d(p-1)}{\lambda} \sin(\theta_{ki}) \right),\ i = 0, 1, \tag{3.1.4}$$

where d is the inter-element spacing, λ is the wavelength of the carrier, and θ_{ki} is user ki signal's direction of arrival (DOA).

Below both low-rate and high-rate signal models will be established, in which the processing intervals are set to be the symbol periods of low-rate users and high-rate users, respectively. For presentation, we define the **spatio-temporal signature** for user ki to be $\tilde{\mathbf{s}}_{ki} \stackrel{\Delta}{=} \mathbf{g}_{ki} \otimes \mathbf{s}_{ki}$, where the **temporal signature** $\mathbf{s}_{ki} = \frac{1}{\sqrt{N_i}}[c_{ki}(1), \ldots, c_{ki}(N_i)]^T$. For the continuous-time signal model (3.1.1), chip-matched filtering followed by chip-rate

sampling yields an N_0-vector

$$\mathbf{y}_p(j) = \sum_{k=1}^{K_0} A_{k0} b_{k0}(j) \mathbf{s}_{k0} g_{k0}^p + \sum_{k=1}^{K_1} \sum_{m=0}^{M-1} A_{k1} b_{k1}(jM+m) \mathbf{s}_{k1}^{(m)} g_{k1}^p + \mathbf{z}_p(j), \tag{3.1.5}$$

where $\mathbf{s}_{k1}^{(m)} = [\underbrace{0, \ldots, 0}_{mN_1}, \mathbf{s}_{k1}^T, \underbrace{0, \ldots, 0}_{N_0-(m+1)N_1}]^T$, and $\mathbf{z}_p(j)$ is a complex AWGN vector with covariance matrix $\sigma_z^2 \mathbf{I}_{N_0}$. Using (3.1.5), the output of P-element antenna array can be written as

$$\mathbf{y}(j) = \sum_{k=1}^{K_0} A_{k0} b_{k0}(j) \tilde{\mathbf{s}}_{k0} + \sum_{k=1}^{K_1} \sum_{m=0}^{M-1} A_{k1} b_{k1}(jM+m) \tilde{\mathbf{s}}_{k1}^{(m)} + \mathbf{z}(j), \tag{3.1.6}$$

where $\mathbf{y}(j) = [\mathbf{y}_1^T(j), \ldots, \mathbf{y}_P^T(j)]^T$, $\tilde{\mathbf{s}}_{k1}^{(m)} = \mathbf{g}_{k1} \otimes \mathbf{s}_{k1}^{(m)}$, and $\mathbf{z}(j) = [\mathbf{z}_1^T(j), \ldots, \mathbf{z}_P^T(j)]^T$.

Let us introduce the following notation:

$$\tilde{\mathbf{S}}_i = [\tilde{\mathbf{s}}_{1i}, \ldots, \tilde{\mathbf{s}}_{K_i i}], \ i = 0, 1,$$

$$\tilde{\mathbf{S}}_1^{(m)} = [\tilde{\mathbf{s}}_{11}^{(m)}, \ldots, \tilde{\mathbf{s}}_{K_1 1}^{(m)}],$$

$$\tilde{\mathbf{S}} = [\tilde{\mathbf{S}}_0, \tilde{\mathbf{S}}_1^{(0)}, \ldots, \tilde{\mathbf{S}}_1^{(M-1)}],$$

$$\mathbf{A}_i = \mathrm{diag}\{A_{1i}, \ldots, A_{K_i i}\}, \ i = 0, 1,$$

$$\mathbf{A} = \mathrm{diag}\{\mathbf{A}_0, \underbrace{\mathbf{A}_1, \ldots, \mathbf{A}_1}_{M}\},$$

$$\mathbf{b}_0(j) = [b_{10}(j), \ldots, b_{K_0 0}(j)]^T,$$

$$\mathbf{b}_1^{(m)}(j) = [b_{11}(jM+m), \ldots, b_{K_1 1}(jM+m)]^T,$$

and

$$\mathbf{b}(j) = [\mathbf{b}_0^T(j), \mathbf{b}_1^{(0)^T}(j), \ldots, \mathbf{b}_1^{(M-1)^T}(j)]^T.$$

Then, (3.1.6) can be rewritten as

$$\mathbf{y}(j) = \tilde{\mathbf{S}} \mathbf{A} \mathbf{b}(j) + \mathbf{z}(j). \tag{3.1.7}$$

By employing Matlab notation, we denote the mth segment of $\mathbf{s}_{k0}$ as $\mathbf{s}_{k0}^{(m)} \triangleq \mathbf{s}_{k0}(mN_1+1:(m+1)N_1)$ and $\tilde{\mathbf{s}}_{k0}^{(m)} \triangleq \mathbf{g}_{k0} \otimes \mathbf{s}_{k0}^{(m)}$. Obviously, M successive subintervals need to be considered for high-rate modelling. Corresponding to the mth subinterval within the jth low-rate symbol period, the output of the antenna array can be represented as a PN_1-vector

$$\mathbf{y}^{(m)}(j) = \tilde{\mathbf{S}}^{(m)}\tilde{\mathbf{A}}\mathbf{b}^{(m)}(j) + \mathbf{z}^{(m)}(j) \ (m = 0, \ldots, M-1), \tag{3.1.8}$$

where $\tilde{\mathbf{S}}^{(m)} = [\tilde{\mathbf{s}}_{10}^{(m)}, \ldots, \tilde{\mathbf{s}}_{K_0 0}^{(m)}, \tilde{\mathbf{S}}_1]$, $\tilde{\mathbf{A}} = \mathrm{diag}\{\mathbf{A}_0, \mathbf{A}_1\}$, and $\mathbf{b}^{(m)}(j) = [\mathbf{b}_0^T(j), \mathbf{b}_1^{(m)^T}(j)]^T$, and $\mathbf{z}^{(m)}(j)$ is the corresponding complex noise vector.

3.2 ST Dual-rate Blind Linear Detectors

Based on the above signal models, this section will derive the subspace-based time-invariant ST low-rate and high-rate blind linear detectors, including blind decorrelators and blind MMSE detectors.

3.2.1 ST Low-rate Blind Linear Detectors

It is easy to see from (3.1.7) that each high-rate user can be viewed as M virtual low-rate users within a low-rate symbol period. Therefore, within a low-rate symbol period, a dual-rate system with K_0 low-rate users and K_1 high-rate users is equivalent to a single-rate system with K_L low-rate users, where $K_L \triangleq K_0 + MK_1$. For convenience, it is assumed that the data bit, the temporal signature, the spatial signature, the spatio-temporal signature and the received amplitude of the kth user are represented by $b_k(j)$,

$\mathbf{s}_k$, $\mathbf{g}_k$, $\tilde{\mathbf{s}}_k$ (i.e., $\mathbf{g}_k \otimes \mathbf{s}_k$), and A_k, respectively, whose physical meanings can readily be understood via (3.1.7).

Assume that $\tilde{\mathbf{S}}$ is of full column rank. By performing an eigen-decomposition, the autocorrelation matrix of the received signal $\mathbf{y}(j)$ can be represented by

$$\begin{aligned}\mathbf{R} &\triangleq \mathbb{E}\{\mathbf{y}(j)\mathbf{y}^H(j)\} \\ &= \mathbf{U}_s\mathbf{\Lambda}_s\mathbf{U}_s^H + \mathbf{U}_n\mathbf{\Lambda}_n\mathbf{U}_n^H,\end{aligned} \tag{3.2.1}$$

where $\mathbf{U}_s$ is an orthonormal basis of the signal subspace and $\mathbf{U}_n$ is that of the noise subspace orthogonal to $\mathbf{U}_s$. $\mathbf{\Lambda}_s$ contains K_L largest eigenvalues of $\mathbf{R}$ and $\mathbf{\Lambda}_n = \sigma_z^2\mathbf{I}_{PN_0-K_L}$. Based on these subspace parameters, a linear detector for demodulating the kth user can be written as [107]

$$\hat{b}_k(j) = \mathrm{sgn}[\mathrm{Re}(\mathbf{d}_k^H\mathbf{y}(j))], \tag{3.2.2}$$

where

$$\mathbf{d}_k = \frac{\mathbf{D}\tilde{\mathbf{s}}_k}{\tilde{\mathbf{s}}_k^H\mathbf{D}\tilde{\mathbf{s}}_k}. \tag{3.2.3}$$

Here $\mathbf{D} = \mathbf{U}_s(\mathbf{\Lambda}_s - \sigma_z^2\mathbf{I}_{K_L})^{-1}\mathbf{U}_s^H$ for ST low-rate blind decorrelator and $\mathbf{D} = \mathbf{U}_s\mathbf{\Lambda}_s^{-1}\mathbf{U}_s^H$ for ST low-rate blind MMSE detector. The scalar constant $\frac{1}{\tilde{\mathbf{s}}_k^H\mathbf{D}\tilde{\mathbf{s}}_k}$ is always positive and thus has no effect on signal detection and can be removed. For ST low-rate blind decorrelator, the BER of the kth user can be given as [107]

$$P_{b_k}^{\mathrm{lr}} = Q\left(\frac{A_k}{\sigma_z\sqrt{[\tilde{\mathbf{R}}^{-1}]_{k,k}}}\right), \tag{3.2.4}$$

where

$$Q(x) = \int_x^\infty \frac{1}{\sqrt{2\pi}} \exp\left(\frac{-t^2}{2}\right) dt, \tag{3.2.5}$$

and $\tilde{\mathbf{R}} = \tilde{\mathbf{S}}^H \tilde{\mathbf{S}}$.

Note that the implicit assumption that the exact signal covariance matrix and thus its eigen-components are known is impractical. Generally, the subspace parameters must be estimated from the received signals using batch eigenvalue decomposition (EVD) of the sample covariance matrix, batch singular value decomposition (SVD) of the sample matrix, or adaptive subspace tracking algorithms. More importantly, the desired spatial signature $\mathbf{g}_k$ is often unknown and thus has to be estimated.

Due to the orthogonality between the signal subspace and the noise subspace and the fact that $\tilde{\mathbf{s}}_k$ is within the range of $\mathbf{U}_s$, we have

$$\mathbf{U}_n^H \tilde{\mathbf{s}}_k = \mathbf{U}_n^H (\mathbf{g}_k \otimes \mathbf{s}_k) = \mathbf{0}. \tag{3.2.6}$$

The above equation set contains $PN_0 - K_L$ equations (for each low-rate user) or $M(PN_0 - K_L)$ equations (for each high-rate user) and P unknown variables. Therefore, if $P \geq \frac{K_L - 1}{N_0 - 1}$ (for low-rate users) or $P \geq \frac{MK_L - 1}{MN_0 - 1}$ (for high-rate users), (3.2.6) is generally an over-determined linear equation set and has a unique nontrivial solution. The principle of ST low-rate blind linear detectors is shown in Fig. 3.1.

3.2.2 ST High-rate Blind Linear Detectors

It can be observed from (3.1.8) that within the mth subinterval, user $k1$ transmits a data bit using $\tilde{\mathbf{s}}_{k1}$, and user $k0$ transmits the mth segment of a data bit using $\tilde{\mathbf{s}}_{k0}^{(m)}$. Equivalently,

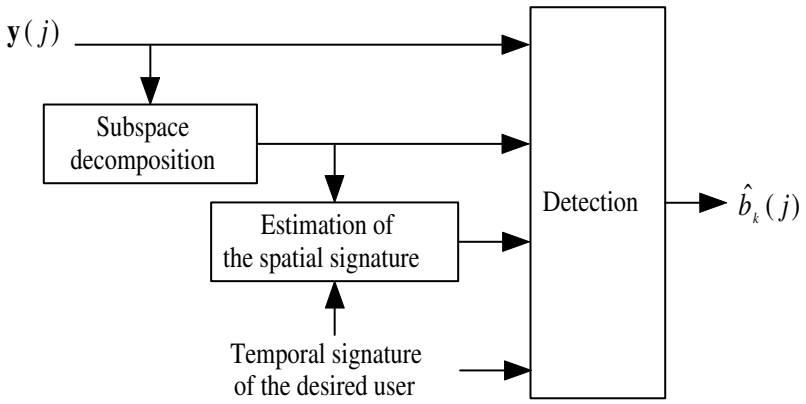

Figure 3.1: The principle of ST low-rate blind linear detectors

it can be perceived that there exist K_H high-rate users simultaneously transmitting one data bit within each subinterval, where $K_H \triangleq K_0 + K_1$. For convenience, we enumerate all active users such that user $k0$ is numbered k while user $k1$ is numbered $K_0 + k$.

Assume that $\tilde{\mathbf{S}}^{(m)}$ has full column rank. The eigen-decomposition can be performed on the autocorrelation matrix of the received signal $\mathbf{y}^{(m)}(j)$, and the subspace parameters such as $\mathbf{U}_s^{(m)}$ and $\mathbf{\Lambda}_s^{(m)}$ can then be obtained. Within the mth subinterval, a linear detector for detecting $b_{k1}(jM+m)$ can be written as

$$\mathbf{d}_{k1}^{(m)} = \frac{\mathbf{D}^{(m)}\tilde{\mathbf{s}}_{k1}}{\tilde{\mathbf{s}}_{k1}^H \mathbf{D}^{(m)} \tilde{\mathbf{s}}_{k1}}, \tag{3.2.7}$$

where $\mathbf{D}^{(m)} = \mathbf{U}_s^{(m)}(\mathbf{\Lambda}_s^{(m)} - \sigma_z^2 \mathbf{I}_{K_H})^{-1}\mathbf{U}_s^{(m)^H}$ for ST high-rate blind decorrelator and $\mathbf{D}^{(m)} = \mathbf{U}_s^{(m)}\mathbf{\Lambda}_s^{(m)^{-1}}\mathbf{U}_s^{(m)^H}$ for ST high-rate blind MMSE detector. As in (3.2.3), the scalar constant $\frac{1}{\tilde{\mathbf{s}}_{k1}^H \mathbf{D}^{(m)} \tilde{\mathbf{s}}_{k1}}$ can also be dropped. For ST high-rate blind decorrelator, the

BER of the kth high-rate user within the mth subinterval can be determined by

$$P_{b_{k1}(m)}^{\text{hr}} = Q\left(\frac{A_{k1}}{\sigma_z\sqrt{[\tilde{\mathbf{R}}^{(m)^{-1}}]_{K_0+k,K_0+k}}}\right), \tag{3.2.8}$$

where $\tilde{\mathbf{R}}^{(m)} = \tilde{\mathbf{S}}^{(m)^H}\tilde{\mathbf{S}}^{(m)}$.

Since the duration of a low-rate symbol spans M subintervals, in order to estimate a data bit of the kth low-rate user, the following decision rule is employed:

$$\hat{b}_{k0}(j) = \text{sgn}\left[\text{Re}\left(\sum_{m=0}^{M-1}\left(\frac{1}{\mathbf{d}_{k0}^{(m)^H}\mathbf{d}_{k0}^{(m)}}\mathbf{d}_{k0}^{(m)^H}\mathbf{y}^{(m)}(j)\right)\right)\right], \tag{3.2.9}$$

where $\mathbf{d}_{k0}^{(m)}$ can be obtained by simply replacing $\tilde{\mathbf{s}}_{k1}$ in (3.2.7) by $\tilde{\mathbf{s}}_{k0}^{(m)}$. We can see from (3.2.9) that a soft decision is applied to each subinterval, and then the sum of the weighted soft outputs from M subintervals is used for the detection of a low-rate data bit. Note that the employed weighting factors are the reciprocal of detector coefficients' energy and need no prior knowledge of the noise level and the interfering users. This means that the contribution from a subinterval to the decision is inversely proportional to the output noise power within this subinterval. The explanation for this strategy is that the noise level is dominant over or comparable to the MAI after multiuser detection is applied, which is particularly true for ST high-rate blind decorrelator where the MAI is completely suppressed. For ST high-rate blind decorrelator, since $\mathbf{d}_{k0}^{(m)^H}\tilde{\mathbf{s}}_{k0}^{(m)} = 1$, $\mathbf{d}_{k0}^{(m)^H}\tilde{\mathbf{s}}_{j0}^{(m)} = 0$ ($j \neq k$), and $\mathbf{d}_{k0}^{(m)^H}\mathbf{d}_{k0}^{(m)} = [\tilde{\mathbf{R}}^{(m)^{-1}}]_{k,k}$ [24], [107], the BER of the kth low-rate user can be given by

$$P_{b_{k0}}^{\text{hr}} = Q\left(\frac{A_{k0}}{\sigma_z}\sqrt{\sum_{m=0}^{M-1}\frac{1}{[\tilde{\mathbf{R}}^{(m)^{-1}}]_{k,k}}}\right). \tag{3.2.10}$$

A similar strategy to (3.2.6) can be used to estimate the desired spatial signature for ST high-rate blind linear detectors. Since the spatial signature information is included in M subintervals, the received signals within M subintervals are exploited for the estimation of the desired spatial signature. Therefore, in this case, the number of available equations for each high-rate or low-rate user is $M(PN_1 - K_H)$. Therefore, if $P \geq \frac{MK_H-1}{N_0-1}$, a unique nontrivial solution exists. The principle of ST high-rate blind linear detectors is summarized in Fig. 3.2.

3.2.3 A Comparison of ST Low-rate and High-rate Blind Linear Detectors

The ST low-rate and high-rate blind linear detectors involve the computation of the subspace parameters and the desired spatial signature. Obviously, the computational complexity of ST low-rate blind linear detectors is much higher than that of their high-rate counterparts as the rate ratio M increases. Moreover, it is easy to see that the use of ST low-rate blind linear detectors incurs a detection delay for high-rate users.

As mentioned before, for the sake of identifying the desired spatial signature, the number of antenna elements should satisfy $P \geq \max\{\frac{K_L-1}{N_0-1}, \frac{MK_L-1}{MN_0-1}\}$ for ST low-rate blind linear detectors and $P \geq \frac{MK_H-1}{N_0-1}$ for ST high-rate blind linear detectors. Since $\frac{MK_H-1}{N_0-1} > \frac{K_L-1}{N_0-1}$ and $\frac{MK_H-1}{N_0-1} > \frac{MK_L-1}{MN_0-1}$ for $M \geq 2$, the ST low-rate blind linear detectors can support no less users than the ST-HR blind linear detectors as long as the desired spatial signature is identifiable (assuming that all the other system parameters are the same). This conclusion can be extended to synchronous multi-rate systems with I different data rates where the higher rates are multiples of the lower rates. The ST rate i $(i = 1, \ldots, I)$

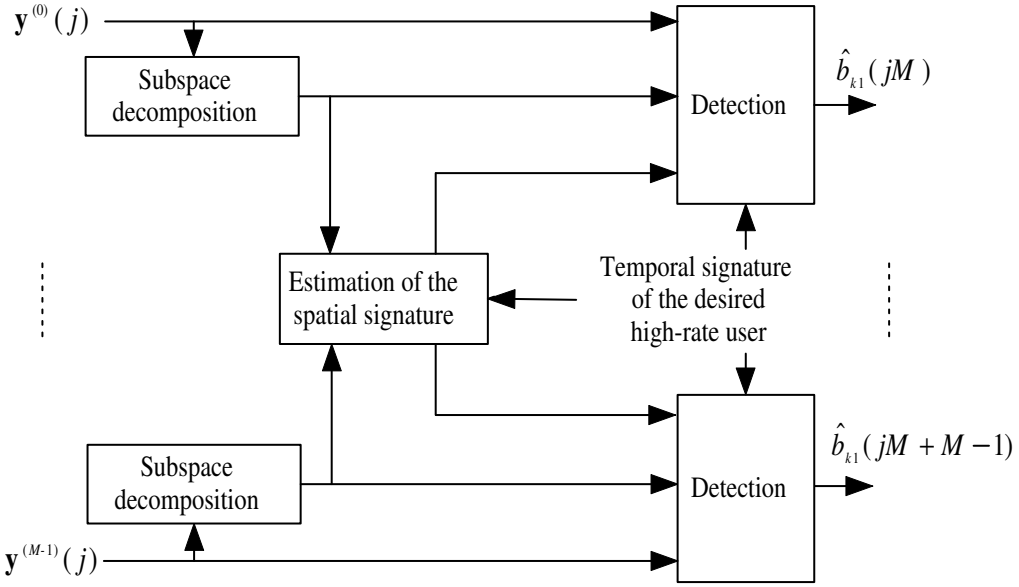

(a) Demodulation of high-rate users

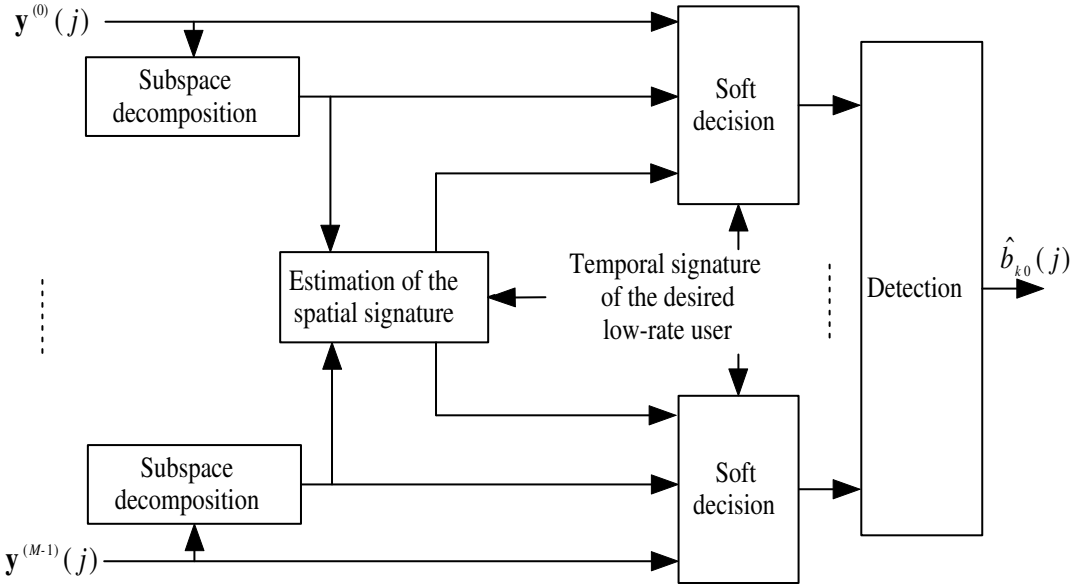

(b) Demodulation of low-rate users

Figure 3.2: The principle of ST high-rate blind linear detectors

blind linear detectors can be developed to match symbol period of rate i users, where a decision rule similar to (3.2.9) can be used to detect those users with rates lower than rate i.

Proposition 3.2.1. *In a synchronous multi-rate system with I different data rates where the higher rates are multiples of the lower rates, if rate l is lower than rate j ($1 \leq l, j \leq I$), the ST rate l blind linear detectors can support no less users than the ST rate j blind linear detectors as long as the desired spatial signature is identifiable (assuming that all the other system parameters are the same).*

Proof. Assume that the number of rate i users is K_i, the symbol period is T_i, and the spreading factor is N_i. It is also assumed that $\frac{1}{T_1} > \frac{1}{T_2} > \cdots > \frac{1}{T_I}$ and $\frac{T_l}{T_j} = M_{lj}$ for $1 \leq j < l \leq I$ where M_{lj} is a positive integer.

Considering that the received signal is cyclostationary with period T_I, M_{Ij} rate j bit intervals should be considered for ST rate j blind linear detectors. Within each rate j bit interval, the number of data bits is $\sum_{q=1}^{j} M_{jq}K_q + \sum_{q=j+1}^{I} K_q$. So the number of available equations for determining the spatial signature of the desired rate d user is $M_{Id}(PN_j - \sum_{q=1}^{j} M_{jq}K_q - \sum_{q=j+1}^{I} K_q)$ for $d < j$, and $M_{Ij}(PN_j - \sum_{q=1}^{j} M_{jq}K_q - \sum_{q=j+1}^{I} K_q)$ for $d \geq j$. Therefore, in order to ensure that the desired spatial signature is identifiable, we must have

$$P \geq \max\{\{P_{jd}^{\perp}, 1 \leq d < j\}, P_j^{\top}\}, \tag{3.2.11}$$

where

$$P_{jd}^{\perp} = \frac{M_{Id}(\sum_{q=1}^{j} M_{jq}K_q + \sum_{q=j+1}^{I} K_q) - 1}{M_{Id}N_j - 1} \tag{3.2.12}$$

$$P_{j}^{\top} = \frac{M_{Ij}(\sum_{q=1}^{j} M_{jq}K_q + \sum_{q=j+1}^{I} K_q) - 1}{M_{Ij}N_j - 1}. \tag{3.2.13}$$

Similarly, for ST rate l blind linear detectors, we must have

$$P \geq \max\{\{P_{ld}^{\perp}, 1 \leq d < l\}, P_{l}^{\top}\}, \tag{3.2.14}$$

where $P_{ld}^{\perp}$ and $P_{l}^{\top}$ are defined by (3.2.12) and (3.2.13), respectively.

Note that

$$\begin{aligned} P_{ld}^{\perp} &< \frac{M_{Id}(\sum_{q=1}^{l} M_{lq}K_q + \sum_{q=l+1}^{I} K_q)}{M_{Id}N_l - 1} \\ &< \frac{M_{Il}(\sum_{q=1}^{l} M_{lq}K_q + \sum_{q=l+1}^{I} K_q)}{M_{Il}N_l - 1} \\ &= \frac{\sum_{q=1}^{l} M_{Iq}K_q + \sum_{q=l+1}^{I} M_{Il}K_q)}{N_I - 1} \triangleq P_l, \end{aligned} \tag{3.2.15}$$

where the second inequality is due to $M_{Id} > M_{Il}$ when $d < l$, and the equality is due to $M_{Il}M_{lq} = M_{Iq}$ and $M_{Il}N_l = N_I$. Since $P_l > P_l^{\top}$ and

$$P_{j}^{\top} - P_l = \frac{(M_{Ij} - M_{Il})\sum_{q=l+1}^{I} K_q + \sum_{q=j+1}^{l}(M_{Ij} - M_{Iq})K_q - 1}{N_I - 1} > 0, \tag{3.2.16}$$

where the inequality is due to the assumption that the higher rates are multiples of the lower rates, Proposition 3.2.1 is proven. □

On the other hand, we have the following proposition for the BER performances of ST low-rate and high-rate blind decorrelators.

Proposition 3.2.2. *For a synchronous dual-rate system, if the desired spatial signature and the exact subspace parameters are known, then*

$$P^{\mathrm{hr}}_{b_{ki}(m)} \geq P^{\mathrm{lr}}_{b_{ki}(m)},\ i = 0, 1, \tag{3.2.17}$$

where $P^{\mathrm{lr}}_{b_{ki}(m)}$ *and* $P^{\mathrm{hr}}_{b_{ki}(m)}$ *are the BERs of ST low-rate and high-rate blind decorrelators for user ki's data bits in any subinterval, respectively. Especially, both achieve the same BER for each low-rate user if the temporal signatures for low-rate users are the same in every high-rate symbol period, i.e., the repetition code is employed.*

Proof. Note that the ST low-rate and high-rate blind decorrelators have similar BER expressions as the non-blind LRD and HRD [71], [72], respectively. They differ as follows:

The BER of LRD (HRD) involves a special diagonal element of $\mathbf{R}^{-1}(\mathbf{R}^{(m)^{-1}})$, i.e., the inverse of the temporal signature correlation matrix within the low-rate (mth high-rate) symbol period, which can be accurately calculated using the known temporal signatures of all active users. On the other hand, the BER of ST low-rate (high-rate) blind decorrelator involves the corresponding element of $\tilde{\mathbf{R}}^{-1}(\tilde{\mathbf{R}}^{(m)^{-1}})$, i.e., the inverse of the spatio-temporal signature correlation matrix within the low-rate (mth high-rate) symbol period, which depends upon the subspace parameters and the desired spatio-temporal signature. Hence, the BER of ST low-rate (high-rate) blind decorrelator can only be approximately estimated from the received signals.

Therefore, inequality (3.2.17) must hold due to the following reasons: i) the special diagonal element of $\tilde{\mathbf{R}}^{-1}(\tilde{\mathbf{R}}^{(m)^{-1}})$ for ST low-rate (high-rate) blind decorrelator can be accurately obtained under the condition that the desired spatial signature and the exact

subspace parameters are known; ii) $\tilde{\mathbf{R}}(\tilde{\mathbf{R}}^{(m)})$ for ST low-rate (high-rate) blind decorrelator has the same matrix structure as $\mathbf{R}(\mathbf{R}^{(m)})$ for LRD (HRD), since $\tilde{\mathbf{R}}(\tilde{\mathbf{R}}^{(m)})$ can be written as the Schur, or element by element, product of $\mathbf{R}(\mathbf{R}^{(m)})$ and the spatial signature correlation matrix without zero elements. In fact, a similar proposition has been proven for the non-blind LRD and HRD based on the above matrix structures [71], [72]. □

In accordance with Proposition 3.2.2 and the fact that the Q function defined by (3.2.5) is monotonically descending, we can conclude that the NFR performances of ST low-rate blind linear detectors are not inferior to those of their high-rate rivals. Furthermore, the above proposition and inference can be extended to synchronous multi-rate systems since a similar extension for the non-blind dual-rate decorrelators has been proven in [72].

3.3 Asynchronous Extension

The ST dual-rate blind linear detectors can be applied to asynchronous DS/CDMA. The same formulae in the synchronous case can be used for asynchronous systems with an increased dimension. This is due to the fact that the number of virtual bits and the number of their associated virtual signatures within the processing interval are larger than those in the synchronous case [87]. For ST low-rate blind linear detectors, if the desired user is a low-rate user, the desired low-rate user is then viewed as the reference user, whose bit interval is taken as the processing interval. Otherwise an arbitrary low-rate user can be chosen as the reference user. For each user other than the reference one, there might be two virtual bits located at both ends of the processing interval, whose full-length

signatures are partitioned into two virtual ones. Therefore, within the processing interval, the number of data bits (including actual and virtual bits) is between $K_0 + MK_1$ and $2K_0 + (M+1)K_1 - 1$. For the detection of the high-rate data bit that is divided into two virtual bits, a similar strategy to (3.2.9) can be used to weight the partial estimates over two successive processing intervals before a final decision is made. It should be noted that for ST low-rate blind linear detectors, the number of data bits and their associated signatures are the same among the different processing intervals.

For ST high-rate blind linear detectors, if the desired user is a low-rate user, an arbitrary high-rate user can be chosen as the reference user. Otherwise the desired high-rate user is viewed as the reference user. Within the processing interval, there might be two virtual bits for each high-rate user other than the reference one and either one or two virtual bits for each low-rate user, resulting in the number of data bits being between $K_0 + K_1$ and $2K_0 + 2K_1 - 1$. A similar strategy to (3.2.9) can be used to demodulate a low-rate data bit. Note that for ST high-rate blind linear detectors, the number of data bits and their associated signatures might change among the different processing intervals. Therefore, special attention should be paid to the implementation of ST high-rate blind linear detectors for asynchronous systems.

For a general asynchronous dual-rate system, the number of data bits within the processing interval, which determines the number of available equations for determining the desired spatial signature, depends on the relative delays of all the users and the choice of the reference user. As a consequence, it is difficult to theoretically compare the number of users which can be supported by ST low-rate and high-rate blind linear detectors.

Fortunately, such a comparison can be performed on some special asynchronous systems. Let us investigate a special asynchronous dual-rate system where only the different rate users are asynchronous. Obviously, for ST low-rate blind linear detectors, the number of data bits within the processing interval is $K_0 + (M+1)K_1$, and thus the number of available equations for determining the spatial signature is $PN_0 - K_0 - (M+1)K_1$ for the desired low-rate user or $(M+1)(PN_0 - K_0 - (M+1)K_1)$ for the desired high-rate user. Consequently, in order to ensure that the desired spatial signature is identifiable, we must have

$$P \geq \max\left\{\frac{K_0 + (M+1)K_1 - 1}{N_0 - 1}, \frac{(M+1)(K_0 + (M+1)K_1) - 1}{(M+1)N_0 - 1}\right\} \triangleq P_L. \tag{3.3.1}$$

For ST high-rate blind linear detectors, the number of data bits is $2K_0 + K_1$ within one of M processing intervals and $K_0 + K_1$ within the others. As a result, the number of available equations for determining the spatial signature is $PN_0 - (M+1)K_0 - MK_1$ for the desired high-rate user. As for the desired low-rate user, the number of available equations is $2(PN_1 - 2K_0 - K_1)$ within the processing interval with $2K_0 + K_1$ data bits, while it is $(M-1)(PN_1 - K_0 - K_1)$ within the others. The total number of available equations is thus equal to $P(N_0 + N_1) - (M+3)K_0 - (M+1)K_1$. So we must have

$$P \geq \max\left\{\frac{(M+1)K_0 + MK_1 - 1}{N_0 - 1}, \frac{(M+3)K_0 + (M+1)K_1 - 1}{N_0 + N_1 - 1}\right\} \triangleq P_H. \tag{3.3.2}$$

Since P_H is not always greater than P_L, Proposition 3.2.1 is invalid for such an asynchronous system. This means that the validity of Proposition 3.2.1 can not be warranted for an asynchronous multi-rate system.

On the other hand, it is easy to see from (3.2.4), (3.2.8) and (3.2.10) that the BER performances of ST dual-rate blind decorrelators are related to the DOAs, the temporal signatures and the delays of all the users as well as the choice of the reference user. This renders it impractical to make a theoretical comparison on the performances of ST dual-rate blind decorrelators. However, it is possible to compare their performances by qualitative analysis.

Intuitively, for asynchronous dual-rate systems, the detection performance would be better as the processing interval is enlarged. On the other hand, it would be worse when a weighting combination strategy similar to (3.2.9) is employed. As a result, the ST low-rate blind decorrelator would outperform the ST high-rate blind decorrelator for detecting the high-rate users due to its actual processing interval being much larger than (more exactly, at least M multiples of) a high-rate bit interval. As for the detection of the low-rate data bit, unlike the ST low-rate blind decorrelator, the ST high-rate blind decorrelator adopts the weighting combination strategy and its actual processing interval is at most $\frac{M+1}{M}$ multiples of a low-rate bit interval. Considering that the actual processing interval of ST high-rate blind decorrelator may be only slightly larger than that of ST low-rate blind decorrelator, the latter should outperform the former for detecting the low-rate users in most cases. This is verified by the simulation results in Section 3.6, where the DOAs, the temporal signatures and the delays of all the users are randomly generated. However, it is still possible that the ST high-rate blind decorrelator offers a better performance than its low-rate counterpart for detecting the low-rate users.

Let us investigate an asynchronous dual-rate system with a low-rate user and a high-rate user, where the rate ratio is two and the high-rate user lags three chips to the low-rate user. For the high-rate user, the DOA is 0° and the signature sequence is $\{1, -1, -1, 1, 1, 1, -1\}$. For the low-rate user, the DOA is 40° and the signature sequence is $\{-1, 1, 1, -1, -1, 1, 1, -1, 1, 1, -1, -1, 1, 1\}$. Both signature sequences are normalized. In accordance with (3.2.4) and (3.2.10), the BERs of the low-rate user are $Q(0.9952 \times A_{10}/\sigma)$ and $Q(0.9971 \times A_{10}/\sigma)$ for ST low-rate and high-rate blind decorrelators, respectively. Since the Q function defined by (3.2.5) is monotonically descending, we can conclude that in the above case, the performance of ST low-rate blind decorrelator is inferior to that of ST high-rate blind decorrelator for detecting the low-rate user. In other words, Proposition 3.3.2 is invalid for such an asynchronous dual-rate system.

3.4 Adaptive Implementations

At first, let us derive the adaptive algorithm for ST low-rate blind MMSE detection. Note that (3.2.6) can also be solved by using the following optimization procedure [107]:

$$\hat{\mathbf{g}}_k = \arg \max_{\|\mathbf{g}_k\|=1} \mathbf{g}_k^H \mathbf{W} \mathbf{g}_k. \tag{3.4.1}$$

The solution of this optimization problem is simply the principal unit-norm eigenvector of the matrix

$$\mathbf{W} = (\mathbf{I}_P \otimes \mathbf{s}_k^H)\mathbf{U}_s\mathbf{U}_s^H(\mathbf{I}_P \otimes \mathbf{s}_k) \tag{3.4.2}$$

for low-rate users, or

$$\mathbf{W} = \sum_{m=0}^{M-1} (\mathbf{I}_P \otimes \mathbf{s}_{k_m}^H)\mathbf{U}_s\mathbf{U}_s^H(\mathbf{I}_P \otimes \mathbf{s}_{k_m}) \tag{3.4.3}$$

for high-rate users, where the virtual user k_m $(m = 0, \ldots, M-1)$ corresponds to the desired high-rate user. This implies that besides prior knowledge of the desire temporal signature, only an orthonormal basis of the signal subspace is required for the estimation of the desired spatial signature. As an alternative to high complexity batch EVD or SVD, adaptive subspace tracking algorithms with lower complexity, e.g., orthonormal PAST algorithm [108], can be employed to estimate an orthonormal basis of the signal subspace. The recursive orthonormal PAST algorithm updates the subspace in a sample-by-sample fashion, which can guarantee the orthogonality of matrix $\mathbf{U}_s$ at each iteration without attendant increase in computational complexity.

By following a similar line to [107], the adaptive algorithm for ST low-rate blind MMSE detection can be summarized as follows:

1. Estimation of an orthonormal basis of the signal subspace from $\mathbf{y}(j)$ using the orthonormal PAST algorithm;

2. Computation of matrix $\mathbf{W}$ via (3.4.2) or (3.4.3);

3. Estimation of the desired spatial signature using the simple power method [106];

4. Construction of the desired spatio-temporal signature;

5. Estimation of the ST low-rate blind MMSE detector based on the updated signal subspace and an intermediate variable of the orthonormal PAST algorithm.

The further details can be found in Table 3.1.

In a similar manner to its low-rate counterpart, the adaptive algorithm for ST high-rate blind MMSE detection can also be obtained easily, in which matrices

$$\mathbf{W} = \sum_{m=0}^{M-1} (\mathbf{I}_P \otimes \mathbf{s}_{k0}^{(m)^H}) \mathbf{U}_s^{(m)} \mathbf{U}_s^{(m)^H} (\mathbf{I}_P \otimes \mathbf{s}_{k0}^{(m)}) \tag{3.4.4}$$

and

$$\mathbf{W} = \sum_{m=0}^{M-1} (\mathbf{I}_P \otimes \mathbf{s}_{k1}^{H}) \mathbf{U}_s^{(m)} \mathbf{U}_s^{(m)^H} (\mathbf{I}_P \otimes \mathbf{s}_{k1}) \tag{3.4.5}$$

are used instead of (3.4.2) and (3.4.3), respectively.

3.5 Two-stage ST Dual-rate Blind Detectors

The ST dual-rate blind linear detectors can also operate at the output of a single antenna by using the temporal signatures instead of the corresponding spatio-temporal signatures in all associated equations. In this case, they are referred to as **purely temporal** dual-rate blind decorrelators and blind MMSE detectors. Their performances are surely inferior to their ST counterparts because angle diversity among all the users is not used. However, they need no estimation of the spatial signature. Moreover, the adaptive algorithms for purely temporal low-rate and high-rate blind MMSE detection will have a much faster convergence than their ST counterparts. This is because the signal subspace can be recursively estimated using the orthonormal PAST algorithm in much less iterations for the former than for the latter due to the smaller dimension of signal vector.

Rather than the adaptive ST dual-rate blind MMSE detectors employing joint spatial-temporal processing, **the basic idea of two-stage ST dual-rate blind detectors is to**

Table 3.1: The adaptive algorithm for ST low-rate blind MMSE detection

Update of the signal subspace using the orthonormal PAST algorithm, where α is a forgetting factor in (0,1]
$$\mathbf{r}(n) = \mathbf{U}_s^H(n-1)\mathbf{y}(n)$$
$$\mathbf{q}(n) = \frac{1}{\alpha}\mathbf{Z}(n-1)\mathbf{r}(n)$$
$$\gamma(n) = \frac{1}{1+\mathbf{r}^H(n)\mathbf{q}(n)}$$
$$\mathbf{p}(n) = \gamma(n)(\mathbf{y}(n) - \mathbf{U}_s(n-1)\mathbf{r}(n))$$
$$\tau(n) = \frac{1}{\|\mathbf{q}(n)\|^2}\left(\frac{1}{\sqrt{1+\|\mathbf{p}(n)\|^2\|\mathbf{q}(n)\|^2}} - 1\right)$$
$$\acute{\mathbf{p}}(n) = \tau(n)\mathbf{U}_s(n-1)\mathbf{q}(n) + (1+\tau(n)\|\mathbf{q}(n)\|^2)\mathbf{p}(n)$$
$$\mathbf{Z}(n) = \frac{1}{\alpha}\mathbf{Z}(n-1) - \gamma(n)\mathbf{q}(n)\mathbf{q}^H(n)$$
$$\mathbf{U}_s(n) = \mathbf{U}_s(n-1) + \acute{\mathbf{p}}(n)\mathbf{q}^H(n)$$
Update of the spatial signature using the power method
$$\mathbf{W}(n) = (\mathbf{I}_P \otimes \mathbf{s}_k^H)\mathbf{U}_s(n)\mathbf{U}_s^H(n)(\mathbf{I}_P \otimes \mathbf{s}_k)$$
$$\mathbf{a}(n) = \mathbf{W}(n)\mathbf{g}_k(n-1)$$
$$\mathbf{g}_k(n) = \frac{\mathbf{a}(n)}{\|\mathbf{a}(n)\|}$$
Update of the ST low-rate blind MMSE detector
$$\tilde{\mathbf{s}}_k(n) = \mathbf{g}_k(n) \otimes \mathbf{s}_k$$
$$\mathbf{d}_k(n) = \mathbf{U}_s(n)\mathbf{Z}(n)\mathbf{U}_s^H(n)\tilde{\mathbf{s}}_k(n)$$

cascade temporal processing and spatial processing. Our aim is to design some two-stage ST dual-rate blind detectors which are comparable to the corresponding adaptive ST dual-rate blind MMSE detectors. At the first stage of temporal processing, an adaptive purely temporal dual-rate blind MMSE detector for each element is a natural choice. Depending upon whether the adaptive purely temporal low-rate or high-rate blind MMSE detector is used at the first stage, it is referred to as two-stage ST low-rate or high-rate blind detector. Although the first stage has the same number of adaptive weights as the corresponding adaptive ST dual-rate blind MMSE detector, the former surely converges much faster than the latter due to its parallel structure. Based on the results in [107], the computational complexity of the former is comparable to that of the latter[1]. At the second stage, a non-adaptive beamformer based on the minimum variance distortionless response (MVDR) criterion is chosen as the spatial processor, since the MVDR beamformer is optimal in the sense that the output SINR is maximized [109]. For two-stage ST low-rate blind detector, the MVDR beamformer always operates at the low-rate symbol rate. For two-stage ST high-rate blind detector, it operates at the low-rate symbol rate for low-rate users while at the high-rate symbol rate for high-rate users.

It is well known that among the linear detectors, the MMSE detectors can maximize the output SINR [5]. Therefore, the two-stage ST dual-rate blind detectors, which combine the adaptive purely temporal dual-rate blind MMSE detectors and the MVDR beamformer, are reasonable counterparts to the adaptive ST dual-rate blind MMSE detectors. We take the two-stage ST low-rate blind detector as an example to see how it works. The

[1]For adaptive ST dual-rate blind MMSE detector, the computational complexity associated with the estimation of the desired spatial signature is not included.

soft output of the pth adaptive purely temporal low-rate blind MMSE detector can be represented by

$$e_k^p(j) = \mathbf{d}_k^{p^H} \mathbf{y}_p(j), \tag{3.5.1}$$

where $\mathbf{d}_k^p$ is a vector of filter tap weights for user k. Then the input of the MVDR beamformer is $\mathbf{e}_k(j) = [e_k^1(j), \ldots, e_k^P(j)]^T$, whose weights can be computed as [109]

$$\mathbf{w}_k = \frac{\mathbf{R}_k^{-1}\mathbf{g}_k}{\mathbf{g}_k^H \mathbf{R}_k^{-1}\mathbf{g}_k}, \tag{3.5.2}$$

where $\mathbf{R}_k = \mathbb{E}\{\mathbf{e}_k(j)\mathbf{e}_k^H(j)\}$. The desired spatial signature can be estimated using Capon's method [109]

$$\hat{\mathbf{g}}_k = \arg \max_{\|\mathbf{g}_k\|=1} \frac{1}{\mathbf{g}_k^H \mathbf{R}_k^{-1}\mathbf{g}_k}. \tag{3.5.3}$$

The solution of this optimization problem is the eigenvector corresponding to the minimal eigenvalue of $\mathbf{R}_k^{-1}$ or the maximal eigenvalue of $\mathbf{R}_k$. Since the number of antenna elements is generally small, the calculation of the beamformer weights is not computationally cumbersome.

3.6 Numerical Examples

The performances of the proposed ST and purely temporal dual-rate blind detectors have been investigated via numerical simulations. Assume that there are five low-rate users and five high-rate users in the system. User 1 is the desired low-rate user and user 6 is the desired high-rate user. A uniform linear array with two elements (spacing = $\frac{\lambda}{2}$) is considered. The spreading factor for high-rate users is 31, and the rate ratio is

2. Therefore, the spreading factor for low-rate users is 62. In order to eliminate any dependence of performance on the spatial-temporal signature correlations, the DOAs of all the users are randomly selected over $[0, 2\pi)$. Also, the binary temporal signatures are randomly generated where the assignment of the low-rate temporal signatures employs the repetition-code scheme [71]. 1500 realizations are used to generate all results.

Fig. 3.3 and Fig. 3.4 show the BER performances of ST dual-rate blind linear detectors and their purely temporal versions versus the near-far ratio[2] in the synchronous and asynchronous cases, respectively, where the SNR of the desired user is 8dB. In these simulations, batch EVD is used for subspace decomposition, and the desired spatial signature is assumed to be known. In the asynchronous case, user 1 and user 6 are chosen as the reference users for low-rate and high-rate blind linear detectors, respectively, and the delay for the kth rate i user is set to be γ_{ki} chips, where γ_{ki} is a randomly selected positive integer between 0 and $N_i - 1$. As proven in Proposition 3.2.2, in the synchronous case, the ST (purely temporal) low-rate blind decorrelator outperforms the ST (purely temporal) high-rate blind decorrelator for high-rate users and they offer the same performances for low-rate users. On the other hand, in the asynchronous case, the ST (purely temporal) low-rate blind decorrelator outperforms its high-rate counterpart for both low-rate and high-rate users. This implies that Proposition 3.3.2 is valid for asynchronous systems in most cases, due to the fact that the DOAs, the temporal signatures and the delays of all the users are randomly generated. In addition, it is obvious that the ST dual-rate blind linear detectors outperform the corresponding purely temporal counterparts, and

[2]Near-far ratio is defined as the power ratio of all the other users to the desired user.

the blind MMSE detectors are upper-bounded by the corresponding blind decorrelators.

In the synchronous case, the performances of ST dual-rate blind linear detectors are also compared to those of their single-rate counterparts proposed in [107]. In order to ensure a fair comparison, the spreading factor for single-rate system is chosen so that the total data rate (bits/s) is conserved in all systems, i.e.,

$$\frac{K_0}{T_0} + \frac{K_1}{T_1} = \frac{K_H}{T_{sr}}, \tag{3.6.1}$$

where $K_H = K_0 + K_1$ is the total number of users in any system, and T_{sr} is the spreading factor of the equivalent single-rate system. In Fig. 3.5, average probability of error over rates are used for dual-rate systems, and the results of non-blind dual-rate decorrelators [71] and single-user limits are also plotted. It is observed that all ST detectors are superior to non-blind dual-rate decorrelators. Furthermore, ST single-rate blind linear detector outperforms ST high-rate blind linear detector but is inferior to ST low-rate blind linear detector.

The performances of two-stage ST dual-rate blind detectors, adaptive ST dual-rate blind MMSE detectors as well as their purely temporal versions in the synchronous case are also evaluated. For the orthonormal PAST algorithm, the forgetting factor is set to be $\alpha = 0.9999$, and the matrix $\mathbf{U}_s$ is initialized to be a random orthonormal matrix. The BERs of adaptive ST dual-rate blind MMSE detectors and their purely temporal counterparts versus the number of iterations are plotted in Fig. 3.6, where the SNRs of all the users are 8dB. Obviously, the adaptive purely temporal dual-rate blind MMSE detectors converge much faster than their ST counterparts. This also means that the

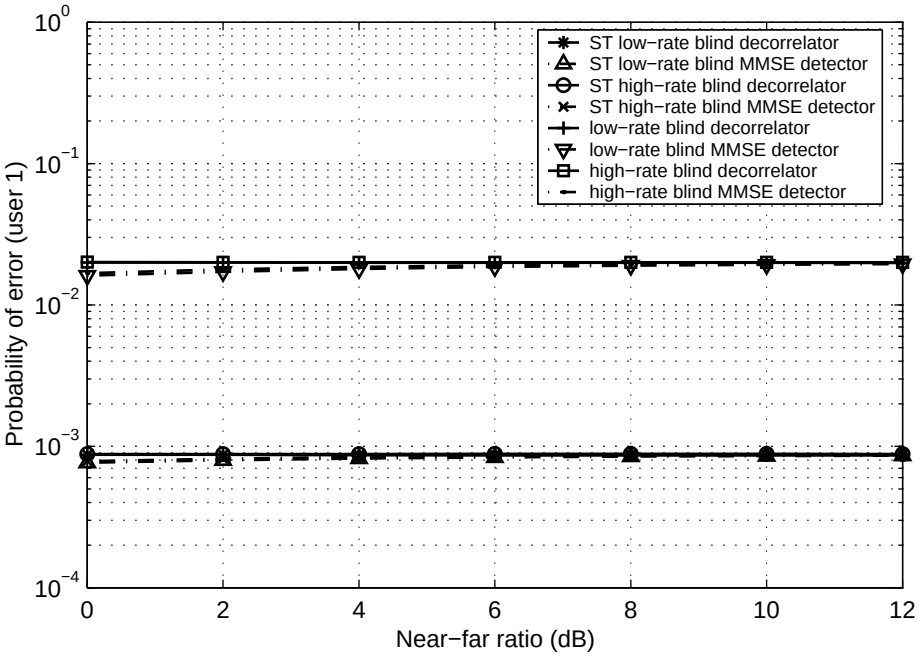

(a)

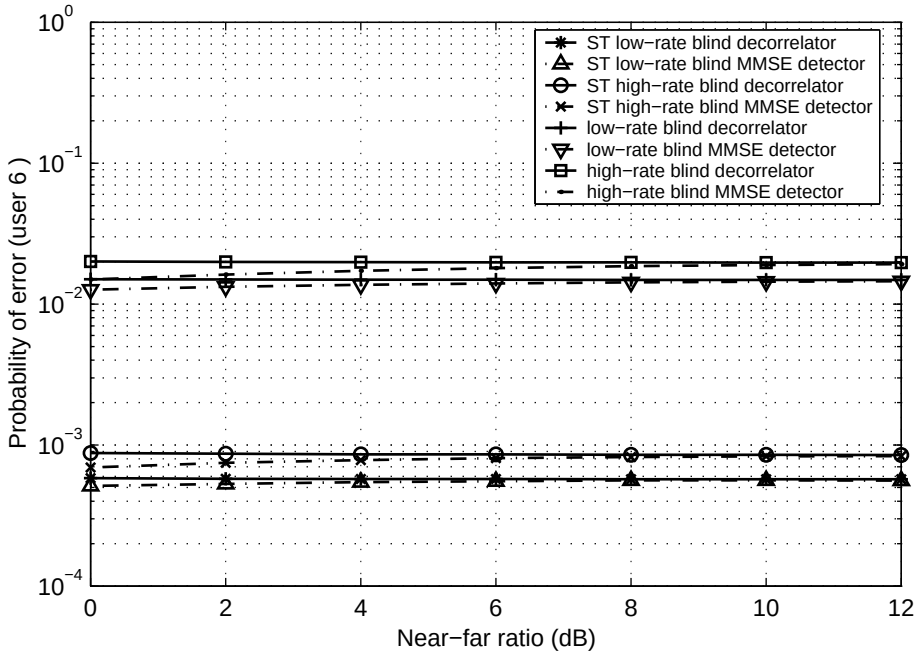

(b)

Figure 3.3: The BER performances of ST dual-rate blind linear detectors and their purely temporal versions for (a) the desired low-rate user and (b) the desired high-rate user in the synchronous case.

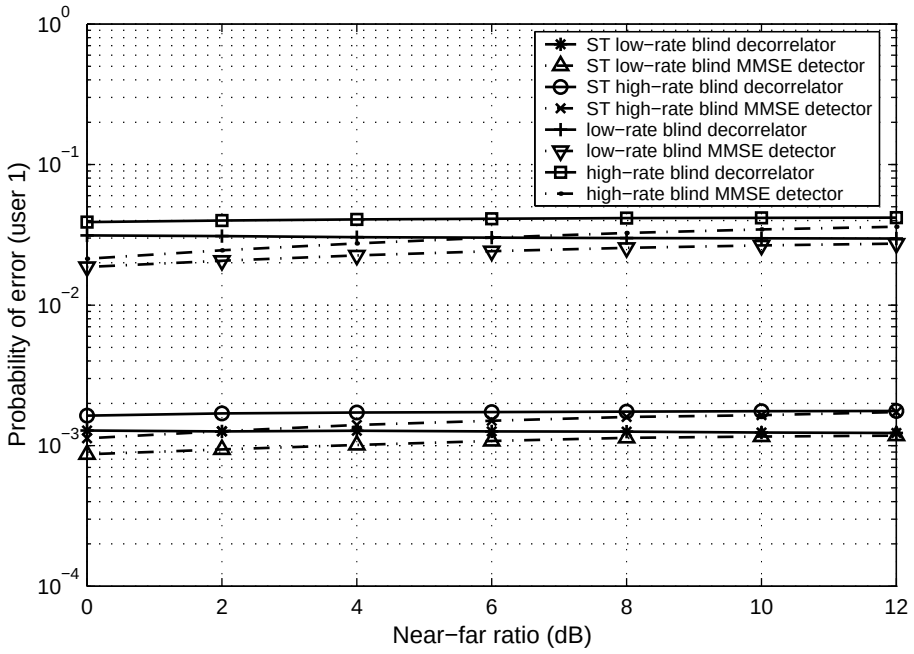

(a)

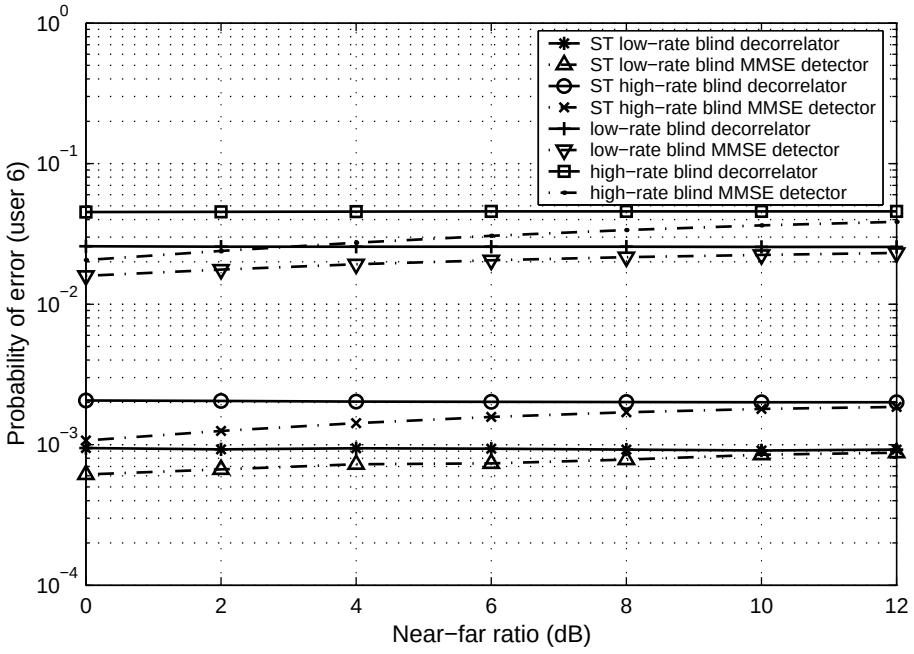

(b)

Figure 3.4: The BER performances of ST dual-rate blind linear detectors and their purely temporal versions for (a) the desired low-rate user and (b) the desired high-rate user in the asynchronous case.

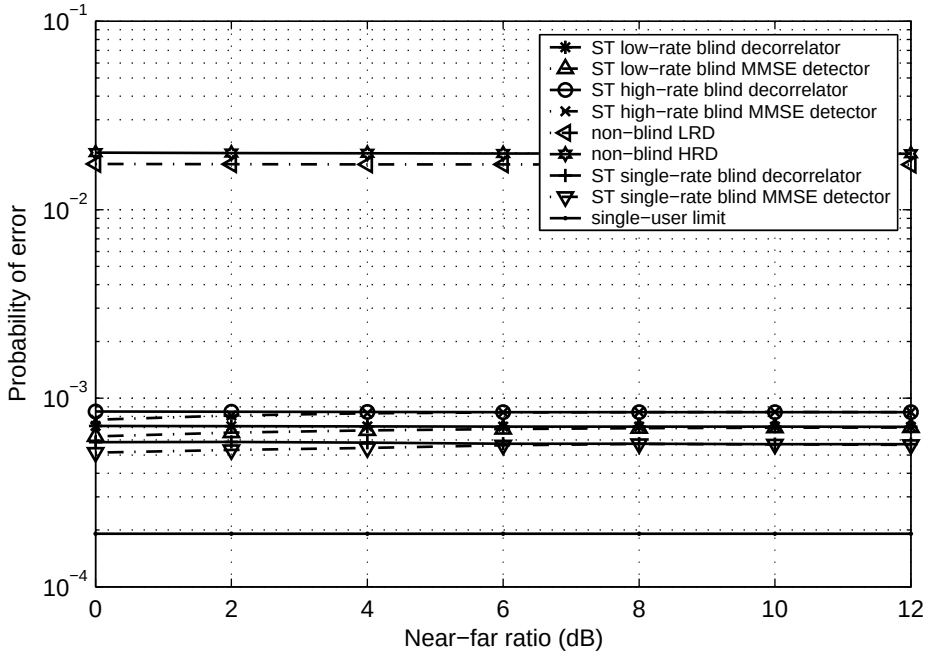

Figure 3.5: Performance comparison between ST dual-rate blind linear detectors and their single-rate counterparts in the synchronous case.

first stages of two-stage ST dual-rate blind detectors have faster convergence than the corresponding adaptive ST dual-rate blind MMSE detectors. Fig. 3.7 indicates the BERs of these dual-rate blind detectors versus the near-far ratio after the adaptive algorithms have converged, where the SNR of the desired user is 8dB. It is shown that the BER performances of adaptive ST dual-rate blind MMSE detectors are superior to those of the corresponding two-stage ST dual-rate blind detectors, while the latter outperform their purely temporal counterparts.

3.7 Summary

This chapter proposes the subspace-based time-invariant ST low-rate and high-rate blind linear detectors for synchronous DS/CDMA systems. It is shown that a) the ST low-rate blind linear detectors can support no less users than their high-rate rivals as long as the desired spatial signature is identifiable (assuming that all the other system parameters are same); b) the BER performance of ST low-rate blind decorrelator is not inferior to that of its high-rate counterpart. The asynchronous extension is also described. Finally, the two-stage ST dual-rate blind detectors, which combine the adaptive purely temporal dual-rate blind MMSE filters with the non-adaptive MVDR beamformer, are presented. Their adaptive stages with parallel structures converge much faster than the corresponding adaptive ST dual-rate blind MMSE detectors, while having a comparable computational complexity to the latter.

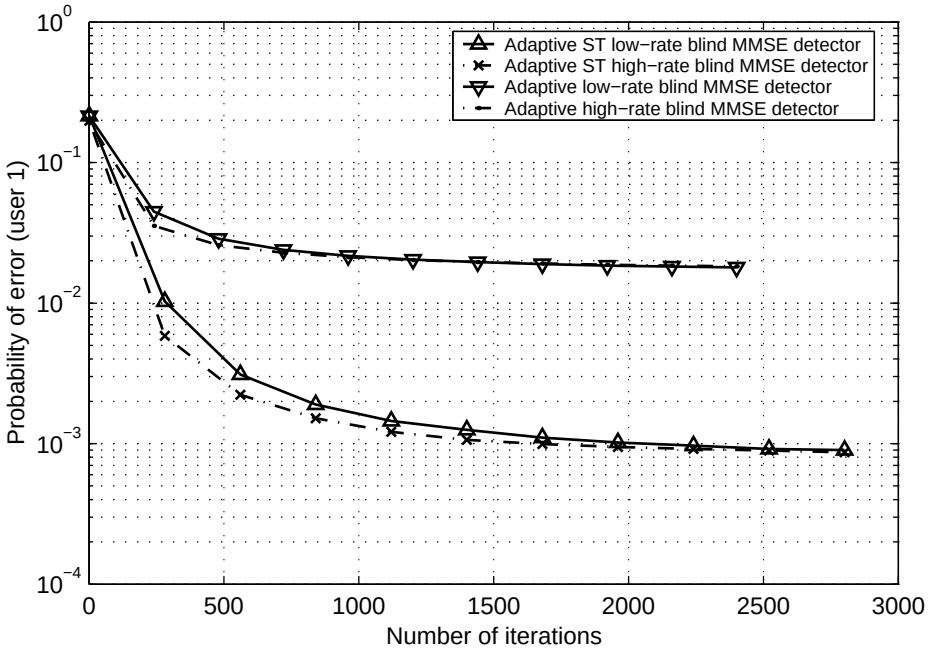

(a)

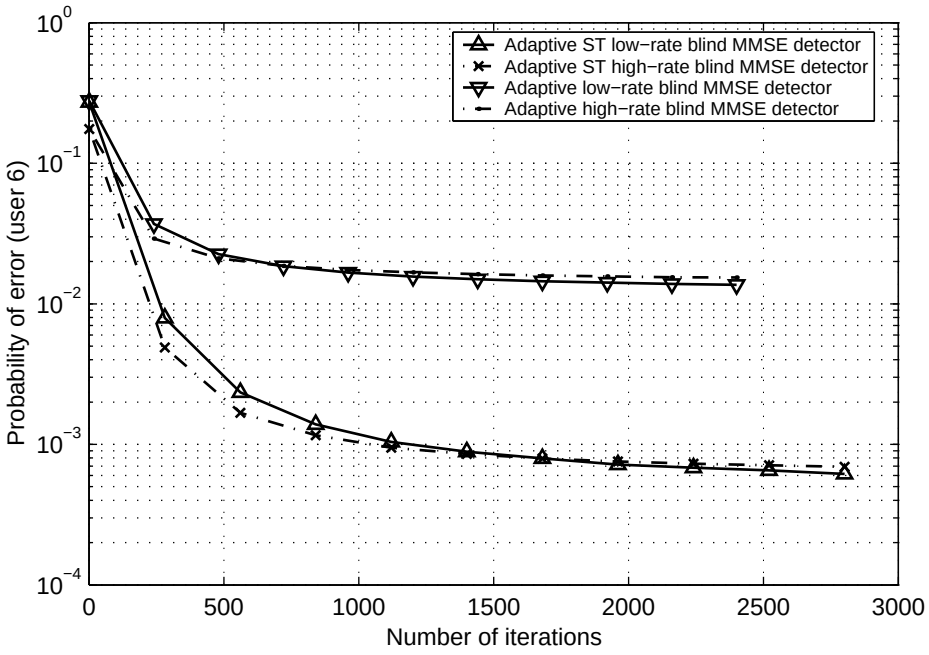

(b)

Figure 3.6: The convergence performances of adaptive ST dual-rate blind MMSE detectors and their purely temporal versions for (a) the desired low-rate user and (b) the desired high-rate user.

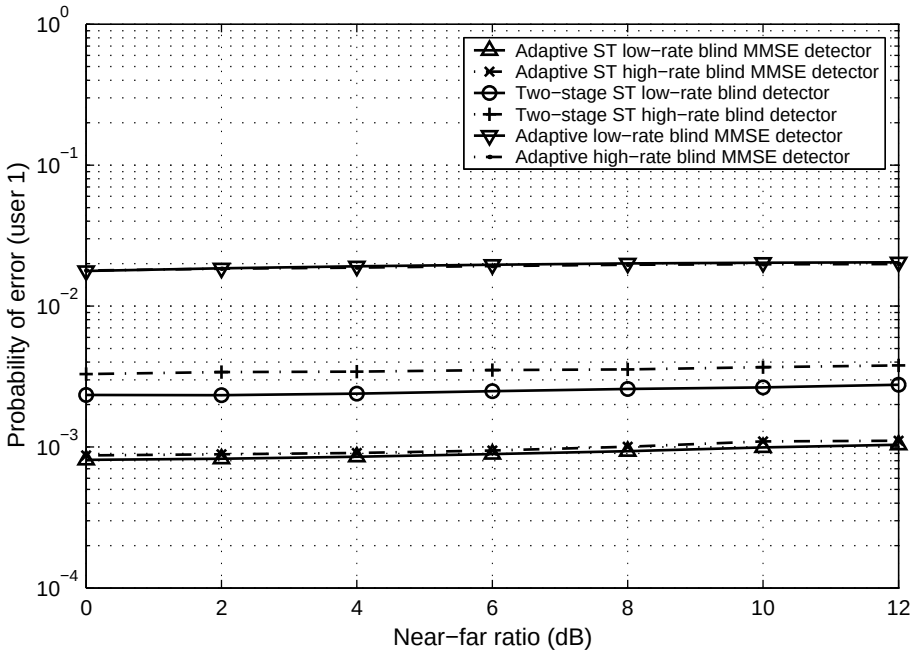

(a)

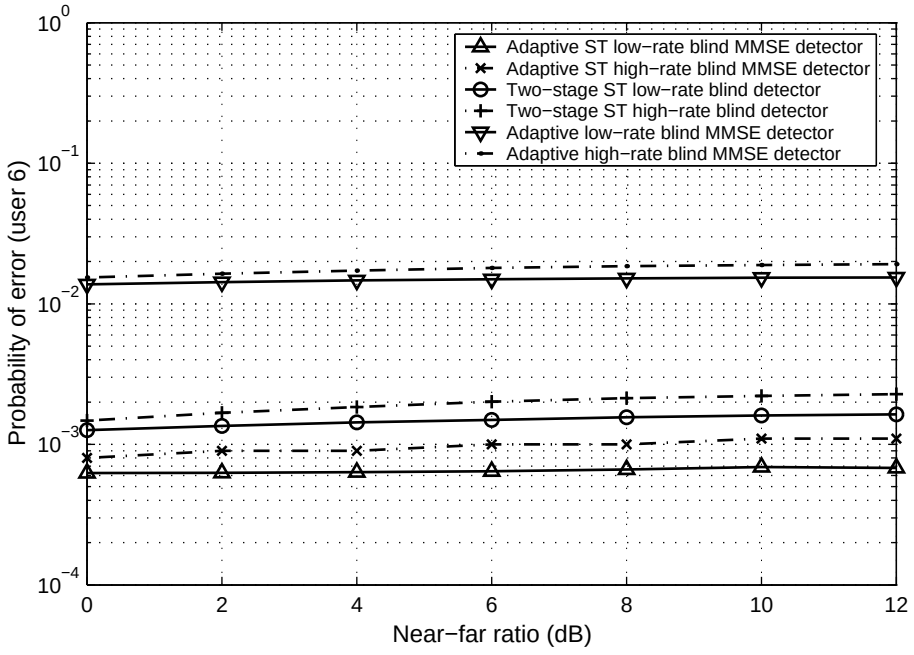

(b)

Figure 3.7: The BER performances of adaptive ST dual-rate blind MMSE detectors, two-stage ST dual-rate blind detectors, and their purely temporal versions for (a) the desired low-rate user and (b) the desired high-rate user.

Chapter 4

Blind Channel Estimation in Dual-rate DS/CDMA Systems

Chapter 3 handles the application of blind techniques for ST multiuser detection to multi-rate DS/CDMA systems over the ideal AWGN channels. Unfortunately, in practice, multi-rate CDMA signals experience multipath fading channels. Furthermore, as described in Chapter 2, they suffer much more severe ISI than their single-rate counterparts.

For multipath fading channels, the design of multi-rate blind multiuser detectors without channel estimation is possible. Such dual-rate blind multiuser detectors were proposed in [91] by applying the MOE criterion. However, this constrained optimization approach only deals with the case where the delay spread is only a small fraction of the symbol period. Moreover, their performances degrade significantly at low SNR.

Alternatively, the channel can be estimated before the multiuser detection process. To this end, the subspace-based blind approaches for channel estimation and multiuser detection in multi-rate DS/CDMA systems have been investigated in [95] and [96], which can handle the case of a large delay spread. In both papers, the basic-rate blind channel

estimators and multiuser detectors are taken into account. However, they have higher computational complexity and do not make full use of the nature of dual-rate signals.

This chapter proposes the subspace-based low-rate and high-rate blind channel estimation algorithms for asynchronous dual-rate DS/CDMA. Compared to the above two works, this work is carried out independently and simultaneously. Especially, the proposed dual-rate blind channel estimation schemes can be implemented adaptively. Moreover, the dual-rate blind MMSE detection for the AWGN channels proposed in Chapter 3 can be extended to frequency-selective multipath channels.

This chapter is organized as follows. In Section 4.1, signal models for an asynchronous dual-rate system over a frequency-selective multipath channel are established. Section 4.2 proposes low-rate and high-rate blind channel estimation schemes. Section 4.3 addresses adaptive algorithms for dual-rate blind channel estimation. The dual-rate blind MMSE detection is presented in Section 4.4. Simulation results are described in Section 4.5. Section 4.6 gives some concluding remarks. Most results in this chapter can also be found in [56] and [60].

4.1 Signal Models

Let us consider an asynchronous VSF dual-rate DS/CDMA system over a frequency selective multipath channel, in which the rate ratio M is an integer greater than 1. As for the notation used below, unless otherwise stated, please refer to Sections 1.6 and 2.2.

At the receiver, in accordance with (2.2.1) and (2.2.2), the received complex baseband

signal is

$$y(t) = \sum_{k=1}^{K_0} \sum_{j=-\infty}^{\infty} A_{k0} b_{k0}(j) s_{k0}(t - jT_0) + \sum_{k=1}^{K_1} \sum_{j=-\infty}^{\infty} \sum_{m=0}^{M-1} A_{k1} b_{k1}(jM + m) s_{k1}(t - jT_0 - mT_1) + z(t), \tag{4.1.1}$$

where

$$s_{ki}(t) = \sum_{l=1}^{N_i} c_{ki}(l) h_{ki}(t - lT_c), \ i = 0, 1, \tag{4.1.2}$$

is the effective spreading waveform for user ki. $c_{ki}(l)$ $(l = 1, \ldots, N_i)$ is the preassigned spreading code for user ki. $h_{ki}(t)$ is the composite channel for user ki, which represents the effects of the fixed transmit/receive pulse shaping filters and the unknown multipath physical channel, and can be modelled as an FIR filter for practical purposes [68].

Sampling the received signal at chip rate, we obtain the discrete-time signal model

$$y(n) = \sum_{k=1}^{K_0} \underbrace{\sum_{j=-\infty}^{\infty} A_{k0} b_{k0}(j) s_{k0}(n - jN_0)}_{y_{k0}(n)} + \sum_{k=1}^{K_1} \underbrace{\sum_{j=-\infty}^{\infty} \sum_{m=0}^{M-1} A_{k1} b_{k1}(jM + m) s_{k1}(n - jN_0 - mN_1)}_{y_{k1}(n)} + z(n), \tag{4.1.3}$$

where

$$s_{ki}(n) = \sum_{l=1}^{N_i} c_{ki}(l) h_{ki}(n - l), \ i = 0, 1, \tag{4.1.4}$$

and $z(n)$ is a complex AWGN sequence with variance σ_z^2. For clarity of presentation, we assume that all the users have the same channel order L and $L < N_0$. Thus $s_{ki}(n)$ has a support equal to $N_i + L$. Note that the channel length in symbol periods for rate i users is

$L_{si} \triangleq \lceil (N_i + L)/N_i \rceil$, where $\lceil x \rceil$ is the smallest integer greater than or equal to x. Clearly, $L_{s0} = 2$. We denote the effective spreading sequence with length $L_{si}N_i$ for user ki to be

$$\mathbf{s}_{ki} = [s_{ki}(1), \ldots, s_{ki}(N_i + L), 0, \ldots, 0]^T, \ i = 0, 1. \tag{4.1.5}$$

In the light of (4.1.4), (4.1.5) can further be written as

$$\mathbf{s}_{ki} = \underbrace{\begin{bmatrix} c_{ki}(1) & & \mathbf{0} \\ \vdots & \ddots & \\ c_{ki}(N_i) & & c_{ki}(1) \\ & \ddots & \vdots \\ & & c_{ki}(N_i) \\ & \mathbf{0} & \end{bmatrix}}_{\mathbf{C}_{ki}} \underbrace{\begin{bmatrix} h_{ki}(0) \\ \vdots \\ h_{ki}(L) \end{bmatrix}}_{\mathbf{h}_{ki}}. \tag{4.1.6}$$

Matrix $\mathbf{C}_{ki}$ can be divided into L_{si} sub-matrices with dimension $N_i \times (L+1)$, i.e., $\mathbf{C}_{ki} = [\mathbf{C}_{ki}^H(1), \ldots, \mathbf{C}_{ki}^H(L_{si})]^H$. Our aim is to estimate the composite channel vector $\mathbf{h}_{ki}$ from the observation $y(n)$, only with the prior knowledge of $c_{ki}(l)$ $(l = 1, \ldots, N_i)$. The low-rate and high-rate signal models will be established below.

4.1.1 Low-rate Signal Model

In order to mitigate the effect of ISI, a processing interval of P_0 low-rate symbol periods should be considered for low-rate signal modelling (See Fig. 4.1). P_0 is termed as **low-rate smoothing factor**.

For user $k0$, collecting the chip-rate samples within an interval of P_0T_0 yields $\mathbf{y}_{k0}(j) = [y_{k0}(jN_0), \ldots, y_{k0}((j + P_0)N_0 - 1)]^T$, which can be represented as

$$\mathbf{y}_{k0}(j) = A_{k0}\mathbf{S}_{k0}\mathbf{H}_{k0}\mathbf{b}_{k0}(j), \tag{4.1.7}$$

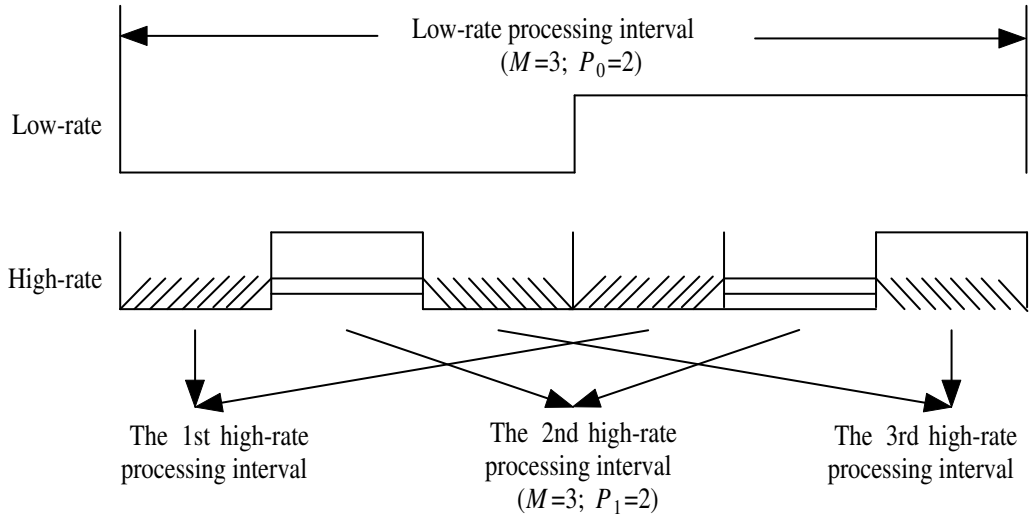

Figure 4.1: The low-rate and high-rate processing intervals

where

$$\mathbf{S}_{k0} = \underbrace{\begin{bmatrix} \mathbf{C}_{k0}(2) & \mathbf{C}_{k0}(1) & & \\ & \ddots & \ddots & \\ & & \mathbf{C}_{k0}(2) & \mathbf{C}_{k0}(1) \end{bmatrix}}_{P_0 N_0 \times (P_0+1)(L+1)}, \tag{4.1.8}$$

$$\mathbf{H}_{k0} = \underbrace{\begin{bmatrix} \mathbf{h}_{k0} & & \\ & \ddots & \\ & & \mathbf{h}_{k0} \end{bmatrix}}_{P_0+1 \text{ blocks}}, \tag{4.1.9}$$

and

$$\mathbf{b}_{k0}(j) = [b_{k0}(j-1), \ldots, b_{k0}(j+P_0-1)]^T. \tag{4.1.10}$$

Furthermore, for each high-rate user, there are $\widetilde{L}_{s1} = M + L_{s1} - 1$ data bits presenting within a low-rate symbol period. Using Matlab notation, we define

- the $2N_0 \times (L+1)$ matrix

$$\hat{\mathbf{C}}_{k1} = \begin{bmatrix} \mathbf{C}_{k1} \\ \mathbf{0} \end{bmatrix};$$

- for $l = 1, \ldots, \widetilde{L}_{s1}$, $\widetilde{\mathbf{C}}_{k1}(l) = \widetilde{\mathbf{C}}_{k1}^{(l)}(1 : N_0, :)$, where

$$\widetilde{\mathbf{C}}_{k1}^{(l)} = \begin{cases} \check{\mathbf{D}}^{(M-l)N_1} \hat{\mathbf{C}}_{k1}, & \text{if } l \le M; \\ \hat{\mathbf{D}}^{(\widetilde{L}_{s1}-l+1)N_1} \hat{\mathbf{C}}_{k1}, & \text{otherwise.} \end{cases} \tag{4.1.11}$$

  Here the shift-down matrix $\check{\mathbf{D}}$ with dimension $2N_0 \times 2N_0$ has all zero entries except 1's in the first lower diagonal, and $\hat{\mathbf{D}} = \check{\mathbf{D}}^T$ and thus a shift-up matrix;

- $\widetilde{\mathbf{C}}_{k1} \triangleq [\widetilde{\mathbf{C}}_{k1}^H(1), \ldots, \widetilde{\mathbf{C}}_{k1}^H(\widetilde{L}_{s1})]^H$.

Then the received signal due to user $k1$ within the above low-rate processing interval can be given by

$$\mathbf{y}_{k1}(j) = A_{k1} \widetilde{\mathbf{S}}_{k1} \widetilde{\mathbf{H}}_{k1} \mathbf{b}_{k1}(j), \tag{4.1.12}$$

where

$$\widetilde{\mathbf{S}}_{k1} = \underbrace{\begin{bmatrix} \widetilde{\mathbf{C}}_{k1}(\widetilde{L}_{s1}) & & \cdots & \widetilde{\mathbf{C}}_{k1}(1) & & \\ & \underbrace{\mathbf{0}, \ldots, \mathbf{0}}_{M-1} & \widetilde{\mathbf{C}}_{k1}(\widetilde{L}_{s1}) & \cdots & \widetilde{\mathbf{C}}_{k1}(1) & \\ & & \ddots & & & \ddots \\ & & & \underbrace{\mathbf{0}, \ldots, \mathbf{0}}_{M-1} & \widetilde{\mathbf{C}}_{k1}(\widetilde{L}_{s1}) & \cdots & \widetilde{\mathbf{C}}_{k1}(1) \end{bmatrix}}_{P_0 N_0 \times (P_0 M - M + \widetilde{L}_{s1})(L+1)}, \tag{4.1.13}$$

$$\widetilde{\mathbf{H}}_{k1} = \underbrace{\begin{bmatrix} \mathbf{h}_{k1} & & \\ & \ddots & \\ & & \mathbf{h}_{k1} \end{bmatrix}}_{P_0 M - M + \widetilde{L}_{s1} \text{ blocks}}, \tag{4.1.14}$$

and

$$\mathbf{b}_{k1}(j) = [b_{k1}(jM - L_{s1} + 1), \ldots, b_{k1}((j + P_0)M - 1)]^T. \tag{4.1.15}$$

If we introduce the following notations:

$$\begin{aligned}
\mathbf{G}_{k0} &= A_{k0}\mathbf{S}_{k0}\mathbf{H}_{k0}, \\
\widetilde{\mathbf{G}}_{k1} &= A_{k1}\widetilde{\mathbf{S}}_{k1}\widetilde{\mathbf{H}}_{k1}, \\
\mathbf{G} &= [\mathbf{G}_{10}, \ldots, \mathbf{G}_{K_0 0}, \widetilde{\mathbf{G}}_{11}, \ldots, \widetilde{\mathbf{G}}_{K_1 1}],
\end{aligned}$$

and

$$\mathbf{b}(j) = [\mathbf{b}_{10}^T(j), \ldots, \mathbf{b}_{K_0 0}^T(j), \mathbf{b}_{11}^T(j), \ldots, \mathbf{b}_{K_1 1}^T(j)]^T,$$

then the resulting received signal within the above low-rate processing interval is

$$\begin{aligned}
\mathbf{y}(j) &= \sum_{k=1}^{K_0} \mathbf{y}_{k0}(j) + \sum_{k=1}^{K_1} \mathbf{y}_{k1}(j) + \mathbf{z}(j) \\
&= \mathbf{G}\mathbf{b}(j) + \mathbf{z}(j),
\end{aligned} \tag{4.1.16}$$

where $\mathbf{z}(j)$ is the corresponding noise vector. A data matrix is formed by concatenating the received signal vectors

$$\begin{aligned}
\mathbf{Y} &= [\mathbf{y}(j), \ldots, \mathbf{y}(j + J_0 - P_0)] \\
&= \mathbf{G}\underbrace{[\mathbf{b}(j), \ldots, \mathbf{b}(j + J_0 - P_0)]}_{\mathbf{B}} + \underbrace{[\mathbf{z}(j), \ldots, \mathbf{z}(j + J_0 - P_0)]}_{\mathbf{Z}}.
\end{aligned} \tag{4.1.17}$$

4.1.2 High-rate Signal Model

For high-rate signal modelling, M processing intervals should be considered. As shown in Fig. 4.1, the mth high-rate processing interval consists of all the mth high-rate bit durations of P_1 successive low-rate symbol periods, where P_1 is referred to as **high-rate smoothing factor**.

For user $k0$, we denote $\mathbf{C}_{k0}^{(m)} \triangleq [\mathbf{C}_{k0}^{(m)^H}(1), \mathbf{C}_{k0}^{(m)^H}(2)]^H$, where $\mathbf{C}_{k0}^{(m)}(l) = \mathbf{C}_{k0}(l)(mN_1 + 1 : (m+1)N_1, :),\ l = 1, 2$. Collecting the chip-rate samples within the mth high-rate processing interval yields $\mathbf{y}_{k0}^{(m)}(j) = [y_{k0}(jN_0 + mN_1), \ldots, y_{k0}(jN_0 + (m+1)N_1 - 1), \ldots, y_{k0}((j + P_1 - 1)N_0 + mN_1), \ldots, y_{k0}((j + P_1 - 1)N_0 + (m+1)N_1 - 1)]^T$, which can be written as

$$\mathbf{y}_{k0}^{(m)}(j) = A_{k0}\mathbf{S}_{k0}^{(m)}\mathbf{H}_{k0}\mathbf{b}_{k0}(j), \tag{4.1.18}$$

where

$$\mathbf{S}_{k0}^{(m)} = \underbrace{\begin{bmatrix} \mathbf{C}_{k0}^{(m)}(2) & \mathbf{C}_{k0}^{(m)}(1) & & \\ & \ddots & \ddots & \\ & & \mathbf{C}_{k0}^{(m)}(2) & \mathbf{C}_{k0}^{(m)}(1) \end{bmatrix}}_{P_1N_1 \times (P_1+1)(L+1)}. \tag{4.1.19}$$

Note that for each low-rate user, the actual number of data bits present within the mth high-rate processing interval might change with the index m. If $0 \leq m < L_{s1} - 1$, the actual number of data bits is $P_1 + 1$; otherwise P_1.

The received signal due to user $k1$ within the mth high-rate processing interval can be written as

$$\mathbf{y}_{k1}^{(m)}(j) = A_{k1}\mathbf{S}_{k1}\mathbf{H}_{k1}\mathbf{b}_{k1}^{(m)}(j), \tag{4.1.20}$$

where

$$\mathbf{S}_{k1} = \underbrace{\begin{bmatrix} \mathbf{C}_{k1}(L_{s1}) & & \cdots & \mathbf{C}_{k1}(1) & & \\ & \underbrace{\mathbf{0},\ldots,\mathbf{0}}_{M-1} & \mathbf{C}_{k1}(L_{s1}) & \cdots & \mathbf{C}_{k1}(1) & \\ & & \ddots & & \ddots & \\ & & & \underbrace{\mathbf{0},\ldots,\mathbf{0}}_{M-1} & \mathbf{C}_{k1}(L_{s1}) & \cdots & \mathbf{C}_{k1}(1) \end{bmatrix}}_{P_1N_1\times(P_1M-M+L_{s1})(L+1)}, \tag{4.1.21}$$

$$\mathbf{H}_{k1} = \underbrace{\begin{bmatrix} \mathbf{h}_{k1} & & \\ & \ddots & \\ & & \mathbf{h}_{k1} \end{bmatrix}}_{P_1M-M+L_{s1}\ \text{blocks}}, \tag{4.1.22}$$

and

$$\mathbf{b}_{k1}^{(m)}(j) = [b_{k1}(jM+m-L_{s1}+1),\ldots,b_{k1}((j+P_1-1)M+m)]^T. \tag{4.1.23}$$

Note that for each high-rate user, the actual number of data bits presenting within each high-rate processing interval depends on the values of M and L_{s1}. If $L_{s1} \geq M$, the actual number of data bits is $P_1M - M + L_{s1}$; otherwise P_1L_{s1}.

If we introduce the following notations:

$$\begin{aligned} \mathbf{G}_{k0}^{(m)} &= A_{k0}\mathbf{S}_{k0}^{(m)}\mathbf{H}_{k0}, \\ \mathbf{G}_{k1} &= A_{k1}\mathbf{S}_{k1}\mathbf{H}_{k1}, \\ \mathbf{G}^{(m)} &= [\mathbf{G}_{10}^{(m)},\ldots,\mathbf{G}_{K_00}^{(m)},\mathbf{G}_{11},\ldots,\mathbf{G}_{K_11}], \\ \mathbf{b}^{(m)}(j) &= [\mathbf{b}_{10}^T(j),\ldots,\mathbf{b}_{K_00}^T(j),\mathbf{b}_{11}^{(m)^T}(j),\ldots,\mathbf{b}_{K_11}^{(m)^T}(j)]^T, \end{aligned}$$

then the resulting received signal within the mth high-rate processing interval is

$$\mathbf{y}^{(m)}(j) = \mathbf{G}^{(m)}\mathbf{b}^{(m)}(j) + \mathbf{z}^{(m)}(j), \tag{4.1.24}$$

where $\mathbf{z}^{(m)}(j)$ is the corresponding noise vector. The data matrix can be formed by

$$\begin{aligned}\mathbf{Y}^{(m)} &= [\mathbf{y}^{(m)}(j), \ldots, \mathbf{y}^{(m)}(j + J_1 - P_1)] \\ &= \mathbf{G}^{(m)} \underbrace{[\mathbf{b}^{(m)}(j), \ldots, \mathbf{b}^{(m)}(j + J_1 - P_1)]}_{\mathbf{B}^{(m)}} + \underbrace{[\mathbf{z}^{(m)}(j), \ldots, \mathbf{z}^{(m)}(j + J_1 - P_1)]}_{\mathbf{Z}^{(m)}}.\end{aligned} \tag{4.1.25}$$

4.2 Dual-rate Blind Channel Estimation

Based on the above signal models, this section develops the low-rate and high-rate blind channel estimators for dual-rate DS/CDMA by exploiting the subspaces of $\mathbf{Y}$ and $\mathbf{Y}^{(m)}$ that contain the relevant channel information due to (4.1.17) and (4.1.25).

4.2.1 Low-rate Blind Channel Estimation

We first consider the noise free case. As in the standard subspace algorithm, a subspace decomposition can be performed on $\mathbf{Y}$ by an SVD

$$\mathbf{Y} = \begin{bmatrix}\mathbf{U}_s & \mathbf{U}_n\end{bmatrix} \begin{bmatrix}\mathbf{\Lambda}_s & \mathbf{0} \\ \mathbf{0} & \mathbf{0}\end{bmatrix} \begin{bmatrix}\mathbf{V}_s^H \\ \mathbf{V}_n^H\end{bmatrix}, \tag{4.2.1}$$

where the vectors in $\mathbf{U}_s$, associated with the singular values in diagonal matrix $\mathbf{\Lambda}_s$, span the signal subspace defined by the columns of $\mathbf{G}$, whereas the vectors in $\mathbf{U}_n$, associated with the zero singular values, span the orthogonal complement of $\mathbf{U}_s$ (and hence of $\mathbf{G}$). The dimension of the signal subspace is $d_s = K_0(P_0 + 1) + K_1(P_0 M - M + \widetilde{L}_{s1})$, and that of its orthogonal complement is $d_n = P_0 N_0 - d_s$. In order to achieve blind identifiability, we assume that $\mathbf{B}$ is full row rank and $\mathbf{G}$ is full column rank [27]. This means that the values of J_0 and P_0 need to be carefully specified.

For convenience of presentation, let us define $\mathbf{U}_n = [\mathbf{U}_n^H(1), \ldots, \mathbf{U}_n^H(P_0)]^H$ and $\mathbf{U}_s = [\mathbf{U}_s^H(1), \ldots, \mathbf{U}_s^H(P_0)]^H$, where $\mathbf{U}_n(p)$ and $\mathbf{U}_s(p)$ $(p = 1, \ldots, P_0)$ are $N_0 \times d_n$ and $N_0 \times d_s$ sub-matrices, respectively. Since $\mathbf{U}_n$ is orthogonal to the columns of $\mathbf{G}$, we have

$$\mathbf{U}_n^H \mathbf{G}_{k0} = \mathbf{0}, \tag{4.2.2}$$

and

$$\mathbf{U}_n^H \widetilde{\mathbf{G}}_{k1} = \mathbf{0}. \tag{4.2.3}$$

For user $k0$, substituting $\mathbf{G}_{k0} = A_{k0}\mathbf{S}_{k0}\mathbf{H}_{k0}$ into (4.2.2), we have

$$\mathbf{U}_n^H \mathbf{S}_{k0} \mathbf{H}_{k0} = \mathbf{0}, \tag{4.2.4}$$

which can be rewritten as

$$\mathbf{Q}_0^H \mathbf{C}_{k0} \mathbf{h}_{k0} = \mathbf{0}, \tag{4.2.5}$$

where

$$\mathbf{Q}_0 = \underbrace{\begin{bmatrix} \mathbf{U}_n(P_0) & \ldots & \mathbf{U}_n(1) & \\ & \mathbf{U}_n(P_0) & \ldots & \mathbf{U}_n(1) \end{bmatrix}}_{2N_0 \times (P_0+1)d_n}. \tag{4.2.6}$$

Equation (4.2.5) yields a set of $(P_0+1)d_n$ linear equations with $(L+1)$ unknown variables. To determine $\mathbf{h}_{k0}$ up to a scalar, a necessary condition is

$$(P_0 + 1)d_n \geq L. \tag{4.2.7}$$

In the presence of noise, since only a perturbed version of $\mathbf{Q}_0$ can be obtained, (4.2.5) can be replaced by the least-squares criterion [107]

$$\hat{\mathbf{h}}_{k0} = \arg \min_{\|\mathbf{h}_{k0}\|=1} \mathbf{h}_{k0}^H \mathbf{C}_{k0}^H \mathbf{Q}_0 \mathbf{Q}_0^H \mathbf{C}_{k0} \mathbf{h}_{k0}. \tag{4.2.8}$$

The solution of this optimization problem is the eigenvector corresponding to the minimum eigenvalue of $\mathbf{C}_{k0}^H \mathbf{Q}_0 \mathbf{Q}_0^H \mathbf{C}_{k0}$.

Similarly, for user $k1$, substituting $\widetilde{\mathbf{G}}_{k1} = A_{k1}\widetilde{\mathbf{S}}_{k1}\widetilde{\mathbf{H}}_{k1}$ into (4.2.3), we have

$$\mathbf{U}_n^H \widetilde{\mathbf{S}}_{k1} \widetilde{\mathbf{H}}_{k1} = \mathbf{0}, \tag{4.2.9}$$

of which an alternative form is

$$\mathbf{Q}_1^H \widetilde{\mathbf{C}}_{k1} \mathbf{h}_{k1} = \mathbf{0}, \tag{4.2.10}$$

where

$$\mathbf{Q}_1 = \underbrace{\begin{bmatrix} \mathbf{U}_n(P_0) & \dots & \mathbf{U}_n(2) & \underbrace{\mathbf{0}, \dots, \mathbf{0}}_{M-1} & \mathbf{U}_n(1) & & \\ & \ddots & & & & \ddots & \\ & & \mathbf{U}_n(P_0) & \dots & \mathbf{U}_n(2) & \underbrace{\mathbf{0}, \dots, \mathbf{0}}_{M-1} & \mathbf{U}_n(1) \end{bmatrix}}_{\widetilde{L}_{s1}N_0 \times (P_0 M - M + \widetilde{L}_{s1})d_n}. \tag{4.2.11}$$

Equation (4.2.10) yields a set of $(P_0 M - M + \widetilde{L}_{s1})d_n$ linear equations, and thus a necessary condition for determining $\mathbf{h}_{k1}$ up to a scalar is

$$(P_0 M - M + \widetilde{L}_{s1})d_n \geq L. \tag{4.2.12}$$

Also, it is easy to see from (4.2.10) that in the least-squares sense, the estimate $\hat{\mathbf{h}}_{k1}$ of $\mathbf{h}_{k1}$ can be obtained as the eigenvector corresponding to the minimum eigenvalue of $\widetilde{\mathbf{C}}_{k1}^H \mathbf{Q}_1 \mathbf{Q}_1^H \widetilde{\mathbf{C}}_{k1}$.

4.2.2 High-rate Blind Channel Estimation

Similar to its low-rate counterpart, for the high-rate blind channel estimator, an SVD can be performed on $\mathbf{Y}^{(m)}$, and then $\mathbf{U}_s^{(m)}$, whose columns span the signal subspace, and

$\mathbf{U}_n^{(m)}$, whose columns span the orthogonal complement of $\mathbf{U}_s^{(m)}$, can be obtained. The dimension of the signal subspace is $d_s^{(m)}$, which is equal to the actual number of data bits presenting within the mth high-rate processing interval. From our previous analysis in Section 4.1, it can be seen that $d_s^{(m)}$ might change with the index m and has a maximum of $K_0(P_1+1)+K_1(PM-M+L_{s1})$. The dimension of the orthogonal complement of the signal subspace is $d_n^{(m)}=P_1N_1-d_s^{(m)}$. In order to achieve blind identifiability, we assume that matrix $\mathbf{G}^{(m)}$ has full column rank, and matrix $\mathbf{B}^{(m)}$ is of full row rank [27]. As a result, the values of J_1 and P_1 need to be carefully specified.

Let $\mathbf{U}_n^{(m)}=[\mathbf{U}_n^{(m)^H}(1),\ldots,\mathbf{U}_n^{(m)^H}(P_1)]^H$, where $\mathbf{U}_n^{(m)}(p)$ $(p=1,\ldots,P_1)$ are $N_1\times d_n^{(m)}$ sub-matrices. For user $k0$, we can derive

$$\mathbf{Q}_0^{(m)^H}\mathbf{C}_{k0}^{(m)}\mathbf{h}_{k0}=\mathbf{0} \tag{4.2.13}$$

from

$$\mathbf{U}_n^{(m)^H}\mathbf{S}_{k0}^{(m)}\mathbf{H}_{k0}=\mathbf{0}, \tag{4.2.14}$$

where

$$\mathbf{Q}_0^{(m)}=\underbrace{\begin{bmatrix}\mathbf{U}_n^{(m)}(P_1) & \ldots & \mathbf{U}_n^{(m)}(1) & \\ & \mathbf{U}_n^{(m)}(P_1) & \ldots & \mathbf{U}_n^{(m)}(1)\end{bmatrix}}_{2N_1\times(P_1+1)d_n^{(m)}}. \tag{4.2.15}$$

Considering that channel information of each low-rate user spans one complete low-rate symbol period, in the least-squares sense, (4.2.13) can be solved by the following optimization problem

$$\hat{\mathbf{h}}_{k0}=\arg\min_{\|\mathbf{h}_{k0}\|=1}\sum_{m=0}^{M-1}\mathbf{C}_{k0}^{(m)^H}\mathbf{Q}_0^{(m)}\mathbf{Q}_0^{(m)^H}\mathbf{C}_{k0}^{(m)}. \tag{4.2.16}$$

Obviously, $\mathbf{h}_{k0}$ can be estimated as the eigenvector corresponding to the minimum eigenvalue of $\sum_{m=0}^{M-1}(\mathbf{C}_{k0}^{(m)^H}\mathbf{Q}_0^{(m)}\mathbf{Q}_0^{(m)^H}\mathbf{C}_{k0}^{(m)})$. Additionally, a necessary condition for determining $\mathbf{h}_{k0}$ up to a scalar is $\sum_{m=0}^{M-1}(P_1+1)d_n^{(m)} \geq L$.

For user $k1$, from

$$\mathbf{U}_n^{(m)^H}\mathbf{S}_{k1}\mathbf{H}_{k1} = \mathbf{0}, \tag{4.2.17}$$

we can obtain

$$\mathbf{Q}_1^{(m)^H}\mathbf{C}_{k1}\mathbf{h}_{k1} = \mathbf{0}, \tag{4.2.18}$$

where

$$\mathbf{Q}_1^{(m)} = \underbrace{\begin{bmatrix} \mathbf{U}_n^{(m)}(P_1) & \dots & \mathbf{U}_n^{(m)}(2) & \underbrace{\mathbf{0},\dots,\mathbf{0}}_{M-1} & \mathbf{U}_n^{(m)}(1) & & \\ & \ddots & & & & \ddots & \\ & & \mathbf{U}_n^{(m)}(P_1) & \dots & \mathbf{U}_n^{(m)}(2) & \underbrace{\mathbf{0},\dots,\mathbf{0}}_{M-1} & \mathbf{U}_n^{(m)}(1) \end{bmatrix}}_{L_{s1}N_1\times(P_1M-M+L_{s1})d_n^{(m)}}. \tag{4.2.19}$$

Then $\mathbf{h}_{k1}$ can be estimated as the eigenvector corresponding to the minimum eigenvalue of $\mathbf{C}_{k1}^H(\sum_{m=0}^{M-1}\mathbf{Q}_1^{(m)}\mathbf{Q}_1^{(m)^H})\mathbf{C}_{k1}$. Also, a necessary condition for determining $\mathbf{h}_{k1}$ up to a scalar is $\sum_{m=0}^{M-1}(P_1M-M+L_{s1})d_n^{(m)} \geq L$.

4.3 Adaptive Implementations

It is noteworthy that for low-rate blind channel estimation, in accordance with (4.2.6), we can obtain

$$\mathbf{Q}_0\mathbf{Q}_0^H = \begin{bmatrix} \mathbf{F}(1) & \mathbf{F}(2) \\ \mathbf{F}^H(2) & \mathbf{F}(1) \end{bmatrix}. \tag{4.3.1}$$

where

$$\mathbf{F}(l) = \sum_{p=l}^{P_0} \mathbf{U}_n(p-l+1)\mathbf{U}_n^H(p),\ l = 1, 2. \tag{4.3.2}$$

Considering that $\mathbf{U}_n\mathbf{U}_n^H + \mathbf{U}_s\mathbf{U}_s^H = \mathbf{I}_{P_0N_0}$, we have

$$\mathbf{F}(1) = P_0\mathbf{I}_{N_0} - \sum_{p=1}^{P_0} \mathbf{U}_s(p)\mathbf{U}_s^H(p) \tag{4.3.3}$$

$$\mathbf{F}(l) = -\sum_{p=l}^{P_0} \mathbf{U}_s(p-l+1)\mathbf{U}_s^H(p),\ l \neq 1. \tag{4.3.4}$$

Therefore, (4.2.8) can also be represented only using the information of the signal subspace.

Let us factorize $\widetilde{L}_{s1}$ as $\widetilde{L}_{s1} = \widetilde{\eta}M + \widetilde{q}$, where both $\widetilde{\eta}$ and $\widetilde{q}$ are integers and $0 \leq \widetilde{q} \leq M-1$. Based on (4.2.11), it is found that the structure of the $\widetilde{L}_{s1}N_0 \times \widetilde{L}_{s1}N_0$ matrix $\mathbf{Q}_1\mathbf{Q}_1^H$ depends on the value of M. For example, when $M = 3$, $\widetilde{q} \in \{0, 1, 2\}$. For $\widetilde{q} = 2$, we have

$$\mathbf{Q}_1\mathbf{Q}_1^H = \begin{bmatrix}
\mathbf{F}(1) & \mathbf{0} & \mathbf{0} & \dots & \mathbf{F}(\widetilde{\eta}) & \mathbf{0} & \mathbf{0} & \mathbf{F}(\widetilde{\eta}+1) & \mathbf{0} \\
\mathbf{0} & & & & & & & \ddots & \mathbf{F}(\widetilde{\eta}+1) \\
\mathbf{0} & & & & & & \ddots & & \mathbf{0} \\
\vdots & & & & & \ddots & & & \mathbf{0} \\
\mathbf{F}^H(\widetilde{\eta}) & & & & \ddots & & & & \mathbf{F}(\widetilde{\eta}) \\
\mathbf{0} & & & \ddots & & & & & \vdots \\
\mathbf{0} & & \ddots & & & & & & \mathbf{0} \\
\mathbf{F}^H(\widetilde{\eta}+1) & \ddots & & & & & & & \mathbf{0} \\
\mathbf{0} & \mathbf{F}^H(\widetilde{\eta}+1) & \mathbf{0} & \mathbf{0} & \mathbf{F}^H(\widetilde{\eta}) & \dots & \mathbf{0} & \mathbf{0} & \mathbf{F}(1)
\end{bmatrix}, \tag{4.3.5}$$

where $\mathbf{F}(l)$ $(l = 1, \dots, \widetilde{\eta}+1)$ are defined by (4.3.3) and (4.3.4). For $\widetilde{q} = 1$ and $\widetilde{q} = 0$, the last one and two, respectively, block matrix rows and columns should be removed from (4.3.5). This means that an equivalent form of $\mathbf{Q}_1\mathbf{Q}_1^H$, which only employs the information

of the signal subspace, is also available. Similarly, for high-rate blind channel estimation, both $\mathbf{Q}_0^{(m)}\mathbf{Q}_0^{(m)^H}$ and $\mathbf{Q}_1^{(m)}\mathbf{Q}_1^{(m)^H}$ can also be expressed by only using the information of the signal subspace. Therefore, for the proposed dual-rate blind channel estimation schemes, channel estimates can be obtained as long as an orthonormal basis of the signal subspace is identified.

As a consequence, the adaptive algorithm for low-rate blind channel estimation can be summarized as follows:

1. Estimation of an orthonormal basis of the signal subspace $\mathbf{U}_s$ from $\mathbf{y}(j)$ using the orthonormal PAST algorithm [108];

2. Computation of matrix $\mathbf{C}_{k0}^H\mathbf{Q}_0\mathbf{Q}_0^H\mathbf{C}_{k0}$ (for low-rate users) or matrix $\widetilde{\mathbf{C}}_{k1}^H\mathbf{Q}_1\mathbf{Q}_1^H\widetilde{\mathbf{C}}_{k1}$ (for high-rate users);

3. Estimation of $\mathbf{h}_{ki}$ by performing the SVD on the matrice obtained in Step 2.

The adaptive algorithm for high-rate blind channel estimation can likewise be derived. As to the details of the orthonormal PAST algorithm, please refer to Table 3.1. The main computational burden of the above algorithms comes from the estimation of the signal subspace. In fact, it can be shown that the computational complexity for low-rate blind channel estimation is $4P_0N_0d_s + O(d_s^2)$ flops per iteration, and that for high-rate blind channel estimation is $4P_1N_1\sum_{m=0}^{M-1} d_s^{(m)} + O(\sum_{m=0}^{M-1} d_s^{(m)^2})$ flops per iteration. Therefore, in the case that $P_0 = P_1$, the complexity of adaptive low-rate blind channel estimation becomes much higher than that of its high-rate rival as the rate ratio M increases.

4.4 Dual-rate Blind MMSE Detection

As mentioned in Section 3.4, after the desired spatial signature is obtained based on the orthonormal PAST algorithm, the desired spatio-temporal signature can be constructed. The adaptive ST dual-rate blind MMSE detection for the AWGN channel can then be developed based on the updated signal subspace and an intermediate variable of the orthonormal PAST algorithm. Accordingly, in the context of frequency selective multipath channel, the adaptive dual-rate blind MMSE detection can also be derived based on the orthonormal PAST algorithm as long as the desired signal vector is identified. The issue to be addressed below is how the desired signal vector is related to the desired channel vector.

For low-rate blind MMSE detection, in accordance with (4.1.7) and (4.1.12), the signal vector corresponding to the data bit $b_{k0}(j)$ can be represented by

$$\mathbf{v}_{k0} = \mathbf{S}_{k0}(:, L+2:2L+2)\mathbf{h}_{k0}, \tag{4.4.1}$$

while the signal vector corresponding to the data bit $b_{k1}(jM+m)$ $(m = 0, \ldots, M-1)$ can be written by

$$\mathbf{v}_{k1}^{(m)} = \widetilde{\mathbf{S}}_{k1}(:, (L_{s1}+m-1)(L+1)+1:(L_{s1}+m)(L+1))\mathbf{h}_{k1}. \tag{4.4.2}$$

For high-rate blind MMSE detection, in terms of (4.1.18), for the data bit $b_{k0}(j)$, the corresponding signal vector within the mth high-rate processing interval can be represented by

$$\mathbf{v}_{k0}^{(m)} = \mathbf{S}_{k0}^{(m)}(:, L+2:2L+2)\mathbf{h}_{k0}. \tag{4.4.3}$$

For the data bit $b_{k1}(jM+m)$ $(m=0,\ldots,M-1)$, in accordance with (4.1.20), the corresponding signal vector can be given by

$$\mathbf{v}_{k1} = \mathbf{S}_{k1}(:,(L_{s1}-1)(L+1)+1:L_{s1}(L+1))\mathbf{h}_{k1}. \tag{4.4.4}$$

4.5 Numerical Examples

In all the simulations, a dual-rate system with three low-rate users and two high-rate users has been considered. User 1 is the desired low-rate user and user 4 is the desired high-rate user. The spreading factor for high-rate users is 16, and the rate ratio is 2. The spreading factor for low-rate users is thus 32. Both low-rate and high-rate smoothing factors are set to be 3. For all the users, the binary code sequences and the channels with order 31 are generated randomly. The near-far ratio is 10dB. For the orthonormal PAST algorithm, the forgetting factor is set to be $\alpha = 0.9999$, and the matrix $\mathbf{U}_s$ is initialized to be a random orthonormal matrix.

First, the performances of the proposed adaptive dual-rate blind channel estimation algorithms are validated. The performance measure is the averaged root mean-squared error (RMSE) between estimated channel and true channel. Note that there is a complex constant ambiguity involved in the channel estimates. During the simulations, the real constant part of ambiguity is handled by assigning the true channels $\mathbf{h}_{ki}$ unit norm. However, without further processing, we can not resolve the phase ambiguity. Thus, to calculate the simulated RMSE, the complex phase ambiguity is compensated by multiplying the estimates by $e^{j\hat{\theta}}$, where the phase estimate $\hat{\theta}$ is obtained by minimizing the distance

$\|\mathbf{h}_{ki} - e^{j\hat{\theta}}\hat{\mathbf{h}}_{ki}\|^2$ and is equal to $\hat{\theta} = \text{phase}(\hat{\mathbf{h}}_{ki}^H \mathbf{h}_{ki})$. As a consequence, the averaged RMSE is

$$\text{RMSE} = \frac{1}{P}\sum_{i=1}^{P}\sqrt{2 - 2\|\hat{\mathbf{h}}_{ki}^H \mathbf{h}_{ki}\|}, \tag{4.5.1}$$

where the number of algorithm runs is $P = 1500$.

Fig. 4.2 shows the channel estimation RMSE versus the number of iterations, where the SNR of the desired user is 10dB. Clearly, the adaptive algorithms for both low-rate and high-rate blind channel estimation converge. However, the low-rate algorithm performs better than the high-rate algorithm, with a cost of increasing the computational complexity. Fig. 4.3 shows the channel estimation RMSE versus the SNR of the desired user after the proposed adaptive algorithms have converged. Note that both algorithms perform better as the SNR of the desired user increases.

Based on channel estimates obtained in the above simulations, the performances of the proposed dual-rate blind MMSE detection algorithms have also been evaluated. Fig. 4.4 shows the output SINR versus the SNR of the desired user after the proposed adaptive algorithms have converged. As a comparison, the single-rate results are also plotted, where the spreading factor for the equivalent single-rate system is determined by (3.6.1), and other system parameters are the same. Obviously, the low-rate and single-rate algorithms outperform the high-rate algorithm. It should also be noted that other than the detection of the desired low-rate user, the performance of the low-rate algorithm is remarkably superior to that of the high-rate algorithm for detecting the desired high-rate user. This is because when the high-rate algorithm is used to detect a high-rate data bit, which

spans multiple high-rate bit durations due to multipath delay spread, it only exploits partial information of this high-rate data bit within the corresponding high-rate processing interval.

4.6 Summary

This chapter has proposed a new adaptive blind channel estimation algorithm for dual-rate DS/CDMA systems in multipath channels. Based on subspace decomposition, this algorithm is capable of dealing with large delay spread channels. Its effectiveness has been confirmed by simulations. Additionally, after the channels are estimated using these algorithms, the adaptive dual-rate blind MMSE detectors developed in Chapter 3 can be extended to multipath fading channels.

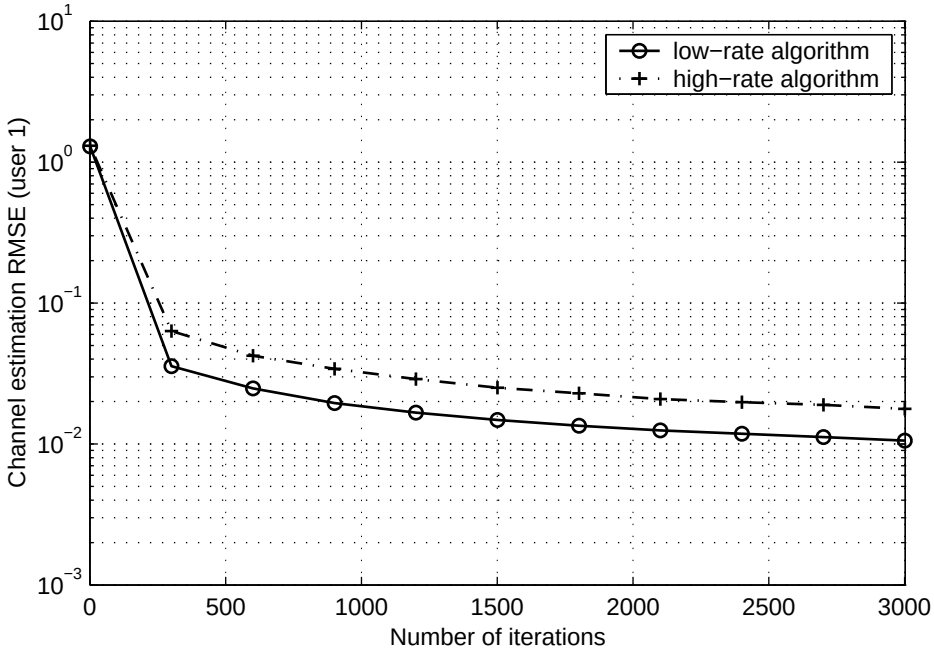

(a)

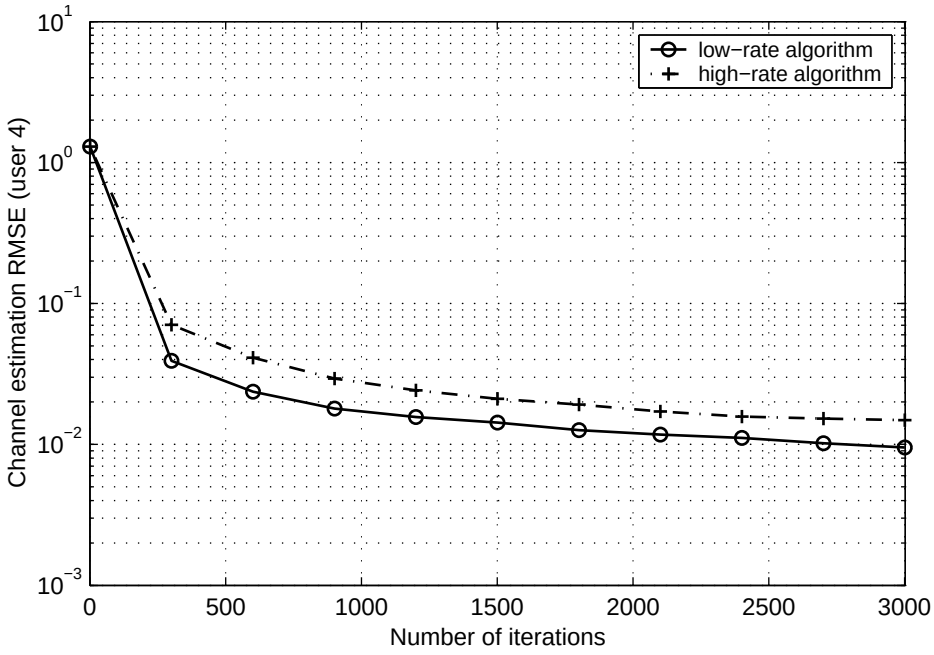

(b)

Figure 4.2: The channel estimation RMSE versus the number of iterations for (a) the desired low-rate user and (b) the desired high-rate user.

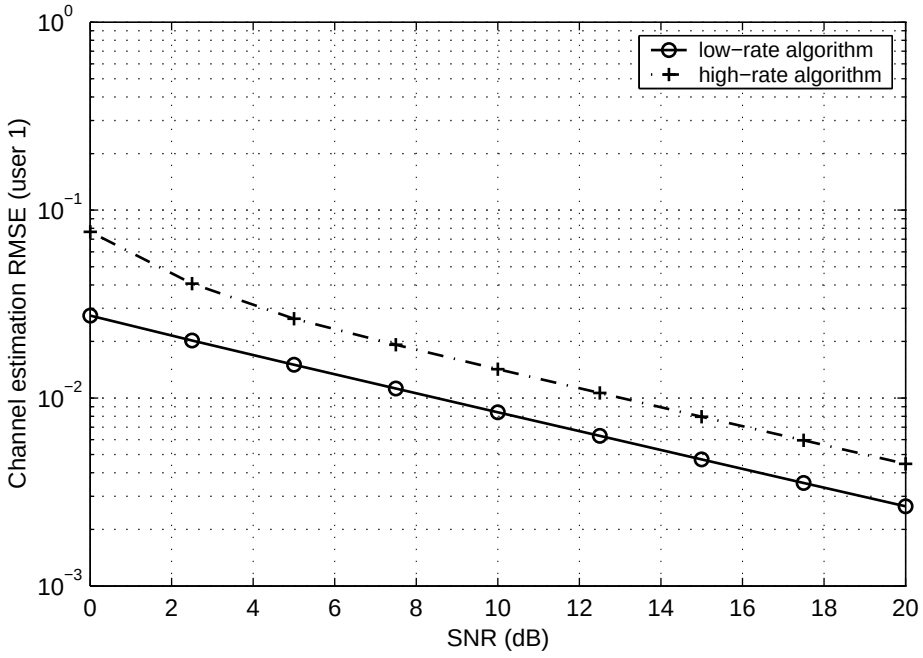

(a)

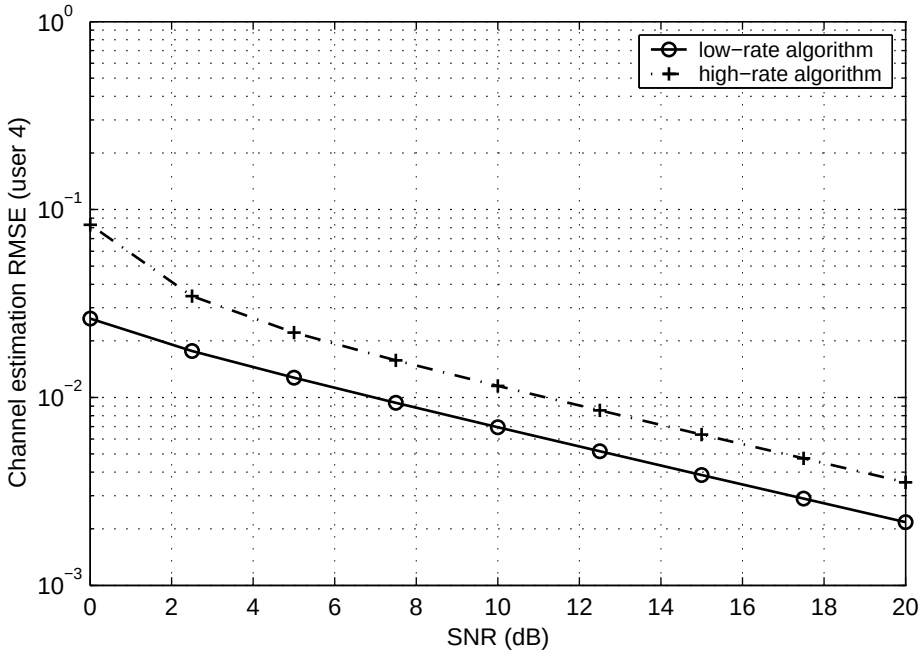

(b)

Figure 4.3: The channel estimation RMSE versus the SNR for (a) the desired low-rate user and (b) the desired high-rate user.

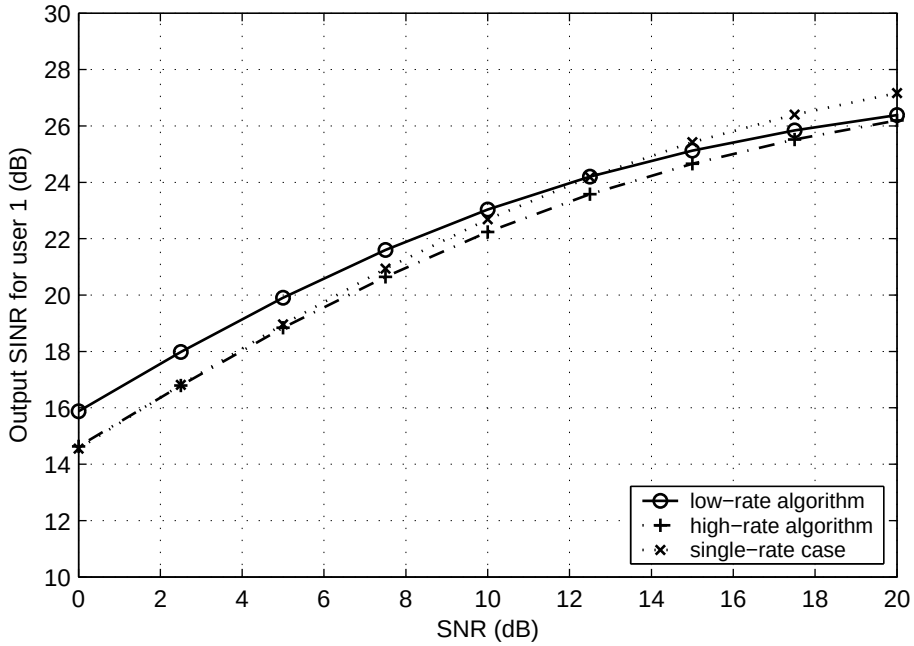

(a)

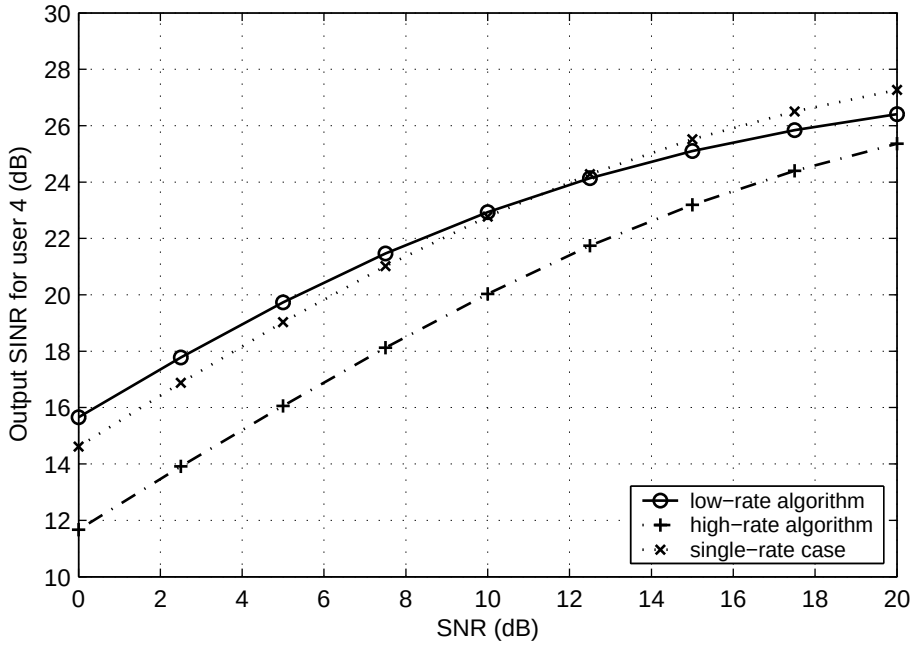

(b)

Figure 4.4: The output SINR versus the SNR for (a) the desired low-rate user and (b) the desired high-rate user.

Chapter 5

Blind Timing Acquisition and Channel Estimation for Multi-rate Multicarrier DS/CDMA

In the preceding two chapters, the subspace-based blind approaches for channel estimation and multiuser detection in multi-rate DS/CDMA systems have been proposed. These approaches target primarily at single-carrier systems. There has been considerable interest in multicarrier CDMA systems due to their robustness to multipath fading channels. However, **little has been reported on channel estimation and multiuser detection for multi-rate multicarrier CDMA**.

As stated in Section 1.4, multicarrier CDMA systems may be classified into two categories, depending upon whether frequency domain or time domain spreading is employed. Both classes of multicarrier CDMA systems show a similar capability in mitigating the effects of fading. However, the time spreading class (the so-called multicarrier DS/CDMA), in general, employs a smaller number of carriers relative to the frequency spreading class,

and thus, is less complex [43]. As a consequence, only multicarrier DS/CDMA is considered in this chapter.

In multicarrier DS/CDMA systems, to achieve frequency diversity, the same data bit spread by a narrowband DS waveform is usually transmitted over each carrier and the received signals are combined to give a more robust data estimate [41]. Such a diversity scheme incurs lower spectral efficiency, and one possible remedy is to employ higher order modulation. For such multicarrier DS/CDMA systems, several receiver structures have been constructed for single-rate systems [43]-[46]. Among these receivers, [46] employed subspace-based techniques to estimate channel coefficients and to construct a multiuser detector.

The major contribution of this chapter is that it addresses the application of the subspace-based technique to timing acquisition and channel estimation issues for multi-rate multicarrier DS/CDMA. Based on a unified signal model, a joint timing acquisition and channel estimation scheme is proposed for both MC and VSF multi-rate systems. It is well known that the operation of any subspace-based technique requires a nonnull noise subspace. Unfortunately, a nonnull noise subspace is unavailable for multicarrier DS/CDMA due to the employed band-limited chip waveform. To tackle this problem, following a similar idea to [46], a finite-length truncation approximation on the chip waveform is performed. Numerical results and theoretical analysis show that this approximation hardly caused any performance degradation of the subspace-based estimators under moderate near-far situations.

The rest of this chapter is organized as follows. Section 5.1 outlines the received

signal model. Problem formulation is described in Section 5.2. The channel estimation and timing acquisition scheme is described in Section 5.3. Simulation results are given in Section 5.4. In Section 5.5, the effect of the finite-length chip waveform truncation on the performance of the proposed scheme is investigated. Section 5.6 concludes the work. Most results presented in this chapter can also be found in [58], [59].

5.1 Signal Model

It has been shown in Section 2.5 that, similar to single-carrier DS/CDMA, MC and VSF access strategies can also be used for multicarrier DS/CDMA to implement multi-rate multiuser communications. In addition, the signal model for a multi-rate multicarrier DS/CDMA system can be established by basic-rate modelling or rate i modelling. Especially, the basic-rate signal model for the VSF case is also applicable to the MC case.

Let us consider a general VSF multi-rate multicarrier DS/CDMA system defined in (2.1.1) and (2.1.2), in which there are I different data rates. As for the notation used below, unless otherwise stated, please refer to Sections 1.6 and 2.2.

Assume that each user uses the same M carriers. The frequency of the mth carrier is w_m. The spreading waveform for the mth carrier of user ki is

$$s_{kim}(t) = \sum_{l=0}^{N_i-1} c_{kim}(l)\phi(t - lT_c), \tag{5.1.1}$$

where $c_{kim}(l)$ $(l = 0, \ldots, N_i - 1)$ is the preassigned spreading code for the mth carrier of user ki. Assume that the chip waveform $\phi(t)$ is band-limited, and the carrier frequencies are well separated so that adjacent frequency bands do not interfere with each other. Also,

$\phi(t)$ is normalized so that $\int_{-\infty}^{\infty} \|\phi(t)\|^2 dt = T_c$.

The channel is assumed to be a slowly varying frequency selective Rayleigh channel. The system parameters (e.g., the number of carriers M) can be chosen suitably so that each frequency band can undergo independent flat fading [43]. Then the received complex signal is given by

$$y(t) = \sum_{i=1}^{I} \sum_{k=1}^{K_i} \sum_{m=1}^{M} A_{ki} x_{kim}(t) \exp(j w_m t) + z(t), \tag{5.1.2}$$

The signal component $x_{kim}(t)$ due to the mth carrier of user ki is given by

$$x_{kim}(t) = \alpha_{kim} \sum_{r=-\infty}^{\infty} b_{ki}(r) s_{kim}(t - rT_i - \tau_{ki}), \tag{5.1.3}$$

where α_{kim} includes the overall effects of phase shifts and fading for the mth carrier of user ki, and $\tau_{ki} \in [0, T_i)$ represents the delay of user ki's signal with respect to the start of the processing interval.

The receiver consists of M branches, each of which is in charge of demodulating one carrier. Assume that the front end filtering at each branch is perfect so that each carrier can be separated. After down-conversion and filtering, the received signal passes through a chip-matched filter followed by chip-rate sampling. At the mth branch, the output of the matched filter at time nT_c is given by

$$y_m(n) = \sum_{i=1}^{I} \sum_{k=1}^{K_i} A_{ki} x_{kim}(n) + z_m(n), \tag{5.1.4}$$

where $z_m(n)$ denotes the component due to AWGN, and

$$\begin{aligned} x_{kim}(n) &= \int_{-\infty}^{\infty} x_{kim}(t)\phi^*(t - nT_c)dt \\ &= \alpha_{kim} \sum_{r=-\infty}^{\infty} b_{ki}(r) \sum_{l=0}^{N_i-1} c_{kim}(l)\hat{\phi}((n - l - rN_i)T_c - \tau_{ki}), \end{aligned} \tag{5.1.5}$$

where the function $\hat{\phi}(t)$ is the output of chip waveform through chip-matched filter, i.e., $\hat{\phi}(t) = \int_{-\infty}^{\infty} \phi(s)\phi^*(s - t)ds$. To avoid interchip interference for the desired signal when it is chip synchronous, the chip waveform is chosen to satisfy the Nyquist criterion, i.e., $\hat{\phi}(nT_c) = T_c$ for $n = 0$ and $\hat{\phi}(nT_c) = 0$ for $n \neq 0$ [46].

Considering that the received signal $y(t)$ is a cyclostationary stochastic process with period T_{br}, to mitigate the effect of interchip interference in the case of chip asynchronism, we set the processing interval with duration PT_{br}, where P is defined as the smoothing factor. It is evident that for each rate i user, at least Pq_i data symbols appear within this processing interval. Assume that N_{br} is the spreading factor for basic rate. At the mth branch, by collecting PN_{br} samples within the processing interval, we can define the following vectors

$$\begin{aligned} \mathbf{y}_m(r) &= [y_m(rN_{br}), \ldots, y_m(rN_{br} + PN_{br} - 1)]^T, \\ \mathbf{x}_{kim}(r) &= [x_{kim}(rN_{br}), \ldots, x_{kim}(rN_{br} + PN_{br} - 1)]^T, \\ \mathbf{z}_m(r) &= [z_m(rN_{br}), \ldots, z_m(rN_{br} + PN_{br} - 1)]^T, \end{aligned}$$

for $i = 1, \ldots, I$, $k = 1, \ldots, K_i$, and $m = 1, \ldots, M$. Then, the corresponding vectors from

M branches can be concatenated into the PMN_{br}-dimensional vectors

$$\mathbf{y}(r) = [\mathbf{y}_1^T(r), \ldots, \mathbf{y}_M^T(r)]^T,$$

$$\mathbf{x}_{ki}(r) = [\mathbf{x}_{ki1}^T(r), \ldots, \mathbf{r}_{kiM}^T(r)]^T,$$

$$\mathbf{z}(r) = [\mathbf{z}_1^T(r), \ldots, \mathbf{z}_M^T(r)]^T,$$

for $i = 1, \ldots, I$ and $k = 1, \ldots, K_i$. Now, (5.1.4) can be rewritten as

$$\mathbf{y}(r) = \sum_{i=1}^{I} \sum_{k=1}^{K_i} A_{ki} \mathbf{x}_{ki}(r) + \mathbf{z}(r). \tag{5.1.6}$$

5.2 Problem Formulation

It is necessary to further explore the structure of $\mathbf{x}_{ki}(r)$ so that the received vector $\mathbf{y}(r)$ can be represented in a more refined manner. According to (5.1.5), by defining

$$h_{kim}^{n'}(p) = \sum_{l=0}^{N_i-1} c_{kim}(l) \hat{\phi}((n'N_i + p - l)T_c - \tau_{ki}),$$

where $n' = jq_i - n$, and then introducing the following notation:

$$\mathbf{g}_{kim}^{n'} = [h_{kim}^{n'}(0), \ldots, h_{kim}^{n'}(PN_{br} - 1)]^T,$$

$$\mathbf{g}_{ki}^{n'} = [\mathbf{g}_{ki1}^{n'T}, \ldots, \mathbf{g}_{kiM}^{n'T}]^T,$$

we can obtain an equivalent form of (5.1.6) as

$$\mathbf{y}(r) = \sum_{i=1}^{I} \sum_{k=1}^{K_i} A_{ki} \mathbf{H}_{ki} \sum_{n'=-\infty}^{\infty} \mathbf{g}_{ki}^{n'} b_{ki}(rq_i - n') + \mathbf{z}(r), \tag{5.2.1}$$

where the $PMN_{br} \times PMN_{br}$ diagonal matrix

$$\mathbf{H}_{ki} = \text{diag}\left(\underbrace{\alpha_{ki1}, \ldots, \alpha_{ki1}}_{PN_{br}}, \ldots, \underbrace{\alpha_{kiM}, \ldots, \alpha_{kiM}}_{PN_{br}} \right).$$

We observe from (5.2.1) that the received signal vector $\mathbf{y}(r)$ is a linear combination of an infinite number of signal vectors. This leads to the null noise subspace and thus disables the subspace-based techniques. To tackle this problem, following the ideas in [46], a fast decaying $\hat{\phi}(t)$ should be chosen in practice. We further assume that $\hat{\phi}(t)$ decays fast enough so that a given symbol of rate i users makes a significant contribution only to $2Q_i$ ($Q_i \geq 1$) adjacent symbols. So we can neglect the vectors in (5.2.1) except for those corresponding to $b_{ki}(rq_i - Q_i), \ldots, b_{ki}(rq_i), \ldots, b_{ki}(rq_i + Pq_i + Q_i - 2)$ for user ki[1]. As a result, (5.2.1) becomes

$$\begin{aligned}\mathbf{y}(r) &= \sum_{i=1}^{I}\sum_{k=1}^{K_i} A_{ki}\mathbf{H}_{ki} \sum_{n'=-Pq_i-Q_i+2}^{Q_i} \mathbf{g}_{ki}^{n'} b_{ki}(rq_i - n') + \mathbf{z}(r) \\ &= \sum_{i=1}^{I}\sum_{k=1}^{K_i} A_{ki}\mathbf{H}_{ki}\mathbf{G}_{ki}\mathbf{b}_{ki}(r) + \mathbf{z}(r), \end{aligned} \tag{5.2.2}$$

where

$$\mathbf{G}_{ki} = [\mathbf{g}_{ki}^{Q_i}, \ldots, \mathbf{g}_{ki}^{-Pq_i-Q_i+2}],$$

$$\mathbf{b}_{ki}(r) = [b_{ki}(rq_i - Q_i), \ldots, b_{ki}(rq_i + Pq_i + Q_i - 2)]^T.$$

Our aim is to estimate the channel vector $\mathbf{h}_{ki} = [\alpha_{ki1}, \ldots, \alpha_{kiM}]^T$ and the delay τ_{ki} from the received vector $\mathbf{y}(r)$, only with the knowledge of spreading sequences of the desired user.

5.3 Timing Acquisition and Channel Estimation

At first, let us estimate the channel vector $\mathbf{h}_{ki}$ on the assumption that τ_{ki} is known. For convenience and without loss of generality, we assume that the columns of matrix $\mathbf{G}$ are

[1] In fact, in the case of $\tau_{ki} = 0$, only $\mathbf{g}_{ki}^{0}, \ldots, \mathbf{g}_{ki}^{-Pq_i+1}$ exist.

linear independent [95], where

$$\mathbf{G} = [A_{11}\mathbf{H}_{11}\mathbf{G}_{11}, \ldots, A_{K_11}\mathbf{H}_{K_11}\mathbf{G}_{K_11}, \ldots, A_{1I}\mathbf{H}_{1I}\mathbf{G}_{1I}, \ldots, A_{K_II}\mathbf{H}_{K_II}\mathbf{G}_{K_II}].$$

The rank of matrix $\mathbf{G}$, d_s, is equal to the number of data symbols within the processing interval. Its value depends on how many users are symbol- or chip-synchronous with respect to the start of the processing interval. d_s has a maximum of $\sum_{i=1}^{I} K_i L_i$ where $L_i \triangleq Pq_i + 2Q_i - 1$.

An eigen-decomposition can be performed on the autocorrelation matrix $\mathbf{R}$ of the received vector $\mathbf{y}(r)$ by

$$\begin{aligned} \mathbf{R} &\triangleq \mathbb{E}\{\mathbf{y}(r)\mathbf{y}^H(r)\} \\ &= \begin{bmatrix} \mathbf{U}_s & \mathbf{U}_n \end{bmatrix} \begin{bmatrix} \mathbf{\Lambda}_s & \\ & \mathbf{\Lambda}_n \end{bmatrix} \begin{bmatrix} \mathbf{U}_s^H \\ \mathbf{U}_n^H \end{bmatrix}, \end{aligned} \tag{5.3.1}$$

where $\mathbf{\Lambda}_s = \mathrm{diag}(\lambda_1, \ldots, \lambda_{d_s})$ contains the d_s largest eigenvalues of $\mathbf{R}$ in descending order, and $\mathbf{U}_s = [\mathbf{u}_1, \ldots, \mathbf{u}_{d_s}]$ contains the corresponding orthonormal eigenvectors; $\mathbf{\Lambda}_n = \sigma^2\mathbf{I}_{PMN_{br}-d_s}$, and $\mathbf{U}_n = [\mathbf{u}_{d_s+1}, \ldots, \mathbf{u}_{PMN_{br}}]$ contains $d_n = PMN_{br} - d_s$ orthonormal eigenvectors that corresponding to the eigenvalue σ^2. The vectors in matrix $\mathbf{U}_s$ span the signal subspace defined by the columns of $\mathbf{G}$ whereas the vectors in $\mathbf{U}_n$ span the noise subspace, orthogonal complement of the signal subspace.

Due to the orthogonality between the noise subspace and the signal subspace, we have

$$\mathbf{U}_n^H\mathbf{H}_{ki}\mathbf{G}_{ki} = \mathbf{0},\ i = 1, \ldots, I;\ k = 1, \ldots, K_i. \tag{5.3.2}$$

It is desirable to represent (5.3.2) in terms of the channel vector $\mathbf{h}_{ki}$. By defining

$$\mathcal{U}_n = \underbrace{\begin{bmatrix} \mathbf{U}_n & & \\ & \ddots & \\ & & \mathbf{U}_n \end{bmatrix}}_{L_i \text{ blocks}},$$

and

$$\mathbf{G}_{ki}^n = \begin{bmatrix} \mathbf{g}_{ki1}^n & & \\ & \ddots & \\ & & \mathbf{g}_{kiM}^n \end{bmatrix}, \; n = -Pq_i - Q_i + 2, \ldots, Q_i,$$

$$\mathcal{G}_{ki} = \begin{bmatrix} \mathbf{G}_{ki}^{Q_i} \\ \vdots \\ \mathbf{G}_{ki}^{-Pq_i - Q_i + 2} \end{bmatrix},$$

for $i = 1, \ldots, I$ and $k = 1, \ldots, K_i$, we can obtain an equivalent form of (5.3.2), i.e.,

$$\mathcal{U}_n^H \mathcal{G}_{ki} \mathbf{h}_{ki} = \mathbf{0}, \; i = 1, \ldots, I; \; k = 1, \ldots, K_i. \tag{5.3.3}$$

Since $\mathcal{U}_n^H \mathcal{G}_{ki}$ has $d_n L_i$ rows, $\mathbf{h}_{ki}$ can be uniquely determined up to a multiplicative constant only if $d_n L_i \geq M - 1$.

Considering that in practice, the noise subspace can just be derived from spectral decomposition of the time-average estimate of $\mathbf{R}$, (5.3.3) can be solved in the least-squares sense [107]

$$\hat{\mathbf{h}}_{ki} = \arg \min_{\|\mathbf{h}_{ki}\|=1} \mathbf{h}_{ki}^H \mathbf{W} \mathbf{h}_{ki}. \tag{5.3.4}$$

The solution of this optimization problem is the eigenvector corresponding to the minimum eigenvalue of $\mathbf{W}$, where

$$\mathbf{W} \triangleq \mathcal{G}_{ki}^H \mathcal{U}_n \mathcal{U}_n^H \mathcal{G}_{ki}. \tag{5.3.5}$$

The above channel estimation scheme assumes that τ_{ki} is known. In practice, we must perform joint timing and channel estimation for the desired user because of the unavailable value of τ_{ki}. Following a similar approach in [46], the procedure for joint timing and channel estimation can be summarized as follows:

1. Hypothesize a value for $\tau_{ki} \in [0, T_i)$ and construct the matrices $\mathcal{G}_{ki}(\tau_{ki})$ and $\mathbf{W}(\tau_{ki})$;

2. Obtain a estimate $\hat{\mathbf{h}}_{ki}(\tau_{ki})$ for this τ_{ki} via (5.3.4);

3. Calculate the cost function

$$C(\tau_{ki}) = \frac{\hat{\mathbf{h}}_{ki}^H(\tau_{ki})\mathbf{W}(\tau_{ki})\hat{\mathbf{h}}_{ki}(\tau_{ki})}{\hat{\mathbf{h}}_{ki}^H(\tau_{ki})\mathcal{G}_{ki}^H(\tau_{ki})\mathcal{G}_{ki}(\tau_{ki})\hat{\mathbf{h}}_{ki}(\tau_{ki})}; \tag{5.3.6}$$

4. Repeat step 1 to 3 for different values of τ_{ki};

5. Choose the timing estimate $\hat{\tau}_{ki}$ which minimizes the cost function $C(\tau_{ki})$ and the corresponding channel estimate is $\hat{\mathbf{h}}_{ki}(\hat{\tau}_{ki})$.

Obviously, in practice, a finite number of hypothesized values of τ_{ki} should be selected in the interval $[0, T_i)$. Since the cost function $C(\tau_{ki})$ is a one-dimensional continuous function of τ_{ki}, an optimal estimate $\hat{\tau}_{ki}$ can be approximated if a sufficient number of hypotheses are given. After the noise subspace is estimated, the overall computational complexity of joint timing and channel estimation algorithm is directly proportional to the number of hypotheses. Therefore, it is necessary to make a performance/complexity tradeoff. In addition, in order to improve computational efficiency, we can store $\mathbf{g}_{ki1}^n, \ldots, \mathbf{g}_{kiM}^n$ ($n = -Pq_i - Q_i + 2, \ldots, Q_i$) for all hypotheses in a lookup table, with a cost of increasing storage requirements.

After timing and channel estimates are obtained via the above scheme, the subspace-based blind MMSE detector can easily be constructed as long as the desired signal vector is identified. The issue now is how the desired signal vector is related to the desired channel vector. In accordance with (5.2.2), the signal vector corresponding to the data bit $b_{ki}(rq_i - n)$ $(n = -q_i + 1, \ldots, 0)$ can be represented by

$$\mathbf{p}_{ki}^n = \mathbf{H}_{ki}\mathbf{g}_{ki}^n = \mathbf{G}_{ki}^n\mathbf{h}_{ki}. \tag{5.3.7}$$

Then the linear MMSE detector for demodulating $b_{ki}(rq_i - n)$ $(n = -q_i + 1, \ldots, 0)$ can be given by [24]

$$\mathbf{w}_n = \mathbf{U}_s\mathbf{\Lambda}_s^{-1}\mathbf{U}_s^H\mathbf{p}_{ki}^n. \tag{5.3.8}$$

5.4 Numerical Examples

We compare the performance of the joint timing and channel estimation scheme for dual-rate MC and VSF systems. The batch EVD is used for subspace decomposition. For a fair comparison, in terms of [95], we established the following baseline:

- Both systems have the same chip rate and thus same system bandwidth;
- The numbers of rate i users are same in both systems;
- Identical duration of observation in both systems;
- Identical length of observation vector $\mathbf{y}(r)$ in both systems, which can be implemented by the suitable choice of the smoothing factor;

Table 5.1: Simulation Settings

Parameters	**VSF System**	**MC System**
Number of users	$K_1 = 3$, $K_2 = 2$	12 basic-rate users
Spreading Factor	$N_1 = 15$, $N_2 = 10$	30
Smoothing Factor	2	2
Number of Carriers	2	2
Duration of Observation	1800 high rate or 1200 low rate symbols	600 basic-rate symbols

- The channel coefficients α_{kim} are generated according to a complex Gaussian distribution with zero mean and unit variance, and the delay τ_{ki} is uniformly generated in $[0, T_i)$;

- The binary spreading sequences are randomly generated in both systems in order to eliminate any dependence of performance on the code correlations.

Let us consider a dual-rate case where the rate ratio is 2:3, i.e., $q_1 = 2$ and $q_2 = 3$. In terms of the above baseline, simulation parameters are shown in Table 5.1. In both systems, a raised-cosine function with roll-off factor 0.15 is used as chip waveform, i.e.,

$$\hat{\phi}(t) = \frac{\sin(\pi t/T_c)}{\pi t/T_c} \frac{\cos(0.15\pi t/T_c)}{1 - 0.09t^2/T_c^2}. \tag{5.4.1}$$

The dimension of the signal subspace is set to be its maximum, i.e., $d_s = \sum_{i=1}^{I} K_i L_i$. Assume that a given symbol of each user only influences two adjacent symbols. Therefore, $d_s = 36$ for the VSF system and $d_s = 45$ for the MC system. The hypothesized values of τ_{ki} are selected within $[0, T_i)$ with spacing $0.05T_c$. Thus, for the VSF system, the number of hypotheses is 300 for low-rate users and 200 for high-rate users; while it is 600 for the MC system. 1500 realizations are used to generate all results.

For both VSF and MC systems, Fig. 5.1 shows the probability of acquisition of the desired user under various near-far ratios. When the obtained timing estimate is more than $0.5T_c$ away from the true value, we assume that an acquisition failure occurs [29]. We can observe that the probability of acquisition for both low-rate and high-rate users can approach 1 as the SNR of the desired user increases. In contrast, an increase of the near-far ratio may cause the probability of acquisition to decrease. However, even in severe near-far situations (near-far ratio=40dB), the probability of acquisition is still larger than 0.983 when the SNR of the desired user is greater than 14dB.

Fig. 5.2 summarizes the RMSE of channel estimation for both VSF and MC systems. It can be seen from Fig. 5.2 that the channel estimation scheme is resistant to moderate near-far effects (near-far ratio$\leq$10dB) for both low-rate and high-rate users. However, in severe near-far situations (near-far ratio=40dB), the channel estimation scheme fails. The reason behind this is that the NFR of the subspace-based channel estimator for multicarrier DS/CDMA with band-limited chip waveform is zero [46]. It is noteworthy that for mild near-far situations (near-far ratio$\leq$10dB) and moderate range of the SNR, the VSF system outperforms the MC system. This is because the desired symbol in the VSF system suffers from less MAI than that in the MC system. However, we can observe that the MC system is less vulnerable to severe near-far situations than the VSF system since the longer spreading factor increases the tolerance of the system toward the MAI.

We employ timing and channel estimates obtained previously to construct the MMSE receivers and investigate their performances. The employed performance measure is the output SINR. As a comparison, the results of the MRC receiver with perfect channel

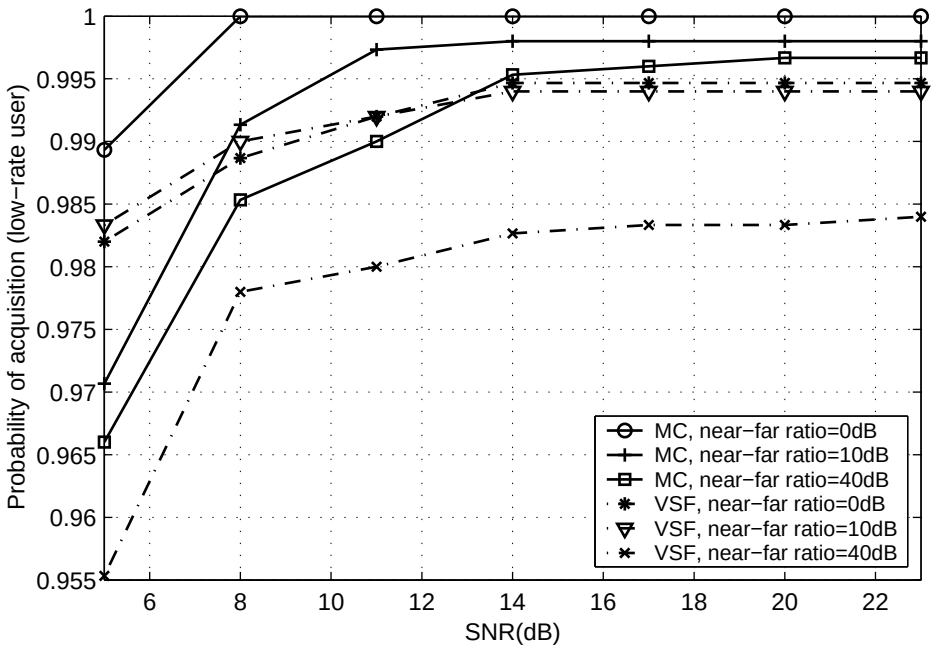

(a)

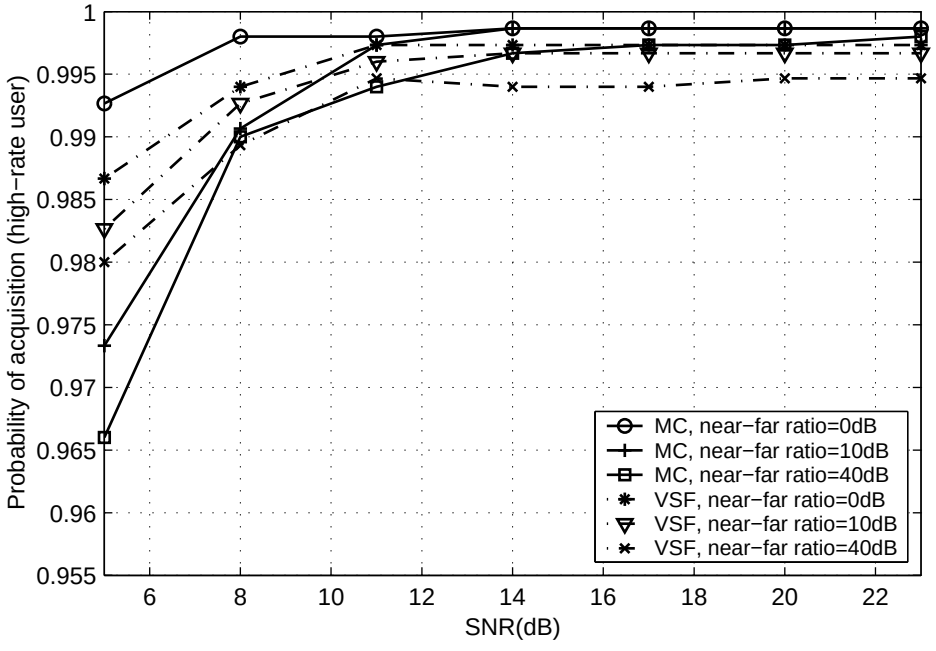

(b)

Figure 5.1: The probability of acquisition for (a) the desired low-rate user and (b) the desired high-rate user.

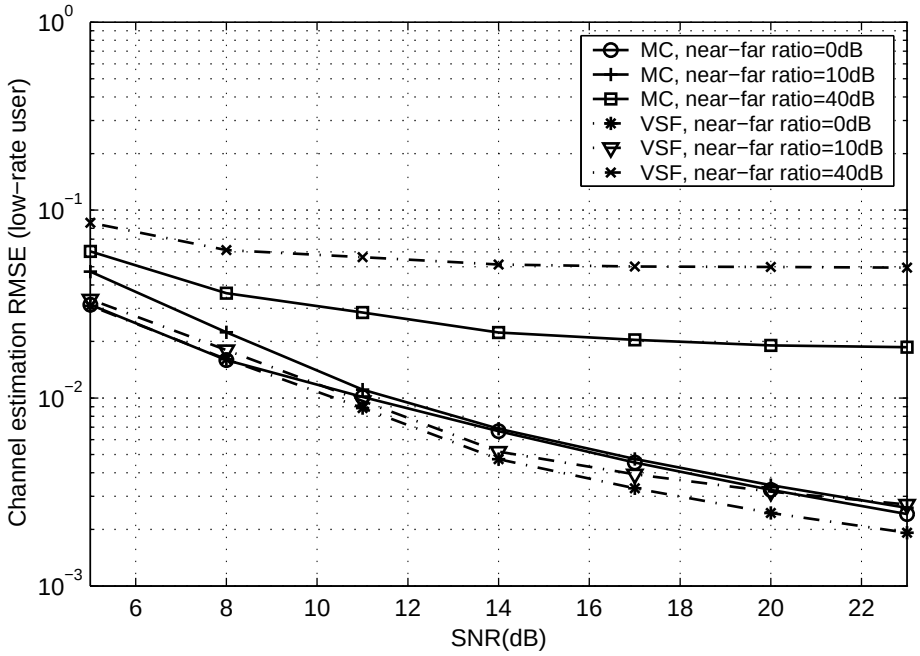

(a)

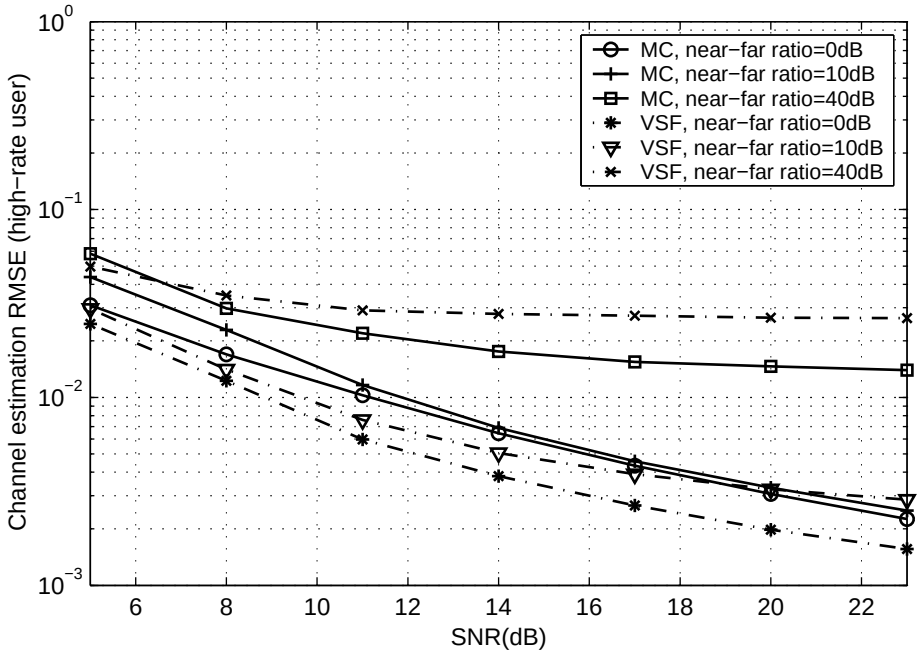

(b)

Figure 5.2: The channel estimation RMSE for (a) the desired low-rate user and (b) the desired high-rate user.

information and the single-rate case are also plotted. For equivalent single-rate system, the spreading factor is determined by (3.6.1) and equal to 12. Thus, in terms of the above baseline, the smoothing factor is 5, and the duration of observation includes 1,500 equivalent single-rate symbols. It can be seen from Fig. 5.3 that for mild near-far situations (near-far ratio$\leq$10dB) and moderate range of the SNR, the output SINR of the VSF system is better than the single-rate system, while the latter outperforms the MC system. In addition, as the SNR of the desired user increases, the MMSE receiver has a prominent advantage over the MRC receiver.

5.5 Performance Analysis

In the development of the subspace-based channel estimator, each rate i user is assumed to contribute at most L_i linearly independent vectors to the received vector $\mathbf{y}(r)$. However, in fact, each user contributes an infinite number of signal vectors because the employed chip waveform is not time-limited. In this section, we analyze the channel estimation error due to the finite-length truncation of chip waveform by exploiting the first-order perturbation approximation in [110]. Similar to [46], we treat the vectors in (5.2.1) from symbols other than $b_{ki}(rq_i - n)$ $(n = -Pq_i - Q_i + 2, \ldots, Q_i)$, for $k = 1, \ldots, K_i$ and $i = 1, \ldots, I$, as perturbations to the unperturbed observation vector $\mathbf{y}(r)$ obtained by the finite-length truncation approximation in (5.2.2). For convenience, we assume that the perturbation vectors are numbered starting from $d_s + 1$.

As stated before, $\mathbf{u}_l$ $(l = 1, \ldots, PMN_{br})$ denote the eigenvectors corresponding to the eigenvalues (in descending order) of the unperturbed correlation matrix $\mathbf{R}$. The first d_s

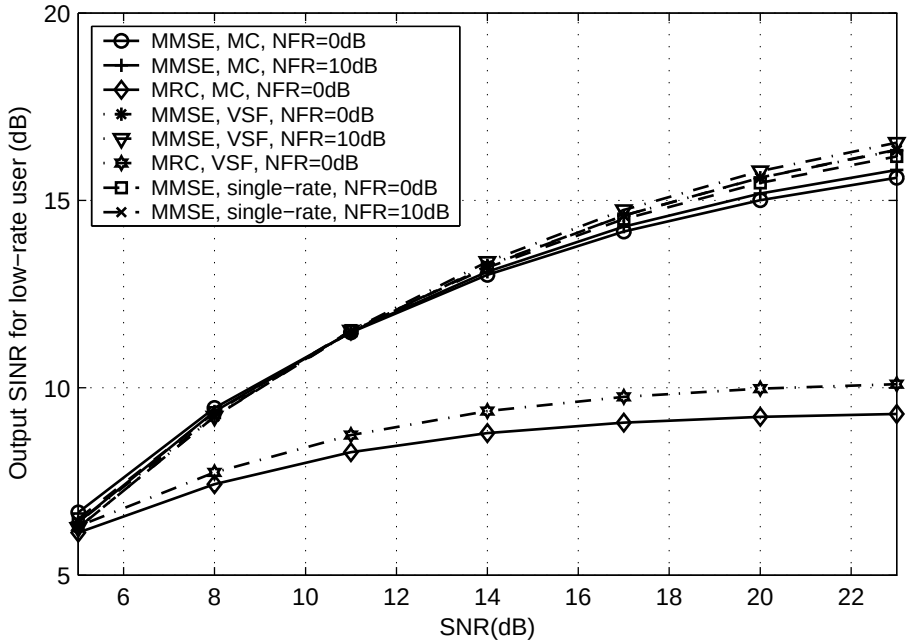

(a)

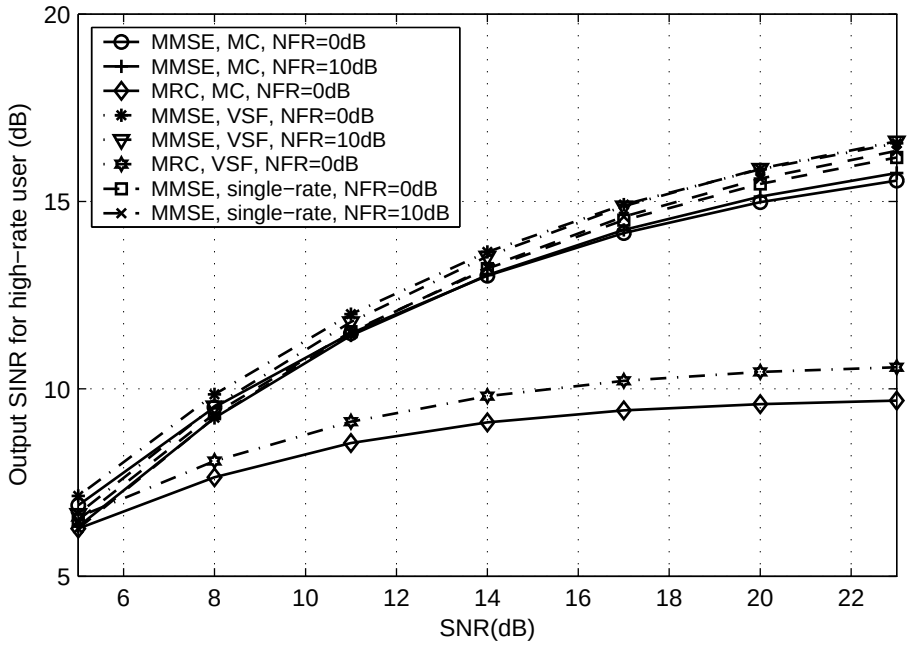

(b)

Figure 5.3: The output SINR for (a) the desired low-rate user and (b) the desired high-rate user.

eigenvectors span the unperturbed signal subspace, and the remaining eigenvectors span the unperturbed noise subspace. Since the signal vectors from all the users span the entire PMN_{br}-dimensional space [46], the perturbation vectors in (5.2.1), denoted by $\mathbf{v}_r$, for $r \geq d_s + 1$, can be represented as

$$\mathbf{v}_r = \sum_{l=1}^{PMN_{br}} e_{rl}\mathbf{u}_l. \tag{5.5.1}$$

By defining a $PMN_{br} \times PMN_{br}$ matrix $\mathbf{\Omega}$, whose (k,l)th element, for $k, l = 1, \ldots, PMN_{br}$, is given by $\epsilon_{kl} = \sum_{r=d_s+1}^{\infty} e_{rk}e_{rl}^*$, and using (5.5.1), we obtain the perturbed correlation matrix $\tilde{\mathbf{R}}$ as

$$\tilde{\mathbf{R}} = \mathbf{R} + \mathbf{E}, \tag{5.5.2}$$

where

$$\begin{aligned}\mathbf{E} &= \sum_{k=1}^{PMN_{br}} \sum_{l=1}^{PMN_{br}} \epsilon_{kl}\mathbf{u}_k\mathbf{u}_l^H \\ &= \begin{bmatrix}\mathbf{U}_s & \mathbf{U}_n\end{bmatrix} \mathbf{\Omega} \begin{bmatrix}\mathbf{U}_s^H \\ \mathbf{U}_n^H\end{bmatrix}.\end{aligned} \tag{5.5.3}$$

For simplicity, we assume that a perfect estimate of the perturbed correlation matrix $\tilde{\mathbf{R}}$ is obtained from the samples of the perturbed vector. An eigen-decomposition can be performed on the perturbed correlation matrix

$$\tilde{\mathbf{R}} = \begin{bmatrix}\tilde{\mathbf{U}}_s & \tilde{\mathbf{U}}_n\end{bmatrix} \begin{bmatrix}\tilde{\mathbf{\Lambda}}_s & \\ & \tilde{\mathbf{\Lambda}}_n\end{bmatrix} \begin{bmatrix}\tilde{\mathbf{U}}_s^H \\ \tilde{\mathbf{U}}_n^H\end{bmatrix}, \tag{5.5.4}$$

where $\tilde{\mathbf{\Lambda}}_n = \sigma^2\mathbf{I}_{d_n}$ and the vectors in $\tilde{\mathbf{U}}_n$ span the perturbed noise subspace. Let us introduce $\Delta\mathbf{U}_n$ as the difference between $\tilde{\mathbf{U}}_n$ and $\mathbf{U}_n$ as well as $\Delta\mathbf{\Lambda}_n$ as the difference between $\tilde{\mathbf{\Lambda}}_n$ and $\mathbf{\Lambda}_n$.

From (5.3.3), the first-order approximation of perturbation to the channel estimation assumes the form [110]

$$\Delta \mathbf{h}_{ki} \approx -(\mathcal{U}_n^H \mathcal{G}_{ki})^\dagger \Delta \mathcal{U}_n^H \mathcal{G}_{ki} \mathbf{h}_{ki}. \tag{5.5.5}$$

What remains is to derive the first-order approximation of $\Delta \mathcal{U}_n^H$. Note that in accordance with (5.5.4), we have

$$\begin{aligned} \tilde{\mathbf{U}}_n^H \tilde{\mathbf{R}} &= \tilde{\mathbf{\Lambda}}_n \tilde{\mathbf{U}}_n^H \\ &= (\sigma^2 \mathbf{I}_{d_n} + \Delta \mathbf{\Lambda}_n)(\mathbf{U}_n + \Delta \mathbf{U}_n)^H \\ &= \sigma^2 \mathbf{U}_n^H + \Delta \mathbf{\Lambda}_n \mathbf{U}_n^H + \sigma^2 \Delta \mathbf{U}_n^H + \Delta \mathbf{\Lambda}_n \Delta \mathbf{U}_n^H. \end{aligned} \tag{5.5.6}$$

We can obtain from (5.5.2) and (5.5.3)

$$\begin{aligned} \tilde{\mathbf{U}}_n^H \tilde{\mathbf{R}} &= (\mathbf{U}_n + \Delta \mathbf{U}_n)^H (\mathbf{R} + \mathbf{E}) \\ &= \mathbf{U}_n^H \tilde{\mathbf{R}} + \Delta \mathbf{U}_n^H \mathbf{R} + \Delta \mathbf{U}_n^H \mathbf{E}. \end{aligned} \tag{5.5.7}$$

By neglecting the second-order terms $\Delta \mathbf{\Lambda}_n \Delta \mathbf{U}_n^H$ in (5.5.6) and $\Delta \mathbf{U}_n^H \mathbf{E}$ in (5.5.7), we have

$$\Delta \mathbf{U}_n^H (\mathbf{R} - \sigma^2 \mathbf{I}_{PMN_{br}}) \approx \Delta \mathbf{\Lambda}_n \mathbf{U}_n^H - \mathbf{U}_n^H (\tilde{\mathbf{R}} - \sigma^2 \mathbf{I}_{PMN_{br}}). \tag{5.5.8}$$

Right-multiplying both sides of (5.5.8) by $\mathbf{U}_s (\mathbf{\Lambda}_s - \sigma^2 \mathbf{I}_{d_s})^{-1} \mathbf{U}_s^H \mathbf{G}_{ki}^n \mathbf{h}_{ki}$ ($n = -Pq_i - Q_i + 2, \ldots, Q_i$) and noting that $\mathbf{G}_{ki}^n \mathbf{h}_{ki}$ ($n = -Pq_i - Q_i + 2, \ldots, Q_i$) lies in the column space of $\mathbf{U}_s$, we have

$$\Delta \mathbf{U}_n^H \mathbf{G}_{ki}^n \mathbf{h}_{ki} \approx -\mathbf{U}_n^H (\tilde{\mathbf{R}} - \sigma^2 \mathbf{I}_{PMN_{br}}) \mathbf{U}_s (\mathbf{\Lambda}_s - \sigma^2 \mathbf{I}_{d_s})^{-1} \mathbf{U}_s^H \mathbf{G}_{ki}^n \mathbf{h}_{ki}. \tag{5.5.9}$$

Note that it is easy to derive from (5.5.2),

$$\mathbf{U}_n^H \tilde{\mathbf{R}} = \sigma^2 \mathbf{U}_n^H + \mathbf{\Upsilon} \begin{bmatrix} \mathbf{U}_s^H \\ \mathbf{U}_n^H \end{bmatrix}, \tag{5.5.10}$$

where $\boldsymbol{\Upsilon}$ is the $d_n \times PMN_{br}$ submatrix of $\boldsymbol{\Omega}$ defined by $\boldsymbol{\Upsilon} = [\mathbf{0}_{d_n \times d_s}\ \mathbf{I}_{d_n}]\boldsymbol{\Omega}$. Substituting (5.5.10) into (5.5.9) leads to

$$\Delta \mathbf{U}_n^H \mathbf{G}_{ki}^n \mathbf{h}_{ki} \approx -\boldsymbol{\Gamma}(\boldsymbol{\Lambda}_s - \sigma^2 \mathbf{I}_{d_s})^{-1} \mathbf{U}_s^H \mathbf{G}_{ki}^n \mathbf{h}_{ki}, \tag{5.5.11}$$

where $\boldsymbol{\Gamma}$ is the $d_n \times d_s$ submatrix of $\boldsymbol{\Upsilon}$ defined by $\boldsymbol{\Gamma} = \boldsymbol{\Upsilon}[\mathbf{I}_{d_s}\ \mathbf{0}_{d_s \times d_n}]^H$. As a result, in accordance with (5.5.5), we have

$$\Delta \mathbf{h}_{ki} \approx (\mathcal{U}_n^H \mathcal{G}_{ki})^\dagger \begin{bmatrix} \boldsymbol{\Gamma}(\boldsymbol{\Lambda}_s - \sigma^2 \mathbf{I}_{d_s})^{-1} \mathbf{U}_s^H \mathbf{p}_{ki}^{Q_i} \\ \vdots \\ \boldsymbol{\Gamma}(\boldsymbol{\Lambda}_s - \sigma^2 \mathbf{I}_{d_s})^{-1} \mathbf{U}_s^H \mathbf{p}_{ki}^{-Pq_i - Q_i + 2} \end{bmatrix}. \tag{5.5.12}$$

We can see from (5.5.12) that the channel estimation error is determined by $\|\boldsymbol{\Gamma}\|$ and the projections of the signal vectors from the desired user onto the eigenvectors of the unperturbed signal subspace, as well as the reciprocals of their corresponding eigenvalues. Intuitively, $\|\boldsymbol{\Gamma}\|$ can be made small (relative to $\|\mathbf{R}\|$) by using a fast decaying chip waveform. Moreover, when the powers of the interferers increase, $\|\boldsymbol{\Gamma}\|$ and the eigenvalues of the unperturbed subspaces increase at roughly the same rate. Hence, the channel estimation error can be made small in moderate near-far situations. However, the increase in interferer powers changes the structure of the signal subspace, which is the basis of the subspace-based techniques. As a consequence, the channel estimation error increases as the near-far effect gets more severe.

To illustrate the discussion above with numerical examples, we reconsider the dual-rate system in Section 5.4. Here we assume that the receiver is synchronized to the desired user. Fig. 5.4 shows the exact value of $\|\Delta \mathbf{h}_{ki}\|$ and its first-order approximation given by (5.5.12). It can be observed that the finite truncation effect is negligible ($\|\Delta \mathbf{h}_{ki}\|$ is

small) in the moderate near-far situation (near-far ratio=10dB). Moreover, the first-order approximation is very accurate.

5.6 Summary

This chapter addresses the timing acquisition and channel estimation issue for multi-rate multicarrier DS/CDMA. Based on finite-length truncated approximation on the band-limited chip waveform, a subspace based scheme has been proposed, which is capable of dealing with both MC and VSF multi-rate systems. The effectiveness of the proposed timing and channel estimation schemes has been confirmed by numerical simulations and theoretical analysis.

Note that a main computational burden of the proposed scheme comes from subspace decomposition using batch EVD. It can be seen from (5.3.5) that an orthonormal basis of the noise subspace, rather than the complete subspace information, is required for the calculation of the matrix $\mathbf{W}$. It is worth noting that $\mathcal{U}_n\mathcal{U}_n^H$ can be further represented by

$$\mathcal{U}_n\mathcal{U}_n^H = \underbrace{\begin{bmatrix} \mathbf{U}_n\mathbf{U}_n^H & & \\ & \ddots & \\ & & \mathbf{U}_n\mathbf{U}_n^H \end{bmatrix}}_{L_i \text{ blocks}}. \tag{5.6.1}$$

Since $\mathbf{U}_s\mathbf{U}_s^H + \mathbf{U}_n\mathbf{U}_n^H = \mathbf{I}_{PMN_{br}}$, an alternative form of (5.3.5), which is based on the signal subspace representation, has been obtained. Therefore, the adaptive subspace tracking algorithms with lower complexity, such as the orthonormal PAST algorithm [108], can be used instead of the batch EVD to estimate an orthonormal basis of the signal subspace, leading to a much reduced complexity.

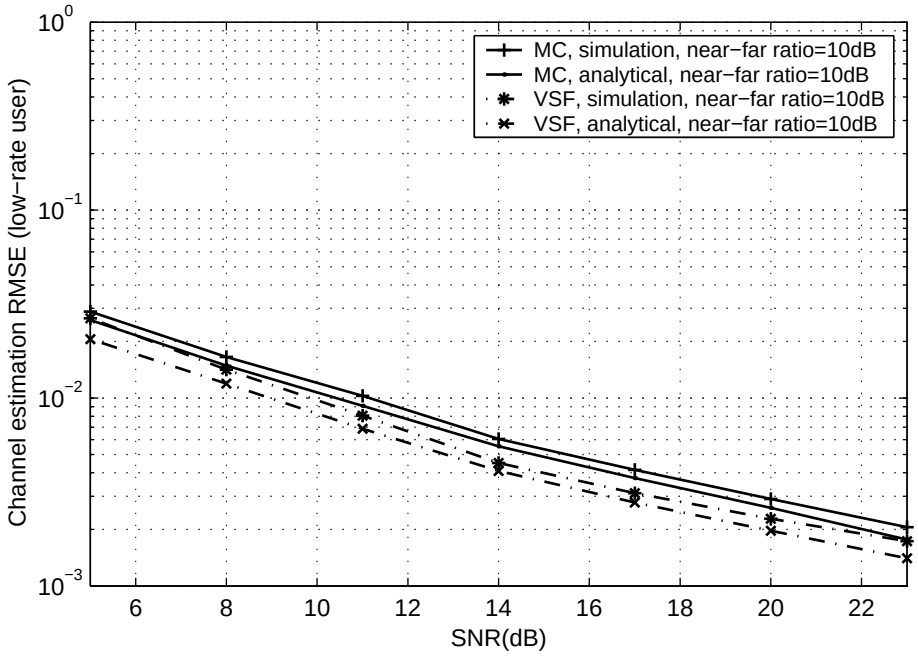

(a)

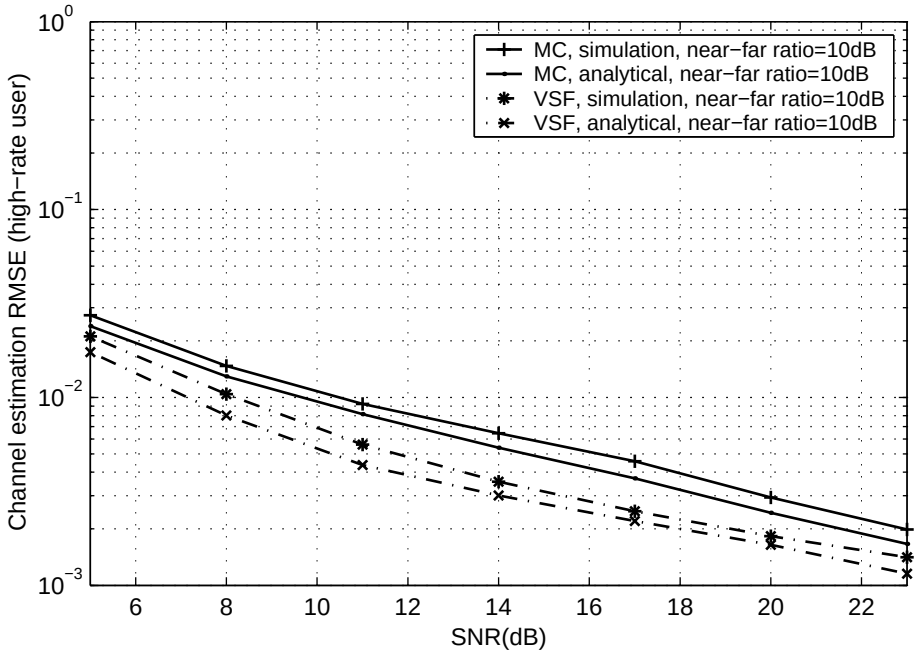

(b)

Figure 5.4: The channel estimation RMSE for (a) the desired low-rate user and (b) the desired high-rate user.

Chapter 6

Conclusions

6.1 Thesis Summary

This thesis consists of two parts. The first part includes the first two chapters. Chapter 1 starts with the basic concepts of cellular wireless communications. The non-blind and blind approaches for multiuser detection and channel estimation in single-rate DS/CDMA systems are then reviewed for both single-carrier and multicarrier cases. Chapter 2 deals with the multiuser detection issue for multi-rate DS/CDMA. After a brief description of multi-rate CDMA access strategies, the methodology for multi-rate signal modelling is summarized. Then the existing multiuser detection and channel estimation techniques for multi-rate DS/CDMA are reviewed, with an emphasis on blind approaches.

It is found that the existing blind approaches for multi-rate multiuser detection focus on constrained optimization methods, which only deal with the case where the delay spread is only a small fraction of the symbol period. Note that for single-rate systems, the subspace-based techniques have been proved to have capability for handling large delay spread cases. As a consequence, the second part of this thesis has investigated the use

of the subspace-based techniques for blind channel estimation and multiuser detection in multi-rate DS/CDMA systems, involving in the following three chapters. Chapters 3 and 4 handle the single-carrier cases, while Chapter 5 deals with multicarrier scenarios.

In Chapter 3, ST low-rate and high-rate blind linear detectors, i.e., blind decorrelators and blind MMSE detectors, are proposed for synchronous dual-rate systems over AWGN channels. It has been proven that a) ST low-rate blind linear detectors can support no less users than their high-rate counterparts (assuming that all the other system parameters are same); b) the BER performance of low-rate blind decorrelator is not inferior to that of high-rate blind decorrelator. The above conclusions are further generalized to synchronous multi-rate scenarios, and the asynchronous extension is discussed. Additionally, the two-stage ST dual-rate blind detectors, which combine the adaptive purely temporal dual-rate blind MMSE detectors and the non-adaptive MVDR beamformer, are presented.

Chapter 4 presents the low-rate and high-rate blind channel estimation schemes for asynchronous dual-rate systems over frequency-selective multipath channels. After adaptive implementations are developed based on the orthonormal PAST algorithm, the dual-rate blind MMSE detection for the AWGN channels is extended to multipath channels. It has been shown that the low-rate algorithm outperforms the high-rate algorithm for both channel estimation and detection.

In Chapter 5, based on a finite-length truncation approximation of the band-limited chip waveform, a blind timing acquisition and channel estimation scheme is developed for multi-rate multicarrier DS/CDMA. It is shown by numerical results and theoretical analysis that this approximation hardly caused any performance degradation of the

subspace-based channel estimation scheme under moderate near-far situations.

6.2 Suggestions for Further Study

In this thesis, subspace-based techniques have been successfully applied to blind channel estimation and multiuser detection for multi-rate DS/CDMA. However, as stated in Section 1.3, the computational complexity of subspace-based approaches is usually prohibitively high, since they typically require not only a long duration of observation, but also some form of eigen-decomposition. Moreover, the channel is often required to be time-invariant during this long observation period, which potentially makes these algorithms impractical for wireless communications. Recently, there has been some interest in semi-blind methods for single-rate systems [32], [111], which exploit the statistics of the unknown data as well as the known pilot signal, and require a shorter duration of observation to achieve the same performance as the blind methods. As a result, the study on semi-blind channel estimation and multiuser detection for multi-rate DS/CDMA is very promising and should become a major area for further study.

One of the new technologies that is being considered for 3G wireless systems and beyond is ST processing. Generally speaking, ST processing involves the exploitation of spatial diversity using multiple transmit and/or receive antennas and, perhaps, some form of coding, e.g., space-time block coding (STBC) that has been adopted in the 3G Wideband CDMA standards. The ST dual-rate blind multiuser detectors proposed in Chapter 3 focus on systems that use one transmit antenna and multiple receive antennas. Recently,

some work has been completed on ST multiuser detection using multiple antennas at both transmitter and receiver. For example, [19] analyzed and compared two different linear receiver structures appropriate for CDMA systems with multiple transmit and receive antennas. It has been shown that the ST structure has many advantages over linear diversity combining, including better BER performance, low complexity, and higher user capacity. Blind adaptive implementation of the ST structure for synchronous CDMA in flat-fading channels and for asynchronous CDMA in fading multipath channels has also been developed. However, the above works target primarily at single-rate systems. Consequently, another interesting option for further study is blind channel estimation and multiuser detection for multi-rate CDMA systems using multiple transmit and receiver antennas.

Bibliography

[1] T.S. Rappaport: *Wireless Communications: Principles and Practice*, Second Edition, Prentice Hall, Upper Saddle River, NJ, 2002.

[2] M. Zeng, A. Annamalai and V.K. Bhargava, "Harmonization of global third-generation mobile systems," *IEEE Commun. Mag.*, vol. 38, pp. 94–104, Dec. 2000.

[3] D. Koulakiotis and A.H. Aghvami, "Data detection techniques for DS/CDMA mobile systems: a review," *IEEE Personal Commun. Mag.*, vol. 7, pp. 24–34, Jun. 2000.

[4] U. Madhow, "Blind adaptive interference suppression for direct-sequence CDMA," *Proc. IEEE*, vol. 86, pp. 2049–2069, Oct. 1998.

[5] S. Verdú: *Multiuser Detection*, Cambridge Univ. Press, UK, 1998.

[6] S. Verdú, "Minimum probability of error for asynchronous Gaussian multiple access channels," *IEEE Trans. Inform. Theory*, vol. 32, pp. 85–96, Jan. 1986.

[7] R. Lupas and S. Verdú, "Linear multiuser detector for synchronous code-division multiple-access channels," *IEEE Trans. Inform. Theory*, vol. 35, pp. 123–136, Jan. 1989.

[8] Z. Xie, R.T. Short and C.K. Rushforth, "A family of suboptimum detectors for coherent multiuser communications," *IEEE J. Select. Areas Commun.*, vol. 8, pp. 683–690, May 1990.

[9] M.K. Varanasi and B. Aazhang, "Multistage detection in asynchronous CDMA communications," *IEEE Trans. Commun.*, vol. 38, pp. 509–519, Apr. 1990.

[10] P. Putel and J. Holtzman, "Analysis of simple successive interference scheme in a DS/CDMA system," *IEEE J. Select. Areas Commun.*, vol. 12, pp. 796–807, Jun. 1994.

[11] D. Koulakiotis and A.H. Aghvami, "Evaluation of a DS/CDMA multiuser receiver employing a hybrid form of interference cancellation in Rayleigh fading channels," *IEEE Commun. Lett.*, vol. 2, pp. 61–63, Mar. 1998.

[12] A. Duel-Hallen, "Decorrelating decision-feedback multiuser detector for synchronous CDMA channel," *IEEE Trans. Commun.*, vol. 41, pp. 285–290, Feb. 1993.

[13] M.K. Varanasi and B. Aazhang, "Near-optimum detection in synchronous code-division multiple-access systems," *IEEE Trans. Commun.*, vol. 39, pp. 725–736, May 1991.

[14] G. Woodward and B.S. Vucetic, "Adaptive detection for DS-CDMA," *Proc. IEEE*, vol. 86, pp. 1413–1434, Jul. 1998.

[15] P.B. Rapajic and B.S. Vucetic, "Adaptive receiver structures for asynchronous CDMA systems," *IEEE J. Select. Areas Commun.*, vol. 12, pp. 685–697, May 1994.

[16] S. Haykin: *Adaptive Filter Theory*, Third Edition, Prentice-Hall, Englewood Cliffs, NJ, 1996.

[17] M. Honig and M.K. Tsatsanis, "Adaptive techniques for multiuser CDMA receivers," *IEEE Signal Processing Mag.*, vol. 17, pp. 49–61, May 2000.

[18] D. Samardzija, N. Mandayam and I. Seskar, "Blind successive interference cancellation for DS-CDMA systems Communications," *IEEE Trans. Commun.*, vol. 50, pp. 276–290, Feb. 2002.

[19] D. Reynolds, X. Wang and H.V. Poor, "Blind adaptive space-time multiuser detection with multiple transmitter and receiver antennas," *IEEE Trans. Signal Processing*, vol. 50, pp. 1261–1276, Jun. 2002.

[20] M. Honig, U. Madhow and S. Verdú, "Blind adaptive multiuser detection," *IEEE Trans. Inform. Theory*, vol. 41, pp. 944–960, Jul. 1995.

[21] M.K. Tsatsanis, "Inverse filtering criteria for CDMA systems," *IEEE Trans. Signal Processing*, vol. 45, pp. 102–112, Jan. 1997.

[22] M.K. Tsatsanis and Z. Xu, "Performance analysis of minimum variance CDMA receivers," *IEEE Trans. Signal Processing*, vol. 46, pp. 3014–3022, Nov. 1998.

[23] Z. Tian, K.L. Bell and H.L. Van Trees, "Robust constrained linear receivers for CDMA wireless systems," *IEEE Trans. Signal Processing*, vol. 49, pp. 1510–1522, Jul. 2001.

[24] X.D. Wang and H.V. Poor, "Blind Multiuser detection: a subspace approach," *IEEE Trans. Inform. Theory*, vol. 44, pp. 677–690, Mar. 1998.

[25] Y. Song and S. Roy, "Blind adaptive reduced-rank detection for DS-CDMA signals in multipath channels," *IEEE J. Select. Areas Commun.*, vol. 17, pp. 1960–1971, Nov. 1999

[26] X.D. Wang and H.V. Poor, "Blind equalization and multiuser detection in dispersive CDMA channels," *IEEE Trans. Commun.*, vol. 46, pp. 91–103, Jan. 1998.

[27] M. Torlak and G. Xu, "Blind multiuser channel estimation in asynchronous CDMA systems," *IEEE Trans. Signal Processing*, vol. 48, pp. 137–147, Jan. 1997.

[28] H. Liu and G. Xu, "A subspace method for signature waveform estimation in synchronous CDMA systems," *IEEE Trans. Commun.*, vol. 44, pp. 1346–1354, Oct. 1996.

[29] E. G. Strom, S. Parkvall, S. L. Miller and B. E. Ottersen, "Propagation delay estimation in asynchronous direct-sequence code-division multiple access sytems," *IEEE Trans. Commun.*, vol. 44, pp. 84–92, Jan. 1996.

[30] S. Bensley and B. Aazhang, "Subspace-based channel estimation for code division multiple access communication systems," *IEEE Trans. Commun.*, vol. 44, pp. 1009-1020, Aug. 1996.

[31] E. Aktas and U. Mitra, "Complexity reduction in subspace-based blind channel identification for DS/CDMA systems," *IEEE Trans. Commun.*, vol. 48, pp. 1392-1404, Aug. 2000.

[32] V. Buchoux, O. Cappe, E. Moulines and A. Gorokhov, "On the performance of semi-blind subspace-based channel estimation," *IEEE Trans. Signal Processing*, vol. 48, pp. 1750–1759, Jun. 2000.

[33] A. Høst-Madsen and K.S. Cho, "MMSE/PIC multiuser detection for DS/CDMA systems with inter- and intra-cell interference", *IEEE Trans. Commun.*, vol. 47, pp. 291–299, Feb. 1999.

[34] H. Ping and T.T. Tjhung, "Decision-feedback blind adaptive multiuser detector for synchronous CDMA systems," *IEEE Trans. Veh. Technol.*, vol. 49, pp. 159–166, Jan. 2000.

[35] X. Wang and A. Høst-Madsen, "Group-blind multiuser detection for uplink CDMA", *IEEE J. Select. Areas Commun.*, vol. 17, pp. 1971–1984, Nov. 1999.

[36] P. Spasojevic, X. Wang and A. Høst-Madsen, "Nonlinear group-blind multiuser detection," *IEEE Trans. Commun.*, vol. 49, pp. 1631–1641, Sep. 2001.

[37] D. Reynolds and X. Wang, "Adaptive group-blind multiuser detection based on a new subspace tracking algorithm," *IEEE Trans. Commun.*, Vol. 49, pp. 1135–1141, Jul. 2001.

[38] A. Høst-Madsen and X. Wang, "Performance of blind and group-blind multiuser detectors," *IEEE Trans. Inform. Theory*, vol. 48, pp. 1849 –1872, Jul. 2002.

[39] T.S. Rappaport, A. Annamalai, R.M. Buehrer and W. H. Tranter, "Wireless communications: past events and a future perspective," *IEEE Commun. Mag.*, vol. 40, pp. 148–161, May 2002.

[40] R. Van Nee and R. Prasad: *OFDM for Wireless Multimedia Communications*, Artech House, Boston, 2000.

[41] A.C. McCormick and E.A. Al-Susa, "Multicarrier CDMA for future generation mobile communication," *Electronics & Communication Engineering Journal*, vol. 14, pp. 52–60, Apr. 2002.

[42] S. Hara and R. Prasad, "Overview of multicarrier CDMA," *IEEE Commun. Mag.*, vol. 35, pp. 126–133, Dec. 1997.

[43] S. Kondo and L.B. Milstein, "Performance of multicarrier DS CDMA systems," *IEEE Trans. Commun.*, vol. 44, pp. 238–246, Feb. 1996.

[44] T.M. Lok, T.F. Wong and J.S. Lehnert, "Blind adaptive signal reception for MC-CDMA systems in Rayleigh fading channels," *IEEE Trans. Commun.*, vol. 47, pp. 464–471, Mar. 1999.

[45] S.L. Miller and B.J. Rainbolt, "MMSE detection of multicarrier CDMA," *IEEE J. Select. Areas Commun.*, vol. 18, pp. 2356–2362, Nov. 2000.

[46] J. Namgoong, T.F. Wong and J.S. Lehnert, "Subspace multiuser detection for multicarrier DS-CDMA," *IEEE Trans. Commun.*, vol. 48, pp. 1897–1908, Nov. 2000.

[47] L. Fang and L.B. Milstein, "Successive interference cancellation in multicarrier DS/CDMA," *IEEE Trans. Commun.*, vol. 48, pp. 1530–1540, Sep. 2000.

[48] H. Liu and H. Yin, "Receiver design in multicarrier direct-sequence CDMA communications," *IEEE Trans. Commun.*, vol. 49, pp. 1479–1487, Aug. 2001.

[49] N.Yee, J.P. Linnartz and G. Fettweis, "Multi-carrier CDMA in indoor wireless radio networks," in *Proc. PIMRC 1993*, Yokohama, Japan, Sep. 1993, pp. 109–113.

[50] Z. Yang, B. Lu and X. Wang, "Bayesian Monte Carlo multiuser receiver for space-time coded multicarrier CDMA systems," *IEEE J. Select. Areas Commun.*, vol. 19, pp. 1625–1637, Aug. 2001.

[51] J. Wu, Y. Wang and K.K.M. Cheng, "Blind channel estimation based on subspace for multicarrier CDMA," in *Proc. VTC 2001-Spring*, Rhodes, Greece, May 2001, vol. 4, pp. 2374–2378.

[52] U. Tureli, D. Kivanc and H. Liu, "Channel estimation for Multicarrier CDMA," In *Proc. ICASSP 2000*, Istanbul, Turkey, Jun. 2000, vol. 5, pp. 2909-2912.

[53] P. Zong, K. Wang and Y. Bar-Ness, "Partial sampling MMSE interference suppression in asynchronous multicarrier CDMA system," *IEEE J. Select. Areas Commun.*, vol. 19, pp. 1605–1613, Aug. 2001.

[54] J.H. Deng, G.J. Lin and T.S. Lee, "A multistage multicarrier CDMA receiver with blind adaptive MAI suppression," in *Proc. ICASSP 2001*, Salt Lake City, UT, May 2001, vol. 4, pp. 2289–2292.

[55] F. Fitzek, A. Kopsel, A. Wolisz, M. Krishnam and M. Reisslein, "Providing application-level QoS in 3G/4G wireless systems: a comprehensive framework based on multirate CDMA," *IEEE Wireless Commun. Mag.*, vol. 9, pp. 42–47, Apr. 2002.

[56] L. Huang, F.-C. Zheng and M. Faulkner, "Blind adaptive channel estimation for dual-rate DS/CDMA signals," *IEEE Commun. Let.*, vol. 6, pp. 129–131, Apr. 2002.

[57] L. Huang and F.-C. Zheng, "Space-time multirate blind multiuser detection for DS/CDMA signals," Accepted for publication by *IEEE Trans. Veh. Technol.*, Apr. 2003.

[58] L. Huang and F.-C. Zheng, "Blind timing acquisition and channel estimation for multi-rate multicarrier DS-CDMA commmnications," in *Proc. GLOBECOM 2002*, Taipei, Taiwan, Nov. 2002.

[59] L. Huang and F.-C. Zheng, "Blind channel estimation in multi-rate multicarrier DS-CDMA systems," in *Proc. PIMRC 2002*, Lisbon, Portugal, Sept. 2002, vol. 4, pp. 1545–1549.

[60] L. Huang and F.-C. Zheng, "Blind channel estimation for dual-rate DS/CDMA," in *Proc. VTC 2002-Spring*, Birmingham, AL, May 2002, vol. 3, pp. 1438–1442.

[61] L. Huang, F.-C. Zheng and M. Faulkner, "Space-time multirate blind multiuser detection for synchronous DS/CDMA systems," in *Proc. GLOBECOM 2001*, San Antonio, TX, Nov. 2001, vol. 1, pp. 146–150.

[62] L. Huang, F.-C. Zheng and M. Faulkner, "Subspace-based blind adaptive multiuser detection for multirate DS/CDMA signals," in *Proc. 11th IEEE Workshop on Statistical Signal Processing*, Singapore, Aug. 2001, pp. 106–109.

[63] T. Ottosson and A. Svensson, "Multi-rate schemes in DS/CDMA systems," in *Proc. VTC 1995*, Chicago, IL, Jul. 1995, vol. 2, pp. 1006–1010.

[64] C.L. I and R.D. Gitlin, "Multi-code CDMA wireless personal communications networks," in *Proc. ICC 1995*, Seattle, WA, Jun. 1995, vol. 2, pp. 1060–1064.

[65] T.H. Wu and E. Geraniotis, "CDMA with multiple chip rates for multi-media communications," in *Proc. 28th Annual Conf. Information Sciences and Systems*, Princeton Univ., Mar. 1994, pp. 992–997.

[66] A.L. Johansson and A. Svensson, "On multirate DS/CDMA schemes with interference cancellation," *Wireless Personal Commun.*, vol. 9, pp. 1–29, Jan. 1999.

[67] H. Holma and A. Toskala: *WCDMA for UMTS: Radio Access for Third Generation Mobile Communications*, John Wiley & Sons, West Sussex, England, 2000.

[68] J.G. Proakis: *Digital Communications*, Fourth Edition, New York: McGraw-Hill, 2001.

[69] U. Mitra, "Comparison of maximum-likelihood-based detection for two multirate access schemes for CDMA signals," *IEEE Trans. Commun.*, vol. 47, pp. 64–77, Jan. 1999.

[70] J.X. Chen and U. Mitra, "Optimum near-far resistance for dual rate DS/CDMA signals: random signature sequence analysis," *IEEE Trans. Inform. Theory*, vol. 45, pp. 2434–2447, Nov. 1999.

[71] M. Saquib and R. Yates and N. Mandayam, "Decorrelating detectors for a dual-rate synchronous DS/CDMA system," *Wireless Personal Commun.*, vol. 9, pp. 197–216, May 1998.

[72] J.X. Chen and U. Mitra, "Analysis of decorrelator-based detectors for multirate DS/CDMA communications," *IEEE Trans. Vehi. Technol.*, vol. 48, pp. 1966–1983, Nov. 1999.

[73] M. Saquib and R.D. Yates and A. Ganti, "An asynchronous multirate decorrelator," *IEEE Trans. Commun.*, vol. 48, pp. 739–742, May 2000.

[74] H. Hiraiwa, M. Katayama and T. Yamazato, "Decorrelating detector for multi-processing gain CDMA systems," *IEICE Trans. Fundamentals*, vol. E82-A, pp. 2774–2777, Dec. 1999.

[75] M.F. Madkour and S.C. Gupta, "Performance analysis of a wireless multirate direct-sequence CDMA using fast Walsh transform and decorrelating detection," *IEEE Trans. Commun.*, vol. 48, pp. 1405–1412, Aug. 2000.

[76] J.W. Ma and H. Ge, "Modified multi-rate detection for frequency selective Rayleigh fading CDMA channels," in *Proc. PIMRC 1998*, Boston, MA, Sep. 1998, vol. 3, pp. 1304–1307.

[77] R. Srinivasan, U. Mitra and R. L. Moses, "Design and analysis of receiver filters for multiple chip-rate DS-CDMA systems," *IEEE J. Select. Areas Commun.*, vol. 17, pp. 2096–2109, Dec. 1999.

[78] M. Saquib, R. Yates and N. Mandayam, "A decision feedback decorrelator for a dual rate synchronous DS/CDMA system," in *Proc. GLOBECOM 1996*, London, UK, Nov. 1996, vol. 3, pp. 1804–1809.

[79] M.J. Juntti, "Performance of multiuser detection in multirate CDMA systems," *Wireless Personal Commun.*, vol. 11, pp. 293–311, Dec. 1999.

[80] A.L. Johansson and A. Svensson, "Multistage interference cancellation in multirate DS/CDMA on a mobile radio channel," in *Proc. VTC 1996*, Atlanta, GA, Apr. 1996, vol. 2, pp. 666–670.

[81] S.R. Chaudry and A.U.H Sheikh, "Performance of a dual-rate DS-CDMA-DFE in an overlaid cellular system," *IEEE Trans. Vehi. Technol.*, vol. 48, pp. 683–695, May 1999.

[82] D.S. Yoo and W.E. Stark, "Interference cancellation for multirate multiuser systems," in *Proc. VTC 2001-Spring*, Rhodes, Greece, May 2001, vol. 3, pp. 1584–1588.

[83] A. Boariu and R.E. Ziemer, "Multiuser detection in multipath environments for variable spreading-factor CDMA systems," *IEEE Trans. Commun.*, vol. 49, pp. 1520–1524, Sep. 2001.

[84] S.H. Han and J.H. Lee, "Objective function based group-wise successive interference cancellation receiver for dual-rate DS-CDMA system," in *Proc. VTC 2002-Spring*, Birmingham, AL, May 2002, vol. 4, pp. 1685–1688.

[85] X. Mestre and J.R. Fonollosa, "ML approaches to channel estimation for pilot-aided multirate DS/CDMA systems," *IEEE Trans. Signal Processsing*, vol. 50, pp. 696–709, Mar. 2002.

[86] S. Bhashyam, A. Sabharwala and U. Mitra, "Channel estimation for multirate DS-CDMA systems," in *Proc. Asilomar Conf. Signals, Systems and Computers*, Pacific Grove, CA, Oct. 2000, vo1. 2, pp. 960–964.

[87] H. Ge, "Multiuser detection for integrated multi-rate CDMA," in *Proc. Internat. Conf. Information, Commun. and Signal Processing*, Singapore, Sep. 1997, pp. 858–862.

[88] H. Ge and J.W. Ma, "Multirate LMMSE detectors for asynchronous multi-rate CDMA systems," in *Proc. ICC 1998*, Atlanta, GA, Jun. 1998, vol. 2, pp. 714–718.

[89] N. Seidl, V. Howitt and J. Richie, "Blind adaptive linear multiuser detection for multirate CDMA systems," in *Proc. VTC 2000-Fall*, Boston, MA, Sep. 2000, vol. 3, pp. 1296–1303.

[90] S. Buzzi, M. Lops and A.M. Tulino, "Blind adaptive multiuser detection for asynchronous dual-rate DS-CDMA systems," *IEEE J. Select. Areas Commun.*, vol. 19, pp. 233–244, Feb. 2001.

[91] M.K. Tsatsanis, Z. Xu and X. Lu, "Blind multiuser detectors for dual rate DS-CDMA systems over frequency selective channels," in *Proc. EUSIPCO 2000*, Tampere, Finland, Sep. 2000, vol. 2, pp. 631–634.

[92] R. Srinivasan, U. Mitra and R. L. Moses, "MMSE receivers for multirate DS-CDMA systems," *IEEE Trans. Commun.*, vol. 49, pp. 2184–2197, Dec. 2001.

[93] V. Kaweevat, S. Jitapunkul, C. Archavawanitchakol, S. Wanichpakdeedecha and N. Rasrikriangkrai, "Blind adaptive decorrelating decision-feedback multiuser detection for multirate synchronous DS/CDMA communications," in *Proc. SPAWC 2001*, Taiwan, China, Mar. 2001, pp. 178–181.

[94] M.F. Madkour, S.C. Gupta and Y.P. Wang, "Successive interference cancellation algorithms for downlink W-CDMA communications," *IEEE Trans. Wireless Commun.*, vol. 1, pp. 169–177, Jan. 2002.

[95] S. Roy and H.B. Yan, "Blind channel estimation for multi-rate CDMA systems," *IEEE Trans. Commun.*, vol. 50, pp. 995–1004, Jun. 2002.

[96] Z. Xu, "Asymptotic performance of subspace methods for synchronous multirate CDMA system," *IEEE Trans. Signal Processing*, vol. 50, pp. 2015–2026, Aug. 2002.

[97] P. Liu and Z. Xu, "Correlation matching in channel estimation for multirate DS/CDMA," in *Proc. ICASSP 2002*, Orlando, FL, May 2002, vol. 3, pp. 2581–2584.

[98] H. Yan and S. Roy, "A frequency domain method for channel estimation in multirate communication systems," in *Proc. ICASSP 2001*, Salt Lake City, UT, May 2001, vol. 4, pp. 2057–2060.

[99] S.Y. Park, H.S. Oh, W.Y. Lee and C.G. Kang, "Performance of pilot/data-combined channel estimation and power allocations for dual-rate DS/CDMA system over mobile radio channels," in *Proc. VTC 2000-Spring*, Tokyo, Japan, May 2000, vol. 3, pp. 1945–1949.

[100] I. Ghauri and D.T.M. Slock, "Blind channel identification and projection receiver determination for multicode and multirate situations in DS-CDMA systems," in *Proc. ICASSP 2001*, Salt Lake City, UT, May 2001, vol. 4, pp. 2197–2200.

[101] Z.Y. Pi and U. Mitra, "Blind delay estimation in multi-rate asynchronous DS-CDMA systems," *Submitted to IEEE Trans. Commun.*, 2000.

[102] T. Ojanpera and R. Prasad: *Wideband CDMA and Third Generation Mobile Communications*, Artech House, Boston, MA, 1998.

[103] K.S. Lim and J.H. Lee, "Performance of multirate transmission schemes for a multicarrier DS/CDMA system," in *Proc. VTC 2001-Fall*, Atlantic City, NJ, Oct. 2001, vol. 2, pp. 767–771.

[104] H. Dai and H.V. Poor, "Iterative space-time processing for multiuser detection in multipath CDMA channels," *IEEE Trans. Signal Processing*, vol. 50, pp. 2116–2127, Sep. 2002.

[105] X. Wang and H.V. Poor, "Space-time multiuser detection in multipath CDMA channels," *IEEE Trans. Signal Processing*, vol. 47, pp. 2356–2374, Sep. 1999.

[106] G.H. Golub and C.F. Van Loan: *Matrix Computations*, The John Hopkins Univ. Press, Baltimore, MD, 1996.

[107] A. Chkeif, K.A. Meraim, G.K. Kaleh and Y.B. Hua, "Spatio-temporal blind adaptive multiuser detection," *IEEE Trans. Commun.*, vol. 48, pp. 729-732, May 2000.

[108] K.A. Meraim, A. Chkeif and Y. Hua, "Fast orthonormal PAST algorithm," *IEEE Signal Processing Lett.*, vol. 7, pp. 60–62, Jul. 2000.

[109] L.C. Godara, "Applications of antenna arrays to mobile communications, Part II: beam-forming and direction-of-arrival considerations," *Proc. IEEE*, vol. 85, pp. 1195–1245, Aug. 1997.

[110] F. Li, H. Liu, and R.J. Vaccaro, "Performance analysis for DOA estimation algorithms: unification, simplification, and observations," *IEEE Trans. Aerosp. Electron. Syst.*, vol. 29, pp. 1170–1183, Oct. 1993.

[111] B. Muquet, M. Courville, and P. Duhamel, "Subspace-based blind and semi-blind channel estimation for OFDM systems," *IEEE Trans. Signal Processing*, vol. 50, pp. 1699–1712, Jul. 2002.

Appendix A

Publications

A.1 Journal Papers

1. L. Huang and F.-C. Zheng, "Space-time multirate blind multiuser detection for DS/CDMA signals," Accepted for publication by *IEEE Trans. Veh. Technol.*, Apr. 2003.

2. L. Huang, F.-C. Zheng and M. Faulkner, "Blind adaptive channel estimation for dual-rate DS/CDMA signals," *IEEE Commun. Let.*, vol. 6, pp. 129–131, Apr. 2002.

A.2 Conference Papers

3. L. Huang and F.-C. Zheng, "Blind timing acquisition and channel estimation for multi-rate multicarrier DS-CDMA commmnications," in *Proc. GLOBECOM 2002*, Taipei, Taiwan, Nov. 2002.

4. L. Huang and F.-C. Zheng, "Multiuser detection and channel estimation for multi-rate DS/CDMA," in *Proc. 2nd ATcrc Telecommunications and Networking Conference*, Perth, Australia, Oct. 2002, pp. 114–118.

5. L. Huang and F.-C. Zheng, "Blind channel estimation in multi-rate multicarrier DS-CDMA systems," in *Proc. PIMRC 2002*, Lisbon, Portugal, Sept. 2002, vol. 4, pp. 1545–1549.

6. L. Huang and F.-C. Zheng, "Blind channel estimation for dual-rate DS/CDMA," in *Proc. VTC 2002-Spring*, Birmingham, AL, May 2002, vol. 3, pp. 1438–1442.

7. L. Huang, F.-C. Zheng and M. Faulkner, "Space-time multirate blind multiuser detection for synchronous DS/CDMA systems," in *Proc. GLOBECOM 2001*, San Antonio, TX, Nov. 2001, vol. 1, pp. 146–150.

8. L. Huang, F.-C. Zheng and M. Faulkner, "Subspace-based blind adaptive multiuser detection for multirate DS/CDMA signals," in *Proc. 11th IEEE Workshop on Statistical Signal Processing*, Singapore, Aug. 2001, pp. 106–109.

9. L. Huang, F.-C. Zheng and M. Faulkner, "Blind multiuser detection for multirate synchronous DS/CDMA signals," in *Proc. 1st ATcrc Telecommunications and Networking Conference*, Perth, Australia, Apr. 2001, pp. 37–38.

10. L. Huang and F.-C. Zheng, "Adaptive neural network based receivers for multirate synchronous DS-CDMA systems," in *Proc. 5th CDMA International Conference*, Seoul, Korea, Nov. 2000, vol. 2, pp. 160–163.